CASPASE-3 AND CALPAIN ACTIVATION IN ALZHEIMER'S DISEASE AND A RAT MODEL OF SEPTO-HIPPOCAMPAL INJURY

By

Carlos Alberto Ayala-Grosso

A thesis submitted to the Faculty of Graduate Studies and Research of McGill University in partial fulfillment of the requirements for the Degree of Doctor of Philosophy

December, 2003

Department of Pharmacology and Therapeutics

McGill University

Montréal, Quebec

Your file Votre référence
ISBN: 0-612-98197-5
Our file Notre référence
ISBN: 0-612-98197-5

This thesis is dedicated to my family, my wife and daughter, Maria Eugenia y Lorena Sofia, to my parents Francisco y Adriana, Aura y Pedro, my brother and sisters, Rodolfo, Carmen and Aida each one has given me support and love. To my nephews Claudia Patricia, Daniel Augusto, David, Alejandro, Elena y Gabriella.

A Maria Eugenia and Lorena Sofia, las siempre me esperan y a quienes ofrezco mi amor.

Abstract

In this study, markers of programmed cell death were examined in the superior temporal, parietal and inferior frontal cortices of age-matched and Alzheimer's brain tissues and in the septum and dorsal hippocampus from fimbria-fornix axotomized rats. Activation of proteases belonging to the caspase and calpain family has been implicated in the mediation of programmed cell death in acute injury and chronic neurodegenerative disorders. The main risk factor for Alzheimer's disease, ageing, is associated with a gradual impairment of critical cellular homeostasis processes such as glucose metabolism, mitochondrial integrity and scavenging of reactive oxygen species. These changes in concert with dysmetabolism of the amyloid precursor protein and/or the microtubule associated protein Tau may compromise cell function beyond a threshold that commits neurons to die. Programmed cell death, a highly regulated pathway that entails an organized disassembly of the cell may contribute to the progression of neuropathology in Alzheimer's disease. Using antibodies to neo-epitopes generated by caspase-3-mediated cleavage of the amyloid precusor protein and spectrin, I have localized by immunohistochemistry these caspase-3-generated neo-epitopes in autopsied Alzheimer's and age-matched control brains, as well as in the forebrain of rats that have been subjected to axotomy of the septo-hippocampal pathway. Elevated levels of caspase-3-cleaved amyloid precursor protein were detected in Alzheimer's disease with respect to age-matched control brains. Immunopositive profiles were observed in particulate elements resembling dystrophic neurites, as well as in dense-core neuritic plaques, and in a subpopulation of neurons and glial cells. Caspase-3 cleaved amyloid precursor protein co-localized with some TUNEL-positive cortical neurons indicating that DNA fragmentation was indeed occurring in neurons undergoing programmed cell death. However, while there was some overlap between caspase-3 cleaved amyloid precursor protein and senile plaques or neurofibrilary tangle-bearing neurons, the fact that was a significant degree of non-overlap between these immunohistochemical markers suggests that programmed cell death may occur independent of classic histopathological features of Alzheimer's disease. Using

an antibody that recognizes nonphosphorylated neurofilaments of medium and high molecular weight (SMI-32) to identify large pyramidal neurons that are vulnerable in Alzheimer's disease, caspase-3 cleaved spectrin was clearly observed in a subset of vulnerable large pyramidal neurons of layers III and V from temporal and frontal association cortices of Alzheimer's patients. Although these neurons showed signs of caspase-3 activation, they still displayed SMI-32 immunoreactivity suggesting that caspase activation may be an early event in the pathological processes that result in the loss of these neurons in Alzheimer's disease. A theoretical model is proposed in which caspase activation triggers cortical pyramidal neuron dysfunction that in turn promotes cortico-cortical disconnection establishing a positive feedback cycle that exacerbates Alzheimer's pathology. Using a rat model of acute septo-hippocampal disconnection, calpain, but not caspase-3, was found to be activated in the terminals and cell bodies of axotomized cholinergic neurons in the septum. Inhibition of axotomy-induced calpain activation by central administration of calpain inhibitors attenuated the cholinergic response in the septum to septo-hippocampal disconnection but did not prevent terminal degeneration. Taken together, these results demonstrate a role for caspase activation in the early events leading to neuronal dysfunction in Alzheimer's disease and calpain activation in the response of septo-hippocampal neurons to axotomy.

RÉSUMÉ

Des marqueurs subrogés de la mort cellulaire programmée ont été évalués dans des tissus de cortex temporal supérieurs, pariétal et frontal inférieurs de cerveaux de patients atteints de la maladie d'Alzheimer, de cerveaux de patients contrôles du même âge ainsi que dans le septum et l'hippocampe dorsal de rats dont la fimbria et le trigone ont été axotomisés. L'activation de protéases des familles des des caspases et de la calpaïne a été mise en cause dans la cascade biochimique de la mort cellulaire programmée subséquente aux traumatismes aigus ainsi que dans les maladies neurodégénératives chroniques. Dans la maladie d'Alzheimer, l'âge, principal facteur de risque, est accompagné de la dégradation graduelle de mécanismes de contrôle de fonctions critiques au maintien de l'homéostasie du tissu. Ces mécanismes sont liés au métabolisme du glucose, à l'intégrité mitochondriale et au système de contrôle des métabolites actifs de l'oxygène. Ces changements biochimiques, ajouté aux troubles du métabolisme de la protéine précurseur de l'amyloïde et/ou à ceux de la protéine Tau, associée aux microtubules, peuvent compromettre la fonction cellulaire au point de dépasser le stade de non retour engageant ainsi la mort cellulaire. Il est probable que la mort cellulaire programmée, une voie métabolique hautement contrôlée impliquant le désassemblage organisé des cellules, puisse contribuer à la progression de la pathologie de la maladie d'Alzheimer.

Nous avons utilisé des anticorps dirigés contre des néo-épitopes générés par l'action de la caspase-3 sur la protéine précurseur de l'amyloïde pour examiner l'expression et pour localiser par immuno-histochimie ces néo-épitopes produits par l'action de la caspase-3 et de la calpaïne dans des tissus d'autopsie de patients atteints de la maladie d' Alzheimer, de patients contrôles du même âge ainsi que dans des tissus de rats ayant reçu une lésion aiguë de la voie septo-hippocampique. Nos résultats montrent, dans la maladie d'Alzheimer par rapport aux cerveaux contrôles, une augmentation du clivage de la protéine précurseur de l'amyloïde par la caspase-3. Le profil immuno-positif que nous avons identifié se localise dans des éléments corpusculaires semblable à des névrites dystrophiques

ainsi que dans des plaques séniles denses et dans une sous population de neurones et de cellules gliales. La co-localisation du produit de clivage de la protéine précurseur de l'amyloïde par la caspase-3 avec des neurones TUNEL positifs, indique que la fragmentation de l'ADN accompagne la mort cellulaire programmée des neurones. Cependent, alors que l'on a pu observer une certaine co-localisation du produit de clivage de la protéine précurseur de l'amyloïde par la caspase-3 avec des plaques séniles et des neurones montrant des enchevêtrements neurofibrilaires, le manque significatif de superposition de ces marqueurs suggère que la mort cellulaire programmée peut avoir lieu indépendamment des marqueurs caractéristiques de l'histopathologie de la maladie d'Alzheimer. L'utilisation d'un anticorps qui reconnaît les neurofilaments non phosphorylés de poids moléculaire moyen et élevé (SMI-32) pour identifier les grands neurones pyramidaux vulnérables dans la maladie d'Alzheimer a permis de clairement observer a la spectrine clivée par la caspase-3 dans une sous population vulnérable ces neurones pyramidaux dans les couches III et V des cortex associatifs frontaux et temporaux chez les patients atteints de la maldie d'Alzheimer. Bien que ces neurones montraient des signes d'activation de la caspase-3, ils montraient aussi de l'immunoréactivité SMI-32. Ceci suggère que l'activation de la caspase peut être un évènement précoce dans les processus qui résultent en la perte de neurones dans la pathology d'Alzheimer. Nous proposons un modèle théorique dans lequel l'activation des caspases produit une dysfonction des neurones corticaux pyramidaux. Cette dysfonction produit à son tour une déconnection cortico-corticale, qui génère ainsi un processus de feedback positif qui exacerberait la pathologie de la maladie d'Alzheimer. Nous avons montré chez le rat, dans un modèle aigu de section septo-hippocampique, que la calpaïne et non pas la caspase-3 était activée dans la terminaisons nerveuses et le somas des neurones septaux cholinergiques axotomisé. Le blocage, par administration central d'inhibiteur, de l'activation de la calpaïne induite par l'axotomie, diminue la réponse cholinergique à la déconnection septo-hippocampique dans le septum mais ne module pas la dégénérescence des terminaisons nerveuses. Ces résultants montrent un rôle de l'activation des caspases dans les évènements précoces qui

mènent à la dysfonction neuronales dans la maladie d'Alzheimer. Ils montreant aussi l'activation de la calpaïne dans la réponse septo-hippocampique à l'axotomie.

Table de contents

Index of figures

Index of tables

Glossary

Aβ: Amyloid Aβ

SP: Senile plaques

NFT: Neurofibrillary tangles

AD: Alzheimer's disease

ANOVA: Analysis of variance

APP: Amyloid precursor protein

$\alpha\Delta C^{csp}$-APP: Caspase cleaved APP

$\alpha\Delta C^{calpain}$-αII-spectrin: Calpain-cleaved -spectrin

$\alpha\Delta N^{caspase}$-αII-spectrin: Caspase-3 cleaved -spectrin

ChAT: Choline acetyl transferase

ODV: Optical density value

BCA: Bincichonic acid

BSA: Bovine serum albumin

DAB: 3'3'- diamino benzidine tetrahydrocholride

EDTA: Ethylendiamine tetraacetic acid

ER: Endoplasmic reticulum

GABA: γ-aminobutiric acid

GFAP: Glial fibrillary acidic protein

HCl: Hydrochloric acid

HRP: Horseradish peroxidase

IgG: Immunoglobulin

MAP: Microtubule associated protein

MAPK: Mitogen activated protein-kinase

NeuN: Neuron specific nuclear antigen

NFT: Neurofibrillary tangles

NGF: Nerve growth factor

NMDA: N-methyl D-aspartate

PAGE: Polyacrylamide gel electrophoresis

PBS: Phosphate buffered saline

PBS + T: Phosphate-buffered saline + 0.2 % tween

SDS: Sodium dodecyl sulfate

TBS: Tris-buffered saline

TBS + T: Tris-bufered saline + 0.1% tween 20

TUNEL: Terminal UTP-nick end labeling

Acknowledgments

I would like to acknowledge my supervisor Dr. George S. Robertson for his support over these 5 years. He offered me incredible possibilities to be explored in science. I particularly thank for his patience in handle my communicational difficulties as foreign student.

I would like also to acknowledge Brian Collier for his splendid disposition and offering me alternatives to develop my PhD studies. Also for listening my experimental observations and reinforce an inquisitive attitude in this matter.

I thank to my advisor Paul Clarke and Guillermina Almazan for their generous disposition of time.

I owe special gratitude to Adriana Ducatenzeiler, Hélène Duplessis and Jean Pierre Fluckiger for adopt me as part of their families and let me share with them moments of pleasure and uncertainty.

To Martín Bruno, Adriana Aguilar-Mahecha, Helen Ashdown, Mathieu Bouchard, Yves Bureau, Susan Crocker, Jing Qji Huang, Elizabeth Wong, Aminah Pradmani, and Betty Panagiotta Stamatiou for their friendship.

I would like to acknowledge the funding support of the Consejo de Desarrollo Científico y Humanístico de la Universidad Central de Venezuela, Caracas, Venezuela.

Finally, I acknowledge Merck Research Laboratories for allow me to develop my research project in their magnificent facilities and receive complete support from his professionals at Laboratory Animal Resources.

Statement of authorship

The following is reproduced in full from the "Guidelines Concerning Thesis Preparations", Faculty of Graduate Studies and Research, McGill University.

Manuscript and Authorship:

Candidates have the option, subject to the approval of their Department, of including, as part of their thesis, copies of the text of a paper(s) submitted for publication, or the clearly-duplicated text of a published paper(s), provided that these copies are bound as an integral part of the thesis. If this option is chosen, connecting texts, providing logical bridges between the different papers are mandatory. The thesis must still conform to all other requirements of the "Guidelines Concerning Thesis Preparation" and should be in a literary form that is more than a mere collection of manuscripts published or to be published. The thesis must include, as separate chapters or sections: (1) Table of Contents, (2) a general abstract in English and French, (3) an introduction which clearly states the rationale and objectives of the study, (4) a comprehensive general review of the background literature to the subject of the thesis, when this review is appropriate, and (5) a final overall conclusion and/or summary. Additional material (procedural and design data, as well as descriptions of equipment used) must be provided where appropriate and in sufficient detail (e.g. Appendices) to allow a clear and precise judgment to be made of the importance and originality of the research reported in the thesis. In the case of manuscripts co-authored by the candidate and others, the candidate is required to make an explicit statement in the thesis of whom contributed to such work and to what extent; supervisor must attest to the accuracy of such claims at the Ph.D. Oral Defense. Since the task of examiners is made more difficult in these cases, it is in the candidate's interest to make perfectly clear the responsibilities of the different authors of the co-authored papers.

Chapter 3/Paper 1 published in Brain Pathology (2002) 12(4): 430-441

Caspase-cleaved amyloid precursor protein in Alzheimer's disease
Carlos Ayala-Grosso, Gordon Ng, Sophie Roy and George S Robertson

Chapter 4/Paper 2 submitted to Neuroscience

Caspase-3 activation in SMI-32 immunoreactive cortical pyramidal neurons is an early event underlying corticocortical disconnection in Alzheimer's disease
Carlos Ayala-Grosso, John Tam, Sophie Roy, Steven Xanthoudakis, Donald W Nicholson and George S Robertson

Chapter 5/Paper 3 submitted to Journal of Comparative Neurology

Effects of Fimbria-Fornix Transection on Calpain and Choline Acetyl Transferase Activities in the Septohippocampal Pathway
C. Ayala-Grosso, J. Tam, S. Xanthoudakis, Y. Bureau, S, Roy, D.W. Nicholson and G.S. Robertson

This thesis is based on the data described in Chapter 3, Chapter 4, and Chapter 5 which (one of them has been already published) and the other two have been submitted for publication. The following statements outline the contributions of each authors.

Dr. George S. Robertson: Principal investigator on all the studies described herein, and main intellectual influence in all matters pertaining to the brain and immunocytological techniques.

Dr. Donald W. Nicholson: main intellectual influence in matters pertaining to Biochemistry of caspases.

Dr. Sophie Roy: main intellectual influence in matters pertaining to Biochemistry of caspases.

Dr. Gordon Ng: main intellectual influence in matters pertaining to biochemistry of calpains.

Dr. Steven Xanthoudakis: Collaborator in the training for the immunoprecipitation experiments of the caspase-cleaved amyloid precursor protein and caspase cleaved spectrin proteolytic fragments. Contributed to the intellectual content of chapter 4.

Dr. Yves Bureau: Collaborator in the tutorial of statistical analysis using the SPSS software. Contributed to alternative statistical analysis in chapter 5.

Mr. John Tam: A research assistant that train me in Western analyses, determination of caspase-3 cleaved spectrin proteolytic fragments who contributed his expertise in the characterization of the caspase-cleaved spectrin antibody in cell lines.

MSc. Carlos Ayala-Grosso: Ph. D. Candidate in the Pharmacology Dpt working at Merck Frosst Research Laboratories under supervision of Dr. Robertson. I did all of immunohistochemical and biochemical work in autopsied human brain tissues that are presented in Chapters 3 and 4 and all *in vivo* work and preparation of rat brain tissues that are presented in Chapter 5. I wrote all of the manuscripts.

Chapter 1

1. Introduction

1.1 Primary Characteristics of Alzheimer's disease

Alzheimer's disease affects more than 12 million people worldwide, being the most prevalent cause of dementia during senescence. If the current rate of 360,000 new cases per year continues, the diagnosed population of patients with this neurodegenerative disorder will double in the next 20 years (Cummings and Cole, 2002). Alzheimer's disease will become an ever-increasing public health issue in the current millennium, because of augmented life expectancy and the high social and economic cost of care-given services for affected individuals.

Named for the German psychiatrist Alois Alzheimer who described its pathological hallmarks in 1907, Alzheimer's disease has been increasing recognized as a multifactorial pathological entity with at least four neurobiological dimensions: (1) *the presence of histopathological features* characterized by the abundant accumulation of extracellular amyloid β (Aβ) peptides in neuritic plaques and neurofibrillary changes, which include intracellular tangles, neuropil threads, and dystrophic neurites investing plaques in specific areas of the brain. The neuronatomical evolution of these changes has been extensively detailed (Braak and Braak, 1991; Katzman et al., 1988; Naslund et al., 2000; Morris and Price, 2001); (2) *dysfunctional metabolism* of classical neurotransmitters and neuromodulators, such as acetylcholine, glutamate and somatostatin (Davies and Maloney, 1976; Perry et al., 1977; Davies et al., 1980; Bartus et al., 1982; Whitehouse et al., 1982; Greenamyre et al., 1989; Francis et al., 1993; Bartus, 2000; Terry and Buccafusco, 2003); (3) *topography of central nervous system involvement*, where neurodegenerative processes tend to selectively involve topographically or functionally related neural systems, as a consequence, the medial temporal, limbic, and temporal-parietal associational cortices are mainly affected becoming atrophic (Pearson, 1985; Braak and Braak, 1991) and (4) *degree of hereditary transmission* encompassing both early onset of autosomal dominant forms, mutations in amyloid precursor protein (APP), presenilin 1 (PS1) and presenilin 2 (PS2) genes, and

some late life sporadic familial forms of the disease, e.g., apolipoprotein E (ApoE) and α-macroglobulin (Corder et al., 1993; Scheuner et al., 1996; Czech et al., 2000; Gomez-Isla et al., 1999; Fraser et al., 2000). Altogether these neurobiological dimensions represent a conundrum of potential etiological factors and consequences associated with the progressive nature of this syndrome leading to a global decline of cognitive function and memory as well as impairment in social and occupational functioning.

1.2 Dynamics of Histopathological Features of Alzheimer's Disease

Definitive diagnosis of Alzheimer's disease relies on *postmortem* determination of density and distribution of histopathological hallmarks on brains from those diagnosed with probable Alzheimer's disease during the last years of their lives. Pathological evaluation of autopsied brain tissues has been useful in characterizing distinct types of degenerative or destructive changes with respect to normal aging or senescence. Although controversy persists as to whether senile plaques (SP), neurofibrillary tangles (NFT) and neuronal loss are disease-specific or also can occur with normal brain aging, recent studies have suggested that when Alzheimer's disease or other disorders are carefully excluded, aging itself may not result in substantial accumulation of senile plaques, neuronal loss and cognitive decline.

Age-related neuronal loss does not occur in most regions of the neocortex, it appears to be specific to the frontal cortex and some hippocampal regions. For instance, West et al., (1993) reported a total neuron loss of about 30% and 50% in the dentate hilus and subiculum (but not in the dentate gyrus), respectively. Furthermore, Simic et al., (1997) reported a significant neuron loss in the subiculum and CA1 area of the hippocampus. More recently, Uylings and de Brabander, (2002) detected a progressive reduction of length of dendritic fields in layer V of the dorso-lateral frontal cortex in aged brains. In agreement with these results, brain mapping by magnetic resonance imaging techniques have estimated a trend for diffuse gray matter loss of around 0.9% per year during healthy senescence (Thompson et al., 2003).

The neuropathology associated with Alzheimer's disease may affect cognitive ability and daily function long before the symptoms become severe enough to warrant a

diagnosis of dementia. Initial clinical symptoms seem not to be directly caused by the deposition of amyloid or the formation of intracellular neurofibrillary tangles, but rather by the loss of neurons and, in particular, synaptic attrition (Hyman et al., 1984; Terry et al., 1991; Dekosky and Scheff, 1990). As the disease progresses, dementia evolves from barely detectable memory loss to widespread cognitive failure with language impairment associated with progressive neuronal loss of the superior temporal sulcus (Gomez-Isla et al., 1997; Price and Morris, 1999; 2001).

Development of neurofibrillary tangles and deposition of amyloid in senile plaques seem to be independent events that can be dissociated both spatially and temporally during the progression of Alzheimer's disease. Tangle density in limbic structures slowly increases with age, whereas plaques are usually absent from aged but nondemented individuals even in the ninth decade of life. However, it seems that with substantial deposition of Aβ peptide in senile plaques, the rate of neurofibrillary tangle formation may be accelerated. As a result, dystrophic neurites and disorganized neuropile may result accompanied by expression of clinical dementia (Braak and Braak, 1997; Price and Morris, 1999; Morris and Price, 2001; Riley et al., 2002).

A variety of factors may explain the poor correlation between the number of senile plaques or end-stage of Aβ deposition and the degree of cognitive impairment in Alzheimer's disease such as the complexity of the kinetics of Aβ accumulation, multiplicity in compartments where Aβ is generated, physical states in which the peptide may exist (soluble or insoluble), as well as its relative degree of secondary structure and state of aggregation (Gomez-Isla et al., 1997; Riley et al., 2002). Using improved techniques of extraction and quantification for $A\beta_{(1\text{-}40)/(1\text{-}42)}$ levels, it has been demonstrated that there is a significant positive correlation between the load of amyloid in the frontal, temporal, parietal and entorhinal cortices and dementia severity measurements as assessed by CDR (clinical dementia ratings) scores in Alzheimer's disease (McLean et al., 1999; Naslund et al., 2000).

Progression of neurofibrillary pathology, as suggested by Braak and Braak, evolves in a predictable sequence across medial temporal lobe structures, subcortical nuclei, and neocortical areas of the brain. The sequence occurs in six stages: In the trans-entorhinal stage (stages I and II), neurofibrillary pathology is essentially confined to the

transentorhinal and entorhinal cortex with mild involvement of the CA1/CA2 sections of the hippocampus. The limbic stage (stages III and IV), involves a higher degree of neurofibrillar pathology in entorhinal areas, moderate tangles in the hippocampus, and spread to the amygdala, thalamus, hypothalamus, and basal forebrain. Finally, the neocortical stage (stages V and VI) involves abundant neurofibrillary pathology in the neocortex. The initial clinical characterization of these stages suggested that the trans-entorhinal stage was "clinically silent" representing a preclinical period of Alzheimer's disease while the limbic stages represent incipient Alzheimer's disease, reflecting the first appearance of clinical symptoms. The neocortical stage is characterized by fully developed Alzheimer's disease from both a pathological and clinical perspective (Braak and Braak, 1991).

The transition from stage to stage is gradual and sequential, extending over a period of two to four decades. In addition to the number and location of neurons involved, another time-dependent process is the evolution of neurofibrillary tangles by itself. Recent work suggests that possession of neurofibrillary tangles within neurons does not indicate immediate cessation of cell function, neurons in which neurofibrillary tangles form may remain alive for many years before they die (Hatanpaa et al. 1996; Morsch et al., 1998).

Adaptive responses in local circuits may precede gross changes in brain architecture because of Aβ deposition and neurofibrillary tangles and may explain the onset of cognitive decline in the elderly Alzheimer's disease subject. Ultrastructural studies of biopsied cortical tissue from the frontal lobe of subjects with mild to moderate Alzheimer's disease have demonstrated a significant reduction in the number of synapses that is accompanied by a significant increase in synapse size. As a consequence, a compensatory enlargement of synaptic size may allow a stable total synaptic contact area (Dekosky and Scheff, 1990). Furthermore, up-regulation of choline acetyl transferase (ChAT) activity in the frontal cortex and hippocampus in mild cognitive impairment is suggestive of an intrinsic property of the cholinergic system to compensate regional deficits at early stages of the disease (Dekosky et al., 2002).

Despite comprehensive research dedicated to understanding the relative contribution of amyloidosis and neurofibrillary pathology to the progression of the

disease, interaction between these histopathological features has remained elusive. However, recent findings from Lewis et al, (2001) and Gotz et al, (2001) have independently established that amyloid precursor protein or accumulation of Aβ may influence generation of neurofibrillary tangles. Crossing of transgenic mice carrying mutated forms of the amyloidal precursor protein (APP) Swedish mutation (APP_{Sw}) (Tg2576) and the fronto-temporal dementia with parkinsonism linked to chromosome 17 (FTDP-17) (JNPL3) have produced a double mutant mice with a marked increase in neurofibrillary tangles in limbic areas. Eventhough, neurofibrillary tangles were not associated with amyloid deposits, these findings are suggestive of an environment of dysfunctional APP or accumulation of Aβ may modulate or promote neurofibrillary tangles. In support of this observation, intrahippocampal administration of $A\beta_{(1-42)}$ results in an increase of neurofibrillary tangles in the amygdala of the FTDP-17 (JNPL3) transgenic mice (Gotz et al., 2001; Lee, 2001).

1.3 How Do Neurons Die in Alzheimer's Disease?

This primary question has been a source of extensive experimental analysis. Although the precise mechanism of cell death in Alzheimer's disease is currently unknown, seminal publications established that neuronal survival requires trophic support. Developing neuronal circuits are shaped by target-derived trophic factors that are in limited supply; when the trophic support is absent, neuronal death may occur by programmed cell death (Oppenheim, 1991; for a review see Yuan and Yankner, 2000).

In contrast with developing neurons and their dependence on trophic factor supply, survival of mature neurons seems to be less dependent on trophic factor support suggesting that loss of trophic factor supply is not a primary pathogenic mechanism in adult neurodegenerative disorders. There is abundant literature suggesting that sporadic Alzheimer's pathology may occur as a consequence of at least two main metabolic conditions: i) energy-depletion (Vander Heyden et al., 2000) and ii) oxidative stress (Slater et al., 1995). Additionally, dysmetabolism of APP and subsequent accumulation of Aβ (Yankner, 1996) as well as increased hyperphosphorylation of Tau may contribute to pathophysiology found in Alzheimer's disease (Cotman and Su, 1996).

There are several epidemiological studies that have identified vascular risk factors and/or vascular disease associated with Alzheimer's disease. For instance, risk factors for Alzheimer's pathology reported in the Rotterdam Study include the following: diabetes mellitus, thrombotic episodes, high blood fibrinogen concentration, high serum homocysteine, atrial fibrillation, smoking, alcoholism, low level of education and atherosclerosis (for a review see de la Torre, 2002). All these conditions share at least one element: the reduction or impairment of optimal brain blood perfusion. For instance, patients with Alzheimer's disease more frequently have asymptomatic or silent brain infarcts on magnetic resonance imaging (MRI) than do control subjects without dementia. The prevalence of silent brain infarcts is also high in elderly populations without dementia.

Energy-depletion and oxidative stress may precede the hypometabolic and neurodegenerative state in Alzheimer's disease. Indeed, de la Torre, (2002) quoted at least 4 conditions that reinforce the proposal that energy-depletion, as a result of cerebral hypoperfusion, may elicit oxidative stress, neurodegeneration and cognitive decline. These conditions are: 1) Regional microvessel degeneration is independent of Alzheimer's stage severity; 2) Regional hypometabolism in Alzheimer's brains appears before senile plaques and does not occur as a consequence of amyloid deposition; 3) abundant density of senile plaques, neurofibrillary tangles that met neuropathological criteria for Alzheimer's disease have been found in a large percentage of cognitively normal, elderly brains at autopsy; 4) abnormal patterns of perfusion similar to those individual with Alzheimer's disease has been found in young patients with Down syndrome at an age when senile plaques and neurofibrillary tangles are still absent from their brains and before any dementia is apparent.

The prevalence of hypometabolism and oxidative stress in several pathological conditions associated with vascular dementia and Alzheimer's disease suggest that cell death in these disorders may occur by similar mechanisms. In the following review, I have summarized the evidence concerning a role for programmed cell death in Alzheimer's disease.

1.4 Programmed Cell Death. Basic Mechanisms

The number of cells that an organism has at a single moment in time is the net result of cell proliferation and cell removal. Under a particular set of conditions, imbalance between these two processes may lead to proliferative disorders such as cancer or neurodegenerative disorders such as Alzheimer's disease.

The starting point in cell death occurs when survival conditions are overcome by apoptotic triggers in such a way that commit a particular population of cells to die. When a cell dies, a characteristic morphological appearance or apoptosis evolves including blebbing of the plasma membrane, chromatin condensation, nuclear fragmentation, loss of adhesion, rounding and shrinkage. Biochemical features associated with these morphological events involve changes in membrane integrity (externalization of phosphatydilserine) (Martin et al., 1995), internucleosomal cleavage of DNA with a subsequent accumulation of oligonucleosomal laddering (Cohen et al., 1994) and proteolytic cleavage of multiple substrates (Fischer et al., 2003).

Programmed cell death is mediated by aspartate-specific cysteine proteases (caspases) that systematically dismantle a cell by cleaving substrates necessary for cell survival (Cohen 1997; Porter and Janicke, 1999). The caspase gene family contains at least 14 mammalian members, of which, 11 human enzymes are known. Caspases share similarities in amino acid sequence, structure, and substrate specificity (Nicholson and Thornberry, 1997). Expressed as zymogens, caspases are activated to fully functional proteases by two cleavage events. The first proteolytic cleavage divides the protein into large and small caspase subunits, and a second cleavage removes the N-terminal prodomain. The active caspase is a tetramer of two large and two small subunits, with two active sites. The large subunit contains the active site thiol (cysteine) group necessary for activity in a conserved QACXG motif (Thornberry and Lazebnik, 1998). Cleavage by caspases occurs with an absolute requirement for cleavage after aspartic acid residues (Stennicke and Salvesen, 1998). Noticeably, the presence of aspartate at the maturation clevage site is consistent with the ability of caspases to auto-activate or to be activated by other caspases as part of an amplification cascade (Zimmermann et al., 2001).

Evidence for the sequential activation of caspases has lead to the concept of a caspase cascade. This cascade begins with autocatalytic activation of initiator caspases (caspase -2, -8, -9 and -10) that, in turn, transmit the signal by cleaving and thereby activating downstream effector caspases (caspases-3, -6 and -7). Coincident with a role of signal integrators for programmed cell death, long prodomain sequences of around 100 amino acids in initiator caspases have distinct motifs, including death effector domains (DED, caspase-8 and -10) and caspase recruitment domains (CARD, caspase-1, -2, -4, -5 and -9) (for a review see Morrison et al., 2002).

Activation of caspases occurs mainly by two signal transduction events: i) an extrinsic pathway triggered by ligation of a death receptor or ii) an intrinsic pathway activated by the release of proactivators from intracellular organelles such as mitochondria sensing disturbances of cellular homeostasis.

1.4.1 Extrinsic Pathway of Programmed Cell Death

1.4.1.1 Death Receptors and Death Ligands in Alzheimer's disease

Death receptor pathways mediated by members of the tumor necrosis factor receptor (TNFR) family are involved in a number of physiological processes, including neuronal cell death during development and after injury. This family of receptors includes Fas/CD95/Apo1, TNFR1, TNFR2, DR3/TRAMP/Wsl-1, TNF-related apoptosis-inducing ligand (TRAIL) receptors and $p75^{NTR}$ that have been characterized mainly in non-neuronal cells (Morrison et al., 2002). In Alzheimer's brain tissues, the Fas/CD95/Apo1 death receptor has been the most extensively characterized thus far.

1.4.1.1.1 *Fas/CD95/Apo1 Death receptor*

Activation of the Fas receptor pathway by binding of Fas ligand (FasL) to this receptor leads to trimerization of the Fas receptor and results in the recruitment of an intracellular adapter protein, FADD (Fas-associated death domain). Multidomains in FADD may interact with homologous sequences such as the DEAD domain in the

Fas/CD95/Apo1 receptor and through the DEAD adaptor domain within the prodomain in caspase 8. The trimeric complex, receptor, FADD and pro-caspase 8 form the death inducing signaling complex (DISC). Pro-caspase 8 subsequently undergoes autocatalytic cleavage to yield its active form, which in turn cleaves and activates the effector caspases -3, -6, or -7. Activation of the death receptor is sufficient for cell death (Morrison et al., 2002).

Fas receptors and Fas ligand (FasL) are expressed on both astrocytes and neurons in normal rat and human brain. Early reports from Nishimura et al. (1995) suggested that Fas death receptor immunoreactivity was associated with senile plaques and a minor subpopulation of glial fibrillary acidic protein immunopositive cells. Increased expression of Fas and p53-immunoreactive neurites and glial cell processes was observed in Alzheimer's brain tissues with respect to age-matched controls. These findings suggested that programmed cell death through the extrinsic pathway was shared by neurons and glial cells in Alzheimer's disease (De la Monte et al., 1997; 1998). More recently, Fas receptor and FasL immunostaining have been reported not to be associated with senile plaques and dystrophic neuritis (Ferrer et al., 2001). In this study, these markers were equally expressed in tangle-bearing and non-tangle bearing neurons in Alzheimer's brain tissues, whereas FasL was highly concentrated in reactive astrocytes (Ferrer et al., 2001). In contrast, Su et al., (2003) have detected FasL expression in both senile plaques and neurofilament-positive dystrophic neurites. These conflicting findings indicate that the role of the death receptor activation in Alzheimer's disease remains undefined.

1.4.1.1.2 Signal Transduction Pathways in Programmed Cell Death

In general, signal transduction of survival and death stimuli may occur through amplification systems based on phosphorylation. Signaling kinases that have either pro- or anti-programmed cell death effects have been described in neuronal cell lines and in Alzheimer's brain tissues.

A signaling pathway of survival involving the mitogen-activated protein (MAP) kinases family (ERK or p42/p44 MAP kinase) and the phosphoinositide 3-kinase (PI3K-

Akt) signaling pathway is counterbalanced by MAP kinase family members known as stress activated protein kinases (SAPKs): c-Jun terminal kinases (JNKs) and the p38 MAP kinase (p38 MAPK) (Morrison et al., 2002).

1.4.1.1.3 *phosphatydil inositide 3- kinase Akt signaling*

The PI3K-Akt pathway functions downstream of growth factor receptors, triggering the expression of proteins involved in the control of glucose uptake, metabolism and cell survival. Loss of regulation of glucose metabolism has particular relevance in senescence and age-related pathologies that may be followed by decreased neuronal activity, which is an essential characteristic of Alzheimer's disease. However, major issues concerning the pathogenesis of Alzheimer's disease are: i) whether histopathological features, e.g., senile plaques and neurofibrillary tangles are causally related to decreased neuronal activity, or vice versa ii) decreased metabolic activity induces SP and NFT or iii) metabolic changes and histopathology are independent. Reports from Swaab et al, (1998) support the proposal that senile plaques, neurofibrillary tangles and decreased metabolic activity would seem to be independent processes in Alzheimer's pathology.

A decreased cerebral metabolic rate ranging from 19% to 40% has been detected in mild to severe Alzheimer's patients (Hoyer et al., 1988; 1991). Furthermore, reduced glucose metabolism in the hippocampus has been observed by positron emission tomography in patients with mild cognitive impairment or Alzheimer's disease with respect to age-matched controls (De Santi et al., 2001). These changes seem to be related to altered insulin action or insulin receptor function in the brain. Decreased levels of insulin in the cerebral spinal fluid, elevated plasma insulin levels and reduced insulin-mediated glucose disposal have all been reported in patients with Alzheimer's disease (Watson and Craft, 2003).

Historically, the main role of insulin has been considered to be the control of glucose utilization in the body. However, recent evidence suggests a role for insulin in the modulation of cerebral function by mechanisms that are independent of its glucoregulatory functions. For instance, epidemiological studies have established a link

between insulin resistance, diabetes mellitus and Alzheimer's disease (For review, see Gasparini et al., 2002).

Recently, compelling evidence has emerged implicating insulin and IGF-1 in the metabolism and clearance of Aβ peptide. Insulin directly increases Aβ secretion and decreases the intracellular levels of Aβ peptides by stimulating their intracellular trafficking in neuronal cultures (Gasparini et al., 2001). In addition, IGF-I stimulates clearance of Aβ through an increase in the translocation of Aβ protein carriers, albumin and transthyretin into the brain through the choroid plexus. After IGF-I administration, entrance of albumin and transthyretin was accompanied by increased levels of Aβ protein bound to these proteins in the cerebrospinal fluid and blood (Carro et al., 2002).

Modulation of the balance between phosphorylation and dephosphorylation of the microtubule associated protein (MAP) Tau has been showed to be influenced by insulin and IGF-I. As a consequence, insulin and IGF-I could play a key role in neurofibrillary tangle formation by increasing phosphorylation of MAP Tau. These findings suggest that insulin and IGF-I may have therapeutic potential in Alzheimer's disease and perhaps in other neurodegenerative disorders (Gasparini and Xu, 2003).

1.4.1.1.4 *Extracellular-signal-regulated kinases (ERK)/MAP kinases signaling*

Early studies on alterations in kinase signaling in neurodegenerative disorders noted an activation of the mitogen-activated protein kinase pathway in Alzheimer's disease autopsied brains (Arendt et al., 1995). More recently, the accumulation of MEK1/2 and ERK1/2 proteins has been found in brain tissues with similar patterns of neurofibrillary pathology in Alzheimer's disease. Furthermore, active forms of MEK1/2 and ERK1/2 were found at initial stages of neurofibrillary pathology prior to the deposition of Aβ. Interestingly, active forms of MEK1/2 and ERK1/2 were found not only in pretangle-like neurons and neurons with classic tangles but also in neurons that did not show abnormally phosphorylated Tau (Pei et al., 2002).

1.4.1.1.5 *c-JUN N-terminal kinase (JNK)/stress activated protein kinases (SAPK) and p38 kinase: MAP kinase signaling*

Among the major pathways involved in regulating cellular responses to genotoxic stress (UV irradiation, pro-inflammatory cytokines, mitogens), activation of JNK and p38 has been implicated in growth arrest and programmed cell death (Morrison et al., 2002). Programmed cell death may occur in mammalian cells subjected to oxidative stress via activation of JNK/SAPK and the p38 kinase. Reactive oxygen species (ROS), by-products of normal mitochondrial respiration, are normally removed promptly, but toxic effects resulting from impaired scavenging efficiency of ROS may accumulate with age. Indeed, increased levels of highly oxidized proteins, DNA and lipids, and the increased appearance of advanced glycation-end products has been found in neurons of Alzheimer's disease brains (Nunomura et al., 1999; Sayre et al., 2001).

Early studies detected increased levels of c-Jun, the nuclear transcription factor activated by JNK/SAPK, in Alzheimer's brain tissues. c-Jun was significantly increased in paired helical filament bearing neurons and in glial fibrillary acidic protein immunopositive cells (Anderson et al., 1994; 1995). More recent studies have demonstrated increased expression of JNK/SAPK and neuronal phospho-JNK/SAPK is associated with neurofibrillary tangles. Localization of inactive JNK/SAPK in the cytosol is associated with neurofibrillary tangles in late stages of Alzheimer's disease. By contrast, prominent nuclear staining of JNK/SAPK in mild cases of Alzheimer's pathology suggests that activation and nuclear translocation of JNK/SAPK is an early event that coincides with the formation of neurofibrillary pathology (Zhu et al., 2001).

1.4.1.1.6 *p38 MAP kinases*

Activation of p38 by multiple stimuli (environmental stressors, growth factors, cytokines) associated with programmed cell death has suggested p38-mediated phosphorylation can be deleterious to neuronal cell survival. Intracerebral administration of $A\beta_{(1-42)}$ in the nucleus basalis of rats produces an increase of phospho-p38 immunoreactivity colocalized with microglial activation (Giovannini et al., 2002). Phospho-p38 immunoreactivity appears in early stages of neurofibrillary tangle formation

that increases as the pathology progresses. However, partial colocalization of p38 immunoreactivity with phospho-Tau immunopositive cells suggests that activation of p38 may be associated with phosphorylation of Tau (Pei et al., 2001; Sun et al., 2003; Johnson and Bailey, 2003).

1.4.2 Organelle-Dependent Programmed Cell Death Pathways

1.4.2.1 *Mitochondria*

Programmed cell death can be induced by external stressors or by ligation of the plasma membrane death (Fas) receptors, which stimulate the extrinsic pathway. It is also conceivable that when stressful or pathogenic stimuli produce damage beyond a critical threshold a sensor system may be activated involving subtle changes in local signal transduction that elicit a convergence of death signals on the mitochondria. According to this theory, a hypothetical self-amplifying system or "central executioner" device involving mitochondrial membrane permeabilization (MMP) and/or caspase activation result in the coordinated disassembly of individual organelles promoting cell death (for review, see Ferri and Kroemer, 2001).

In many cell types, MMP involves loss of protein from the outer membrane and a reduction of the normal electrochemical proton gradient generated by the electron transport chain used to generate ATP. MMP triggers extrusion of proteins normally confined to the mitochondrial intermembrane space, such as cytochrome c, which stimulate the cytosolic assembly of the apoptosome and subsequent activation of caspase-9 that in turn triggers capase-3 activation. Caspase-3 has been shown activated a DNase capable of translocating to the nucleus where it promotes DNA fragmentation and chromatin condensation (Morrison et al., 2002). A variety of second messengers elicited by cellular stressors such as elevated intracellular Ca+2, oxygen radicals, nitric oxide, ganglioside GD3, arachidonic acid and peroxynitrate, toxic metabolites such as bile salts and Aβ, proteins encoded by infectious agents and classic inhibitors of the respiratory chain may induce MMP and subsequent programmed cell death (Ferri and Kroemer et al., 2001).

1.4.2.2 *Nucleus*

Early evidence of DNA damage in Alzheimer's disease came from studies where DNA fragmentation was determined using TdT-mediated dUTP nick-end labeling (TUNEL) (Su et al., 1994; Lassman et al., 1995; Smale et al., 1995; Cotman and Anderson, 1995; Troncoso et al., 1996). Although DNA laddering has been considered a typical feature of programmed cell death, TUNEL has been demonstrated to be a more sensitive marker. TUNEL labeled cells are significantly increased with respect to age-matched controls and some of them were positively identified as undergoing programmed cell death on the basis of morphological characteristics such as apoptotic cell bodies (Su et al., 1994; Cotman and Anderson, 1995). However, several groups have seldom found cells positive for DNA fragmentation and morphological features of apoptosis in Alzheimer's brain (Lassman et al., 1995; Troncoso et al., 1996; Lucassen et al., 1997; Stadelmann et al., 1998). These contradictory findings have suggested that the TUNEL technique is not a reliable indicator of programmed cell death and that neuronal cell death may occur independently of morphological changes indicative of apoptosis.

Activation of the phospho-nucleoprotein p53 may occur as a direct consequence of DNA damage as well as a diverse array of cellular stresses, including accumulation of reactive oxygen species (Kitamura et al., 1999; Morrison et al., 2002). Mitochondria are particularly vulnerable to oxidative damage. As a result, the increase in oxidative stress associated with aging is likely accompanied by damage to mitochondrial DNA and mitochondrial adenine nucleotide translocase (ANT). ANT is a component of the mitochondrial permeability transition pore, which is a key regulator of programmed cell death (Vieira et al., 2000).

Increased p53 immunoreactivity has been reported in DNA-fragmented cortical neurons and glial cells of temporal and frontal cortices from Alzheimer's disease brains (Kitamura et al., 1997; de la Monte et al., 1997). *In vitro* studies have shown that accumulation of Aβ-induced oxidative species is associated with activation of p53. Pretreatment of neurons with α-pifithryn, a specific p53 inhibitor, resulted in a 50-60% reduction of Aβ-induced programmed cell death (Tamagno et al., 2003).

One of the actions of this transcription factor is to cause up-regulation of pro- and down regulation of anti-apoptotic members of the B cell leukemia-2 (Bcl-2) family. Increased permeability of the outer mitochondrial membrane also recruits Bcl-2 proteins that may modulate the voltage-dependent anion channel (VDAC) and other components of the mitochondrial permeability transition pore (Harris and Thompson, 2000). A complex interaction may occur between Bcl-2 and Bcl-X_L, and their pro-apoptotic counterpart Bax, Bak and Bad. The ability of Bcl-2 family members to form dimers is essential for functional activity. For instance, homodimerization or heterodimerization between pro- and anti-apoptotic members of the Bcl-2 family following the principle of mass action will promote survival or cell death. In addition, the ratio of phosphorylated forms of Bcl-2 family members may also play a role in cell survival (Hengartner, 2000).

Formation of the MMP allows release of intermembrane proteins like cytochrome *c*, and the mitochondrial-derived activator (Smac/DIABLO), that promote proteolytic activation of caspases through interaction with members of the inhibitors apoptotic protein (IAPs) family and a third apoptosis-inducing factors (AIF), which activates a nuclear DNAse that induces chromatin condensation and DNA fragmentation in a caspase independent manner.

Activation of caspases occurs by two distinct pathways: i) the extrinsic pathway, and the ii) the intrinsic pathway. In the extrinsic pathway, initiator caspases either -8, and -10, or -2 and -9 through their death effector domain or caspase recruitment domain, respectively, interact with a death inducing signaling complex at the death receptor. Otherwise, the intrinsic pathway is initiated by the release of cytochrome c that triggers formation of the apoptosome. The apoptosome consist of caspase-9, cytochrome c and apoptotic protease activating factor-1 (Apaf-1), which activates caspase-9. Once initiator caspases are activated, they can promote proteolysis and activation of executioner caspases-3, -6 and -7. As a result of caspase executioner activity, a large number of proteins with caspase-3 consensus sequences (DEXD) that are responsible for cellular homeostasis are cleaved by this protease and result in an orderly loss of cell function and integrity. A comprehensive review of caspase substrates has been recently published (Hengartner, 2000; Fisher et al., 2003).

1.4.2.3 *Endoplasmic reticulum*

Accumulation of unfolded proteins and elevated intracellular calcium levels may elicit activation of caspase-12 and up-regulation of pro-apoptotic Bcl-2 proteins. Indeed, mutations in presenilin-1 gene which are associated with early familial forms of Alzheimer's disease generate an increased production of $A\beta_{(1-41)}$ that likely affects mobilization of calcium from the endoplasmic reticulum that subsequently activates calpain, which in turn may promote caspase-12 activation (Nakagawa et al., 2000). Once caspase-12 is activated it cleaves Bcl-x_L converting it into a pro-apoptotic MMP inducer protein (Ferri and Kroemer, 2001).

1.5 Activation of Caspases in Alzheimer's Disease

The balance between promoters (Bak and Bad) and inhibitors (Bcl-2 and Bcl-x_L) of programmed cell death may be critical to the survival of individual neurons. According "the rheostat model", an increase of promoters of programmed cell death is accompanied with an increase in inhibitors of both members of the Bcl-2 family. These findings support the role of a counterbalanced activity of pro- and anti-apoptotic modulators in Alzheimer's pathology (Kitamura et al., 1998; Shimohama et al., 2000). In agreement with this hypothesis, Masliah et al., (1998) reported an increase of Bcl-2 immunopositive pyramidal neurons in the frontal cortex and a positive correlation between pro-caspase-3 immunoreactivity in neurons and the extent of DNA fragmentation (Masliah et al., 1998). Furthermore, increased expression of pro-caspase-2, -3, -8 and -9 has been found in Alzheimer's disease when compared to age-matched control brains (Shimohama et al., 1999; Engidawork et al., 2001). A recent study has also shown changes in caspase gene expression as a function of clinical progression in Alzheimer's pathology. Up-regulation of caspases was accompanied by cognitive impairment as assessed by clinical dementia ratings (Pompl et al., 2003).

Studies of caspase activation in Alzheimer's disease have yielded conflicting results. Extremely low levels of active caspase-3 in neurons and granulo-vacuolar deposits of Alzheimers's patients have been reported by Stadelmann et al., (1999). While

Su et al., (2001) found high numbers of neurons displaying DNA fragmentation but no to low colabeling of active caspase-3 with senile plaques and neurofibrillary tangles suggesting that programmed cell death as defined by caspase-3 activation may occur independently of Alzheimer's pathology. In support of this proposal, increases of active caspase-3 have been observed in subjects with mild cognitive impairment but not in late stages of Alzheimer's disease. Consequently, caspase activation may occur as an early but not a late event in this pathology (Gastard et al., 2003).

In neurons compromised by oxidative stress, due to amyloid burden, caspase activation may occur resulting in impaired cellular homeostasis, and the initiation of mechanisms associated with programmed cell death. If an adverse environment either at the cell body or in the synaptic terminal challenges cell integrity, an anterograde or retrograde wave of death signaling may spread from the site of origin. Overactivation of glutamate receptors located in postsynaptic regions of dendrites appears to be an important trigger of neuronal death in both acute and chronic neurodegenerative conditions. Conversely, activation of programmed cell death resulting from trophic factor withdrawal is based on the rational that insufficient pro-survival trophic factor signaling from target cells to presynaptic neurons will trigger cell death. Compelling evidence has been accumulated indicating that altered signaling in synaptic compartments triggers both developmental and pathological neuronal death. Degeneration of the neuronal axon may therefore precede the death of the cell body in many different neurodegenerative disorders including Alzheimer's disease, stroke, epileptic seizures, traumatic brain injury, Parkinson's and Huntington's disease (for review, see Mattson and Duan, 1999). In support of this proposal, exposure of cortical synaptosomes to Aβ results in membrane lipid peroxidation, impairment of glucose and glutamate transporters that may triggers neuronal cel death. In addition, Aβ induces expression of prostatic apoptotic related 4 protein (Par-4), caspase activation and mitochondrial dysfunction (Mattson and Duan, 1999).

In apparent contradiction with these findings, reports from Finn et al., (2000) have defined at least two independent mechanisms of degeneration when the cell body is subjected to nerve growth factor deprivation and the axon is trasected. After axonal transection, a process called Wallerian degeneration occurs involving degradation of the

axolemma and axonal cytoskeleton in a Ca^{+2} dependent manner, through activation of the calcium dependent proteases, calpains, but independent of caspase activation. By contrast, in the cell body, axotomy or nerve growth factor deprivation produced activation of programmed cell death and subsequent accumulation of active caspase-3.

Evidence of several mechanisms of cell death has been observed in the Wallerian degeneration slow (Wld^s) mice. In Wld^s mice, after axotomy, axonal degeneration is significantly delayed with respect to wild type animals in both peripheral nervous system and central nervous system. Nerve growth factor deprivation experiments on neurons from this animals have shown that cell bodies rapidly undergoes programmed cell death, whereas the axon survives for 6 days or more, then when axons start to degenerate administration of caspase inhibitors fail to block or slow this degeneration. These findings indicate that in Wld^s mice axonal degeneration occurs independent of caspases activation (For a review see Raff et al., 2002).

Differential activation of calpain and caspases has been historically related to two conceptually different processes. Calpain-mediated proteolysis has been related to necrotic neuronal death whereas caspase activation has been associated with programmed cell death. It has generally been accepted that acute degenerative neuronal death, such as that seen in cerebral ischemia, traumatic brain injury and spinal-cord injury is necrotic in nature. However, evidence of DNA fragmentation, and lately, description of caspase activation have challenged that idea. As a result, it has to be considered that neuronal death in acute and chronic neurodegenerative disorders could result in both, activation of calpain and caspase proteases (Chan and Mattson, 1999; Wang, 2000).

Dysregulated neuronal calcium homeostasis during acute ischemic insults, epileptic seizures, and traumatic brain injury and in chronic neurodegenerative disorders such as Alzheimer's disease may result in excessive calpain activation (Nixon et al., 1994; for review, see Nixon, 2000; Huang and Wang, 2001; Nixon, 2003). As a consequence, activation of calpains may lead to neuronal death through: i) degradation of cytoskeletal proteins such as actin and fodrin (Saido et al., 1993; Robert-Lewis et al., 1994; for a review see Chan and Mattson, 1999), ii) activation of caspase-12 and subsequent execution of programmed cell death (Nakagawa et al., 2000), and iii)

activation of cyclin-dependent kinase 5 (cdk5) activator protein p35 to p25 may induce hyperphosphorylation and aggregation of Tau (Lee et al., 2000; Nath et al., 2000).

The family of calcium-activated cysteinyl proteases or calpains, include several tissue-specific isoforms and two ubiquitous isozymes μ-calpain (calpain I) and m-calpain (calpain II). These isoforms bind calcium with an affinity range from millimolar (m-calpain) to micromolar (μ-calpain) and have been found to be expressed in a variety of cell types and tissues (Siman et al., 1983; Sorimachi et al., 1997). In the central nervous tissue, μ-calpain is located mainly in neurons, existing in high concentration in the dendrites and cell bodies, whereas m-calpain seems to be located predominantly in axons and glia (Nixon, 1986). Calpains are expressed as proenzyme heterodimers consisting of an 80 kDa catalytic subunit, unique to each isozyme and a 29 kDa regulatory subunit, encoded by a different gene and shared by both isozymes. Each subunit of the heterodimer contains and EF hand domain characteristic of most calcium binding proteins. The 29 kDa subunit also contains, a hydrophobic glycine-rich domain that maintains the enzyme in association with cell membranes. The catalytic site containing the critical cysteine and histidine residues is located on the larger subunit of the dimer (Sorimachi et al., 1997).

Physiologically, the activity of calpains is stimulated by an increase in intracellular free calcium concentration, that promotes autocatalytic processing to produce a heterodimer of 78 kDa and 18 kDa that is negatively regulated by low concentrations of calcium and the endogenous protein inhibitor calpastatin. Activation of caspases and calpain by physiological activity and subsequent cleavage of structural proteins such as actin and spectrin, or APP is suggestive that these proteases are also involved in remodeling of growth cone during development and synaptic plasticity that occurs in the mature nervous system (for a review see Chan and Mattson, 1999).

There are several potential confounding factors involved in examining the activation of caspases and calpains in the Alzheimer's disease brain. First, in the case of caspases, these enzymes are expressed at nominal concentration within neurons, and therefore, detecting a true signal above background is difficult. Secondly, the turnover of caspase is so rapid that active pools are inactivated and cleared before they can be captured in a single section of autopsied brain tissues. Finally, in chronic

neurodegenerative disorders, coincident with the protracted duration of disease, neuronal death as a result of activation of caspase and calpains may have occurred under strongly controlled conditions as a discrete phenomena, as a result only a small amount of cells in a particular period of time may be expected to show accumulation of active proteases.

Many of these limitations using antibodies to the active fragments of proteases may be overcome by directing antibodies to calpain- and caspase- cleaved substrates. Calpain- and caspase- cleavage products are stable, accumulate over time and are present even when the neurons die and, therefore may represent better targets to examine caspase- and calpain activation in the Alzheimer's brain or in acutely injure models. A major drawback of these tools is production of a reliable antibody without significant cross reactivity with parental forms of cleaved substrates.

Site-directed calpain-cleavage fodrin antibodies were first used to show spatial resolution of fodrin proteolysis in gerbil postischemic brains (Saido et al., 1993). Because fodrin is also a substrate for caspase, accumulation of calpain or caspase-cleaved proteolytic fragments may indicate differential activation of these proteases. Subsequent development of caspase- and calpain- cleaved fodrin antibodies has been useful in understanding the role of these proteases in acute neuronal injury (Robert-Lewis et al., 1994; for see a review Wang et al., 2000).

The first report using sequence-directed caspase-cleaved actin antibody, showed a significant accumulation of caspase-cleaved actin proteolytic fragments in processes and neurons as well as in plaque-associated microglia in Alzheimer's disease with respect to age-matched control brains. Noteworthy, the authors also reported double-labeling with TUNEL and a caspase-cleaved actin antibody, indicating that execution of programmed cell death occurrs in this disorder (Yang et al., 1998). A short time there after, using a similar approach, our laboratory developed a neo-epitope directed caspase-cleavage antibody to APP. These studies had important implications, first, as a consequence of the dysmetabolism of APP, elevated levels of Aβ produce amyloidosis and subsequent amyloid deposits in the Alzheimer's disease brain. Because elevated concentrations of Aβ may activate the programmed cell death cascade, caspases may further process APP to Aβ and feed a vicious cycle that amplifies this deleterious cascade even more. Second, caspase-cleaved APP immunoreactivity was detected in Aβ senile

plaques in Alzheimer's disease brain, suggesting that activation of programmed cell death occurs in this disorder (Gervais et al., 1999). I have reviewed the literature and dedicated a particular section to discussion.

Studies from Rohn et al., (2001) reported significant accumulation of caspase-cleaved spectrin in Alzheimer's brain with respect to age matched controls. Findings from these studies also showed a correlation between neurofibrillary tangle formation and caspase-3 cleavage of spectrin in Alzheimer's disease, suggesting that caspase-3 activation occurs in tangle-bearing neurons. In this study, application of the caspase-cleaved APP antibody was used to characterize caspase-3 activation and to identify immunoreactive profiles in Alzheimer's and age-matched controls brains. In the present study, I asked whether programmed cell death is the mechanism responsible for neuronal cell death associated with Alzheimer's disease. I have devoted a chapter of this thesis to this hypothesis, results from this study have been reported and published. I also developed caspase-3 and calpain- cleaved spectrin antibodies to assessed programmed cell death in association cortices of Alzheimer's and age-matched control brains.

1.6 Axotomy of the Fimbria-Fornix Pathway: A model of cholinergic septo-hippocampal dysfunction

Studies of the brains of those of advanced age and Alzheimer's disease have consistently found histopathological features such as neurofibrillary tangles, Lewy bodies and cell loss in the nucleus de Meynert, together with deficits in the cholinergic system in the neocortex and hippocampus (Whitehouse et al., 1982). These changes have been linked to cognitive and memory decline and might be related to alterations in consciousness experienced by patients with Alzheimer's disease (Perry et al., 1999). As a result, decline in the cholinergic innervation in the central nervous system correlates with deficits in memory performance (Bartus et al., 1982; 2000). These findings have led to the proposal of the so-called "cholinergic hypothesis" that attempts to explain the key role of ACh in cognitive decline associated with advanced age and Alzheimer's disease.

The septo-hippocampal projection consist of cholinergic and GABAergic neurons of the medial septum-diagonal band (MS-DB) complex, that form an essential

neurotransmitter system controlling function of the hippocampus. The key role of the septo-hippocampal cholinergic system in regulating memory is supported by findings that indicate that memory performance is correlated with cholinergic activity in the hippocampus assessed by changes in choline acetyl transferase activity (ChAT), acetylcholine (ACh) levels and particularly high-affinity choline uptake. As a proof of concept, disruption of the fimbria-fornix septo-hippocampal projection interferes with memory retention (For review see, Van der Zee and Luiten, 1999).

Cholinergic efferents of the MS-DB complex project through the fimbria-fornix pathway to innervate all major hippocampal cell types that are, glutamatergic pyramidal, granule and GABAergic interneurons, while septal GABAergic neurons innervate GABAergic interneurons (Shute and Lewis, 1966; Freund and Antal, 1988). A subpopulation of hippocampal GABAergic cells, projects back to the GABAergic cells of the MS-DB complex. As a result, the major reciprocal communication between the septum and the hippocampus is mediated by ACh and GABA from the MS-DB to hippocampal glutamatergic and GABAergic neurons (Gulyas et al., 1991; Leranth et al., 1992).

The extent to which septo-hippocampal neurons degenerate following transection of the fimbria-fornix pathway and the factors that contribute to the degeneration process have been a matter of controversy. Certainly, the finding that numerous septo-hippocampal projection neurons that were first retrogradely labeled and then axotomized survived over extended periods of time of up to 10 weeks, is indicative that cholinergic cells of the MS-DB complex do not die after axotomy (Peterson et al., 1990). In agreement with these results, reports from Sofroniew and Isacson, (1988) have showed that cell loss in the MS-DB complex is a function of the distance between the cell bodies and the place of transection, i.e. the further from cell bodies the axotomy is performed the less cell loss occurs.

We have developed a paradigm of axotomy of the fimbria-fornix pathway in order to identify whether caspase or calpain activation occur after septo-hippocampal transection.

1.7 Amyloid Precursor Protein Promotes Programmed Cell Death in Alzheimer's disease

Despite extensive research on APP, its role in the pathogenesis of Alzheimer's disease remains unclear. Historically, once senile plaques were successfully extracted from Alzheimer's disease brains, identification of its major constituent, a protein of around 4 kDa, was characterized biochemically. This hydrophobic peptide aggregates to form a characteristic β-pleated sheet structure, due to a spontaneous tendency to self-aggregation and organization on fibers and fibrils (Glenner and Wong, 1984; Masters et al., 1985; Kang et al., 1987). Subsequent cloning of the APP gene and mapping to chromosome 21, and the discovery that Alzheimer's neuropathology was invariable linked to trisomy of chromosome 21 (Down's syndrome) as well as the finding that mutations in the APP gene occur in autosomal dominantly inherited familial Alzheimer's disease have lead to the proposal that Aβ derived from APP is a a causative agent for familial Alzheimer's disease.

Epidemiological studies have determined that the majority of cases diagnosed with Alzheimer's disease are not related to familial forms of the disease, around 95% of Azheimer's disease cases are sporadic. The discovery that senile plaques and neurofibrillary tangles are common histopathological features in familial and sporadic cases, lead to "the amyloid cascade hypothesis". According to this hypothesis, dysfunctional metabolism of APP is the main cause of the accumulation of Aβ, triggering pathological changes in the brain of Alzheimer's patients (Selkoe, 1994; Hardy, 1997; Sommer, 2002; Hardy and Selkoe, 2002). Identification of familial forms of Alzheimer's disease resulting from mutations of the microtubule associated protein Tau led to the alternative proposal of "the TAU hypothesis" in development of Alzheimer's pathology (Hardy et al., 1998; Spillantini and Goedert, 1998; Lewis et al., 2000).

The physiological role of APP still remains a matter of controversy, known as a multidomain molecule, APP may be involved in several cellular processes, such as cell adhesion, neuronal remodeling and neuronal death (for a review see Mattson, 1997). Encoded by a gene that by alternative splicing yields eight isoforms containing 677 to 770 amino acids, APP is a typical type I protein consisting of an extracellular amino-terminal

domain followed by a single transmembrane segment and a short intracellular carboxy-terminal domain.

Proteolytic processing of APP by α-secretase produces APPsα and a carboxy-terminal fragment of 83 residues precluding the production of the amyloid Aβ protein. Alternative cleavage of APP by β-secretase produces a soluble form of APP (APPsβ) and a carboxy-terminal fragment of 99 residues. Subsequent proteolysis of the carboxy-terminal fragment by γ-secretase generates amyloid $A\beta_{(1-40)}$ and $A\beta_{(1-42)}$ proteins. Most of Aβ, in particular $A\beta_{(1-40)}$, is secreted from cells and can be detected in the cerebrospinal fluid as well as in the plasma of normal subjects, whereas in Alzheimer's disease brain, greater accumulation of $A\beta_{(1-42)}$, with respect to $A\beta_{(1-40)}$, is the first species to be deposited, which is followed by subtle accumulation of $A\beta_{(1-40)}$ protein (for review, see Bayer et al., 2001; Morishima-Kawashima and Ihara, 2002).

In addition to the cleavages that result in the formation of Aβ, APP can be cleaved at its C-terminus by caspases (Gervais et al., 1999; LeBlanc et al., 1999; Pellegrini et al., 1999; Weidemann et al., 1999). Several studies have shown that cleavage of amyloid precursor protein by caspases may favor the event of production of Aβ (Gervais et al., 1999; LeBlanc et al., 1999). Indeed, previous studies shown that serum deprivation, a known inducer of programmed cell death may increase generation of Aβ (LeBlanc et al., 1995).

Accumulation of caspase-3 cleaved proteolytic fragments of APP, either the N- or the C-terminal portion (C-31), are increased in Alzheimer's with respect to age-matched controls brains (Gervais et al., 1999; Lu et al., 2000; Ayala-Grosso et al., 2002; Su et al., 2002). Activation of caspases and subsequent the cleavage of amyloid precursor protein may generates a C-terminal fragment that seems to have neurotoxic properties (Lu et al, 2000; Dumanchin-Njock et al., 2001; Bertarndt et al., 2001; Nishimura et al., 2001) dissociated from generation of Aβ (Soriano et al., 2001). Recent studies have shown that Aβ-induced neurotoxicity and C-31 induced programmed cell death are dependent on the presence of amyloid precursor protein (Lu et al., 2003).

1.8 Amyloid β Protein: Physiology and Neurotoxicity

The physiological role of the amyloid β protein is uncertain. Several studies have established conditions by which Aβ may promote growth and survival as well as cell death (for review, see Iversen, 1995). Abundant literature has been generated concerning a main role of Aβ as a neurotoxin. However, lack of consistency in the data generated has been pointed out based on the complex properties of the Aβ molecule that changes as a function of its concentration, state of aggregation, size and composition of the peptide (Mattson, 1997).

The precise mechanism by which Aβ induces neuronal damage is still a matter of discussion. Early studies showed that Aβ interacts with the plasma membrane because its intrinsic hydrophobic properties. Indeed, aggregated amyloid may form amphipathic structures that may disturb the plasma membrane leading to intracellular ionic unbalance. The current literature suggests a central role for oxidative stress in Aβ induced neurotoxicity and subsequent activation of programmed cell death. ROS such as the superoxide anion and hydrogen peroxide, as well as 4-hydroxynonenal, a major product of lipid peroxidation, may mediate Aβ induced cytotoxicity. For instance, Aβ deposition is accompanied by generation of ROS, in conjunction with binding of redox-active transition metals, or through interaction of Aβ fibrils with cell-surface receptors associated with the inflammatory response. Microglia, which are the most frequent cell surrounding senile plaques are major sites of ferritin-bound iron and in addition a source of nitric oxide and superoxide anion. Trace metals such as aluminum, iron, zinc and copper accelerate aggregation of Aβ and seem to be redox active and thus capable of mediating ROS production (Sayre et al., 2001).

Studies from Lorenzo et al, (2000) have suggested that fibrillar Aβ interacts with membrane-bound-holo-APP in order to produce neurotoxicity. Fibrils of Aβ co-precipitate with APP to detergent-extractable neuronal membrane proteins at high nanomolar concentrations. Lack of interaction between Aβ with soluble APP have suggested that fibrillar Aβ may interact with APP transmembrane, carboxy-terminal or particularly topologically oriented APP membrane-inserted domains in order to produce cytotoxicity.

So far, the literature suggests that the main mechanism for neurotoxicity of Aβ is through dysregulated metabolism of APP followed by an increase in the turnover of Aβ that may lead to accumulation of insoluble $A\beta_{(1-42)}$ and subsequent generation of ROS. However, accumulation of ROS and reactive nitrogen intermediates can cause cell death either by necrosis or programmed cell death. A role for oxidative stress in the induction of apoptosis is suggested by studies where the addition of low levels of ROS induce programmed cell death and the observation that various antioxidants such as N-acetylcysteine can inhibit cell death (for a review see Curin et al., 2002). A dynamic interaction between increased ROS and activation of programmed cell death has been shown to be dependent on the APP molecule. Binding of a monoclonal antibody that recognizes an epitope of 34 aminoacid residues in the extracellular domain of APP is followed by accumulation of surrogate markers of oxidative stress and subsequent activation of programmed cell death. Attenuation of cell death by the epitope used to raise the antibody or after administration of antioxidants and pan caspase inhibitors serve to demonstrate that APP itself may be linked to a transduction signaling pathway that eventually promotes increased oxidative stress and caspase activation followed by subsequent cell death (Rohn et al., 2000).

Chapter 2

Objectives

2.1 To determine the extent of colocalization of the caspase-3 cleaved APP fragment ($\alpha\Delta C^{csp}$ –APP) and Aβ amyloid peptide in autopsied Alzheimer's disease brains.

2.2 To determine whether caspase-3 cleaved spectrin occurs in specific populations of neurons in the cerebral cortices of Alzheimer's disease, and age-matched control autopsied brains.

2.3 To determine the role of caspase-3 and calpain activation in a model of cholinergic septohippocampal disconnection produced by transection of the fimbria-fornix pathway.

Chapter 3

Caspase-cleaved amyloid precursor protein in Alzheimer's disease

Carlos Ayala-Grosso*, Gordon NgØ, Sophie Roy § and George S RobertsonØ**
*Department of Pharmacology, McGill University, McIntyre Medical Sciences Building, 3655 Promenade Sir-William-Osler, Montreal H3G 1Y6, Canada, §Department of Biochemistry and Molecular Biology and ØDepartment of Pharmacology, Merck Frosst Centre for Therapeutic Research, C.P./ P.O. Box 1005, Pointe Claire, Dorval, Quebec, Canada H9R 4P8

Published in Brain Pathology (2002) 12(4):430-431

3.1 Abstract

Caspase-3 mediated cleavage of the amyloid precursor protein (APP) has been proposed as a putative mechanism underlying amyloidosis and neuronal cell death in Alzheimer's disease. We utilized an antibody that selectively recognizes the *neo* epitope generated by caspase-3 mediated cleavage of APP ($\alpha\Delta C^{csp}$–APP) to determine if this proteolytic event occurs in senile plaques in the inferior frontal gyrus and superior temporal gyrus of autopsied Alzheimer's disease and age-matched control brains. Consistent with a role for caspase-3 activation in Alzheimer's disease pathology, $\alpha\Delta C^{csp}$-APP immunoreactivity colocalized with a subset of TUNEL-positive pyramidal neurons in Alzheimer's disease brains. $\alpha\Delta C^{csp}$-APP immunoreactivity was found in neurons and glial cells, as well as in small and medium size particulate elements, resembling dystrophic terminals and condensed nuclei, respectively, in Alzheimer's disease and age-matched control brains. There were a larger number of $\alpha\Delta C^{csp}$–APP immunoreactive elements in the inferior frontal gyrus and superior temporal gyrus of subjects with Alzheimer's disease pathology than age-matched controls. $\alpha\Delta C^{csp}$–APP immunoreactivity in small and medium size particulate elements were the main component colocalized with 30% of senile plaques in the inferior frontal gyrus and superior temporal gyrus of Alzheimer's disease brains. In some control brains, $\alpha\Delta C^{csp}$ –APP immunoreactivity appeared to be associated with a clinical history of metabolic encephalopathy. Our results suggest that apoptosis contributes to cell death resulting from amyloidosis and plaque deposition in Alzheimer's disease.

3.2 Introduction

Amyloid plaques and neurofibrillary tangles that extend progressively to neocortical brain areas accompanied by an extensive synaptic and neuronal loss are prominent features of Alzheimer's disease (Cummings et al., 1998; Dekosky et al., 1999; Delacourte et al., 2000). Programmed cell death or apoptosis has been proposed as a mechanism of neuronal cell death in acute and chronic neurological diseases including stroke, Parkinson's disease, amyotrophic lateral sclerosis, frontotemporal dementia (FTD) and Alzheimer's disease (For review see Zheng et al., 2000; Nijhawan et al., 2000; Robertson et al., 2000; Mattson et al., 2001).

In Alzheimer's disease, a role for apoptosis is supported by studies linking Alzheimer's disease-associated genes such as APP, presenilin 1 and presenilin 2 with neuronal cell death. (Yamatsuji et al., 1996; Guo et al., 1997; Wolozin et al., 1996; Ivins et al., 1999; Pellegrini et al., 1999; for review see Neve et al., 2000). Mutations in the secretase cleavage sequences of APP generate recognition sites prone to cleavage by caspases enzymes (Gervais et al., 1999). Moreover, a caspase-cleaved APP proteolytic fragment called C31 that induces apoptosis in cell lines is elevated in Alzheimer's brains (Lu et al., 2000).

Apoptosis effectors such as, Bcl-2, Bcl-x, Bax, Bak and Bad, as well as cysteine proteases such as caspase-2 (ICH-1) and caspase-3 (CPP-32) have been found to be up-regulated in Alzheimer's disease (Kitamura et al., 1999; Masliah et al., 1998; Shimohama et al., 1999). In addition, a variety of proteins responsible for structural and metabolic integrity have been shown to be substrates for caspase-3, suggesting a key role for this primary cell death effector protease in neuronal apoptosis in Alzheimer's disease (Marks and Berg, 1999).

Senile plaques and neurofibrillary tangles as well as apoptotic-like mechanisms are present in Alzheimer's disease, but the question of whether these features are causally related to cell death remains an unresolved issue. DNA fragmentation assessed by TUNEL labeling has been observed in Alzheimer's disease brains (Su et al., 2001; Smale et al., 1995; Troncoso et al., 1996). However, despite large numbers of cells with DNA

fragmentation, only a few cells display the morphological characteristics of apoptosis such as membrane blebbing and chromatin condensation (Lassman et al., 1995; Troncoso et al., 1996; Lucassen et al., 1997), or labeling for the c-jun/activating protein-1 (apoptosis-specific protein) (Stadelmann et al., 1999). Furthermore, DNA fragmentation has also been observed in necrotic cells injured by oxidative damage (Tsang et al., 1996) or by postmortem autolysis (Stadelmann et al., 1999) indicating that this event is not a specific marker of apoptosis.

Increased expression of prostate apoptosis response-4 (Par-4) in a subset of neurons that show accumulations of abnormal tau protein is strong evidence that neuronal death in Alzheimer's disease may be due to apoptosis (Guo et al., 1998). Besides, colocalization of neurofibrillary tangles and caspase-cleaved fodrin proteolytic fragments as well as active caspase-3 have been recently reported in Alzheimer's disease brains (Rohn et al., 2001; Su et al., 1994). In contrast, several studies have reported a lack of colocalization between neurofibrillary tangles and putative apoptotic markers such as DNA fragmentation (Su et al., 1997; Bancher et al., 1997; Lassman et al., 1995). Furthermore, lack of active caspase-3 in Alzheimer's disease (Selznick et al., 1999) or exceptionally low numbers in Down syndrome (DS) autopsied brains (Stadelmann et al., 1998) suggest that a specific role for caspase activation in neuronal death in Alzheimer's disease is still unclear.

To further investigate whether caspase-cleaved APP is associated with the progression of amyloidogenesis in Alzheimer's disease, we utilized immunohistochemical methodologies to determine the extent of colocalization of the caspase-3 cleaved APP fragment ($\alpha\Delta C^{csp}$ –APP) and Aβ amyloid peptide in autopsied Alzheimer's disease brains. Caspase-3 dependent processing of APP has been proposed as a putative mechanism that may contribute to the amyloid burden and subsequent amplification of the apoptotic cascade in Alzheimer's disease (Gervais et al., 1999). If caspase activation contributes to Alzheimer's disease pathology by generating a pro-amyloidogenic fragment such as $\alpha\Delta C^{csp}$–APP, we reasoned that there should be an increase in $\alpha\Delta C^{csp}$–APP immunoreactivity associated with senile plaques in Alzheimer's disease brains.

We report here a significant association between $\alpha\Delta C^{csp}$–APP immunoreactive profiles and Alzheimer's disease pathology. Consistent with this finding, $\alpha\Delta C^{csp}$-APP immunoreactivity was present in a subset of pyramidal neurons in early or advanced stage of DNA fragmentation and chromatin condensation in some cases of Alzheimer's disease. In some age-matched control brains, elevated $\alpha\Delta C^{csp}$–APP immunoreactive elements were associated with a clinical history of metabolic encephalopathy rather than Alzheimer's disease. These results suggest that apoptosis may contribute to the widespread cell death that occurs in Alzheimer's disease.

3.3 Materiales and methods

3.3.1Antibodies

The antibody directed against the caspase-cleaved APP neo-epitope, CHGV**VEVD**, $\alpha\Delta C^{csp}$ –APP has been extensively characterized by Gervais et al. (1999). This antibody was used at a dilution of 1/2000. A monoclonal antibody directed against amyloid $A\beta_{(1-12)}$ was used at a concentration of 1/2000 as previously described by Grant et al. (2000). This antibody was kindly provided by A.C. Cuello (McGill University, Montreal, Canada). Glial fibrillary acidic protein (GFAP) was detected with a monoclonal antibody from Sigma Chemical Co. (St Louis, MO) and used at a dilution of 1/2400. Active caspase–3 immunoreactivity was detected using a polyclonal purified rabbit antibody from Pharmingen (San Diego, CA) at 1/2000. An enhanced Vectastain ABC Elite or ABC alkaline phosphatase kit was used from Vector Laboratories (Burlingame, CA) to visualize $\alpha\Delta C^{csp}$–APP, $A\beta_{(1-12)}$ positive senile plaques and GFAP immunoreactivities. All other chemicals were of reagent grade and obtained commercially.

3.3.2 Human brain tissue

Brain tissues from the inferior frontal gyrus (IFG) and superior temporal gyrus (STG) were obtained at autopsy from 31 subjects, 16 clinically diagnosed and identified histopathologically as having Alzheimer's disease (average age ± SEM = 84.6 ± 1.12 years, postmortem index mean 3.55 ± 0.76 h) and 15 age-matched non-demented control

subjects (81.9 ± 1.42 years; postmortem index = 2.34 ± 0.09 h). Braak and Braak staging (2) was based on Gallyas (7), silver-pyridin Campbell-Switzer (3) and Thioflavine S staining methods. The human brain tissue used in this study was provided by the Sun Health Research Institute, (Sun City, AZ). A demographic summary of these cases is presented in Table 3.1.

3.3.3 Immunoprecipitation of $\alpha\Delta C^{csp}$–APP from human brain

Tissue samples of the superior parietal cortex from at least 3 age-matched controls and 3 Alzheimer's disease cases were homogenized in lysis buffer containing 50 mM Tris-HCl pH 7.4 (Gibco), 1% nonidet-40 (Sigma), 2 mM EDTA (Gibco), a minicomplete protease inhibitor cocktail (Roche) and 1 mM caspase-3 inhibitor. The homogenates were centrifuged at 16000g (4°C) for 20 min. The supernatant was removed and precleared with protein A sepharose (Amersham) at 4°C for 1 h. Precleared extracts were incubated at 4°C in a circular rotator with $\alpha\Delta C^{csp}$–APP antibody and protein A. Next, the samples washed at least 4 times with lysis buffer.

Samples were electrophoresed on a 6% Tris-glycine gel (Novex) for 120 min (110 V) and electrically transferred to a nitrocellulose membrane (0.45 µm pore size) overnight. Blots were then incubated for 2h with the anti-APP monoclonal antibody 22C11 (Chemicon) (diluted 1/2000 in 5% non-fat milk) and incubated with antirabbit~horseradish peroxidase (Amersham), the immunoreactivity was detected with luminol (ECL, Amersham). Consistency of protein loading for each lane was verified by Ponceau red staining.

3.3.4. Immunohistochemistry

Autopsied brain tissues were snap frozen, cryostat sectioned at 10 µm of thickness, mounted on superfrost slides and stored at –80°C until staining. Tissue sections were post fixed in 4% paraformaldehyde buffered with sodium phosphate (0.1 M, pH 7.4) at 4°C for 5 min, then treated with 0.3% hydrogen peroxide in 100% methanol for 15 min at

RT, and permeabilized with PBS (0.01 M) containing 0.1% Triton X-100 at RT for 30 min.

Nonspecific sites were blocked with 0.05% bovine serum albumin for 15 min and with 15% normal goat serum for 30 min. Slides were then incubated with the primary antibody at 4°C overnight. Biotinylated secondary antibodies (Vector Labs) at a dilution of 1/200 were applied for 1 h at RT and immunoreactivity detected using diaminobenzidine (DAB) brown or alkaline phosphatase (AP) with DAB and AP substrate kits (Vector). No specific staining was detected on slides lacking the primary antibody. Slides from cases diagnosed with Alzheimer's disease as well as age-matched controls were routinely stained side by side in a single and double labeling paradigm using the same batch of antibodies.

We examined immunohistochemical labeling in cortical layers containing plaques and $\alpha\Delta C^{csp}$–APP immunoreactivity from 1-3 sections/brain sample. All histological and immunohistochemical images were acquired from a Zeiss Axioplan 2 microscope equipped with an Axiophoto 2 system adapted to a Sony 3 CCD DXC-950 color video camera. The video signal was routed via a Sony camera adaptor CMA-D2 into a microcomputer. Images were analyzed by a custom designed program implemented in Northern Eclipse, an image analysis system produced by Empix Imaging, Inc. (Mississauga, Ontario, Canada). Quantification of positive labeling was performed on longitudinal bands following a linear sampling pattern using a micrometer scale in the ocular as an external calibrator. Each determination represented the mean ± SEM of 20 measurements per brain section performed on different regions of the frontal and temporal cortices. The number of plaques and $\alpha\Delta C^{csp}$–APP profiles were counted over an area of 350 µm x 280 µm.

3.3.5. Tunel labeling

A modified version of the TUNEL method originally described by Gavrieli et al., 1992 was used in this study. In brief, free 3'OH DNA termini were labeled *in situ* with digoxigenin tagged nucleotides, which were then recognized by an anti-digoxigenin peroxidase antibody, that was visualized by bright field microscopy. TUNEL labeling

was performed according to the Apoptag Plus Peroxidase In Situ Apoptosis Detection Kit (Intergen Company, Purchase, NY). Once the TUNEL procedure was performed, slides were then blocked with 15% normal goat serum (Vector) and incubated with $\alpha\Delta C^{csp}$–APP antibody at 4°C overnight. Biotinylated secondary antibodies (Vector Labs) at a dilution of 1/200 were applied for 1 h at RT and immunoreactivity detected using diaminobenzidine (DAB) with a NovaRed kit (Vector). Slides from cases diagnosed with Alzheimer's disease as well as age-matched controls were routinely stained side by side in a single and double labeling paradigm using the same batch of antibodies.

3.3.6. Data analysis

$\alpha\Delta C^{Csp}$–APP immunoreactivity profiles appeared as multiple elements in Alzheimer's disease and aged–matched control brains. These elements consisted of particulates that were small ($\alpha\Delta C^{Csp}$–APPsp; 3 μm) or medium sized ($\alpha\Delta C^{Csp}$–APPmp; 6 μm) or neuronal ($\alpha\Delta C^{csp}$–APPn) in nature. These elements were either associated ($\alpha\Delta C^{csp}$–APPpl^{+}) or unassociated with senile plaques ($\alpha\Delta C^{csp}$–APPpl^{-}).

Analysis of variance (ANOVA) mixed design (two factor-within subjects, one factor-between subjects), was carried out to compare the mean density of $\alpha\Delta C^{csp}$–APPpl^{+}, $\alpha\Delta C^{csp}$–APPpl^{-}, $\alpha\Delta C^{csp}$–APPsp, $\alpha\Delta C^{csp}$–APPmp, and $\alpha\Delta C^{csp}$–APPn immunoreactive elements in the IFG and STG of Alzheimer's disease and age-matched control brains. A statistical test was considered significant at $P < 0.05$. Data analyses were performed using the SPSS statistical package (Version 10.0, 1998).

TABLE 3.1

Age-matched Control and Alzheimer's disease Case Demographic Information

Patient	Age	Sex	PMI (h)	ApoE	Braak Index	Neuropathological Diagnosis
C1-9710	79	M	2.00	3/3	I	Control
C2-9714	76	M	2.50	3/3	I	Control
C3-9717	78	M	2.66	3/3	I	Control
C4-9639	73	F	2.50	3/3	I	Control
C5-9702	81	M	2.75	3/3	I	Control
C6-9833	82	F	2.00	3/3	I	Control
C7-9914	86	M	2.50	3/3	I	Control/small numbers of senile plaques and tangles
C8-9750	88	F	2.15	Nd	I	Control/Alzheimer type II glia, consistent with metabolic encephalopathy. Incidental Lewy bodies.
C9-9613	85	F	2.75	3/3	II	Control/spasmodic dysphonia
C10-9745	79	F	2.00	3/3	II	Control/
C11-9834	73	F	2.00	3/3	II	Control/ Alzheimer type II glia, consistent with metabolic encephalopathy
C12-9746	86	M	2.00	Nd	III	Control/mild amyloid angiopathy, focal concentration of diffuse plaques, Incidental Lewy bodies.
C13-9753	91	M	2.66	Nd	III	Control/sparse neocortical neuritic plaques and numerous neurofibrillary tangles.
C14-9819	87	F	2.00	3/3	III	Control
C15-9807	85	M	2.66	3/3	III	Control/sparse neocortical neuritic plaques and neurofibrillary tangles.

AD1-9751	84	M	3.00	3/3	III	Early Alzheimer's disease
AD2-9818	91	F	2.16	3/3	III	Early Alzheimer's disease
AD3-9822	90	M	2.50	3/3	III	Alzheimer's disease
AD4-9921	86	M	3.33	3/3	IV	Alzheimer's disease
AD5-9701	78	F	2.50	3/3	IV	Early Alzheimer's disease
AD6-9605	87	F	2.00	3/3	V	Alzheimer's disease
AD7-9609	75	M	2.50	3/3	V	Alzheimer's disease/Cerebral amyloid angiopathy
AD8-9626	85	M	3.25	3/3	V	Alzheimer's disease/seizure disorder
AD9-9642	85	M	14.66	3/3	V	Alzheimer's disease
AD10-9707	87	F	2.50	2/2	V	Alzheimer's disease
AD11-9725	88	M	1.75	3/3	V	Alzheimer's disease
AD12-9727	77	F	4.00	2/3	V	Alzheimer's disease
AD13-9733	85	M	2.33	3/3	V	Alzheimer's disease
AD14-9805	88	M	4.00	3/3	V	Alzheimer's disease
AD15-9828	84	F	2.00	3/3	VI	Alzheimer's disease
AD16-9812	84	M	4.33	Nd	VI	Alzheimer's disease

PMI: Postmortem interval in hours; ApoE: Apolipoprotein genetic load: Nd: Not determined

3.4. Results

The caspase-cleaved APP *neo*-epitope antibody ($\alpha\Delta C^{csp}$-APP) has been extensively characterized *in vitro* by Gervais et al., (1999). In the present study, we detected caspase-cleaved APP proteolytic fragments in tissue extracts from parietal cortex of some cases of Alzheimer's disease but not in age-matched controls (Fig 3.1). The $\alpha\Delta C^{csp}$-APP antibody recognized a protein approximately 110 kDa in size that corresponds to the molecular weight of APP processed by active caspase-3 as was reported by Gervais etal., (1999). $\alpha\Delta C^{csp}$-APP (110 kDa) was predominant in 1 of three Alzheimer's disease cases selected from our sample population.

Densities of $\alpha\Delta C^{csp}$-APPmp and $\alpha\Delta C^{csp}$-APPsp immunoreactive elements were consistently higher in Alzheimer's disease that in age-matched control brains. $\alpha\Delta C^{csp}$-APPmp and $\alpha\Delta C^{csp}$-APPsp were round elements approximately 3 μm and 6 μm in diameter, respectively, with a size and morphologic appearance suggestive of dystrophic terminals and remnant nuclei (Fig 3. 2A).

In a few control brains, $\alpha\Delta C^{csp}$-APPmp and $\alpha\Delta C^{csp}$-APPsp immunoreactive elements were colocalized with diffuse plaques (Fig 3.2B). Occasionally, $\alpha\Delta C^{csp}$-APP immunoreactive pyramidal neurons were also found (results not shown). In Alzheimer's disease brains, $\alpha\Delta C^{csp}$-APPmp and $\alpha\Delta C^{csp}$-APPsp immunoreactive elements were predominantly located in the middle and/or the periphery of diffuse and dense-core senile plaques (Fig 3.3B, 3.3C) and associated with dystrophic neurites (Fig 3.3B). In addition, $\alpha\Delta C^{csp}$-APP immunoreactivity was found in neurons (Fig 3.2C, Fig 3.3A, 3.3B) and glial cells with astrocytic morphology (Fig 3.3A). In some Alzheimer's disease cases, $\alpha\Delta C^{csp}$-APP immunoreactivity was also colocalized with cell bodies containing intracellular Aβ (Fig 3.2D).

$\alpha\Delta C^{csp}$-APP immunoreactivity was detected in pyramidal neurons associated with dense-core senile plaques (Fig 3.4A). However, $\alpha\Delta C^{csp}$-APPmp and $\alpha\Delta C^{csp}$-APPsp immunoreactive elements were the most common features detected in senile plaques (Fig 3.4B). In some cases, $\alpha\Delta C^{csp}$-APP immunoreactivity was located in both neurons and GFAP positive cells in the absence of senile plaques (Fig 3.4C, 3.4D).

Counts of neuritic plaques associated or unassociated with caspase-3 cleaved APP immunoreactive profiles, as well as counts of $\alpha\Delta C^{csp}$-APPn, $\alpha\Delta C^{csp}$-APPmp and $\alpha\Delta C^{csp}$-APPsp immunoreactive components in the IFG and STG of Alzheimer's disease and age-matched controls are shown in Fig 3.5. The density of senile plaques was considerably greater in Alzheimer's disease brains than age-matched controls ($F = 71.97$, $df = 1$, $P < 0.0001$; Fig 3.5A). We found no difference in the number of neuritic plaques in the IFG and STG of Alzheimer's disease brains. In the IFG and STG of Alzheimer's disease patients, senile plaques that lacked $\alpha\Delta C^{csp}$-APP immunoreactive components ($\alpha\Delta C^{csp}$-APPpl$^-$) were significantly more numerous than senile plaques containing $\alpha\Delta C^{csp}$-APP immunoreactive components ($\alpha\Delta C^{csp}$-APPpl$^+$) ($F = 13.41$, $df = 1$, $P = 0.001$).

Overall, densities of $\alpha\Delta C^{csp}$-APPn, $\alpha\Delta C^{csp}$-APPmp and $\alpha\Delta C^{csp}$-APPsp immunoreactive elements were significantly higher in Alzheimer's disease patients with respect to age-matched controls ($F = 40.50$, $df = 1$, $P < 0.0001$; Fig 3.5B). Similar numbers of $\alpha\Delta C^{csp}$-APP immunoreactive elements were found in the IFG and STG of Alzheimer's disease brains. There was a positive association between $\alpha\Delta C^{csp}$-APP immunoreactive profiles and Alzheimer's disease pathology ($F = 14.88$, $df = 2$, $P = 0.0001$).

We found elevated numbers of $\alpha\Delta C^{csp}$-APPn, $\alpha\Delta C^{csp}$-APPmp, and $\alpha\Delta C^{csp}$-APPsp in the IFG of some control cases with Alzheimer type II glia consistent with metabolic encephalopathy (C8-9750, C11-9834). This suggests that caspase-3 cleaved APP fragments can be generated in Alzheimer's disease as a consequence of mechanisms that are independent of amyloidosis and plaque deposition.

By examining individual cases, we detected a remarkable elevation in the number of $\alpha\Delta C^{csp}$–APPn in some preclinical cases of Alzheimer's disease diagnosed with mild amyloid angiopathy and an assigned Braak and Braak index of III (C12-9746, C13-9753). In contrast, the number of $\alpha\Delta C^{csp}$-APPn in Alzheimer's disease brains was highly variable, and in some cases a few or no $\alpha\Delta C^{csp}$–APPn counts were observed, although these patients had been classified with a Braak and Braak index of V. These results suggest that $\alpha\Delta C^{csp}$-APP immunoreactivity is not correlated with the severity of pathology defined according to the Braak and Braak index. Furthermore, we found in

sections from Alzheimer's disease cases with elevated counts of $\alpha\Delta C^{csp}$–APPn, a lack of colocalization of $\alpha\Delta C^{csp}$–APPn with thioflavine S positive cells (results not shown), suggesting that neurofibrillary tangles and caspase-cleaved APP proteolysis may be independent events in Alzheimer's disease.

TUNEL positive cells were rarely observed in age-matched controls (Fig 3.6A). In contrast, we found a relatively high number of cells undergoing DNA fragmentation and chromatin condensation in Alzheimer's disease brains (Fig 3.6B, 3.6C arrows). Furthermore, we found that $\alpha\Delta C^{csp}$–APPn immunoreactivity colocalized with a subset of TUNEL-positive pyramidal cells (Fig 3.6B, 3.6D circles).

Counts of $\alpha\Delta C^{csp}$–APPpl^{-} were significantly more numerous than $\alpha\Delta C^{csp}$–APPpl^{+} in the frontal and temporal cortices of Alzheimer's disease brains. This result is consistent with the fact that approximately 70% of senile plaques in the IFG and STG of Alzheimer's disease brains did not contain $\alpha\Delta C^{csp}$–APP immunoreactivity.

In aged-matched control and Alzheimer's disease brains (C1-9710, AD6-9605, AD13-9733, AD14-9805) we observed intraneuronal $\alpha\Delta C^{csp}$–APP immunoreactivity. However, we found evidence for only weak active caspase-3 immunoreactivity in just a very few neuronal cell bodies in each of these cases (results not shown).

3.5. Discussion

In the present study, we examined the colocalisation of caspase-cleaved amyloid precursor protein ($\alpha\Delta C^{csp}$–APP) in neuritic plaques in the IFG and STG of Alzheimer's disease and age-matched control brains.

Our antibody specifically recognizes a 116 kDa proteolytic fragment extracted from human parietal cortex of Alzheimer's disease cases that corresponds with the predicted molecular weight of the caspase-cleaved amyloid precursor protein proteolytic fragment ($\alpha\Delta C^{csp}$–APP). This result is consistent with previous *in vitro* findings where activation of caspase-3, as a consequence of apoptotic stimuli, may generate a similar fragment from APP during execution of the cell death program. Furthermore, accumulation $\alpha\Delta C^{csp}$–APP is consistent with studies that have reported a significant

increase of caspase-cleaved fodrin (Rohn et al., 2001) and actin in Alzheimer's disease brains (Yang et al., 1998).

In several control cases that demonstrated elevated numbers of $\alpha\Delta C^{csp}$–APPmp immunoreactivity, there was an association with a clinical history of metabolic encephalopathy and stroke rather than Alzheimer's disease. Elevated $\alpha\Delta C^{csp}$ –APP immunoreactivity in sections of age-matched controls may be the result of Alzheimer type II glia consistent with metabolic encephalopathy (C8-9750, C11-9834). In addition to the progression of Alzheimer's disease pathology, a clinical history of ischemia (AD14-9805) may also contribute to elevated counts of $\alpha\Delta C^{csp}$ –APP immunoreactive components. Consistent with these findings, several reports have described elevated apoptosis in aged-conditions or in pathologies not related to Alzheimer's disease (Masliah et al., 1998; Selznick et al., 1999; Su et al., 1994).

In this study, $\alpha\Delta C^{csp}$–APP immunoreactivity colocalized with 30% of senile plaques in the IFG and STG of Alzheimer's disease brains. $\alpha\Delta C^{csp}$–APP immunoreactive small and medium size particulate elements were colocalized to a greater extent with early and mature plaques than in older dense-core plaques. These findings suggest that during the progression of Alzheimer's disease pathology, amyloidosis and plaque deposition may promote caspase activation that triggers neuronal cell death, resulting in the accumulation of $\alpha\Delta C^{csp}$–APP immunoreactive particulate elements in injured cells and dystrophic neurites. The clearance of $\alpha\Delta C^{csp}$–APP immunoreactive profiles from older plaques may be responsible for the low incidence of $\alpha\Delta C^{csp}$–APP labeling in dense-core plaques. An alternative explanation is that in late stages of Alzheimer's disease, multiple neuromodulatory mechanisms may be disturbed as a consequence of amyloid burden and neurofibrillary tangles that may potentially lead to cell death by both apoptotic and non-apoptotic mechanisms.

The mean counts of $\alpha\Delta C^{csp}$ –APPn were highly variable in Alzheimer's disease but they were more frequent in AD than age-matched control brains. In addition, we found a lack of colocalization between $\alpha\Delta C^{csp}$ –APPn and thioflavine S positive cells (results not shown). This finding is in agreement with reports indicating a mismatch between the distribution of TUNEL positive nuclei and senile plaques (Troncoso et al., 1996). Furthermore, it has been shown that amyloid burden is not correlated with either

cell loss or neurofibrillary tangles (Gomez-Isla et al., 1997). Therefore, the accumulation and subsequent deposition of amyloid Aβ peptide may be a risk factor rather than a primary mechanism of neurodegeneration in Alzheimer's disease.

We found a higher numbers of TUNEL-positive cells in Alzheimer's disease brains than age-matched controls. In addition, a subset of TUNEL-positive pyramidal cells colocalized with $\alpha\Delta C^{csp}$ –APP immunoreactivity. Mismatches between the estimates of TUNEL-positive cells and $\alpha\Delta C^{csp}$–APPn immunoreactive profiles suggests that DNA fragmentation and chromatin condensation assessed by TUNEL seem to follow a temporal course different from that for activation of caspase-3, one of the key steps in apoptotic cell death.

$\alpha\Delta C^{csp}$–APPmp and $\alpha\Delta C^{csp}$ –APPsp were the most frequent components in a subset of senile plaques containing $\alpha\Delta C^{csp}$–APP profiles. In these plaques, there may be at least three potential independent sources of $\alpha\Delta C^{csp}$–APP immunoreactivity: A) as a consequence of amyloidosis and plaque deposition as occurs in Alzheimer's disease; B) as a result of intracellular accumulation of Aβ; or C) subsequent to multiple local events occurring during senescence.

Our data support the hypothesis recently proposed by Terry (2000) in which a differential incidence in the cognitive impairment in AD may occur as a consequence of distinct pathological processes leading to the loss of synaptic and somatic neuronal components. Caspase-3 activation may produce localized synaptic loss and terminal dystrophy. For instance, $\alpha\Delta C^{csp}$–APPn, $\alpha\Delta C^{csp}$–APPmp and $\alpha\Delta C^{csp}$–APPsp immunoreactive elements may represent different stages of these events. This suggestion is supported by the detection of $\alpha\Delta C^{csp}$–APP immunoreactivity in neurons, and dystrophic neurites as well as in GFAP positive cells not associated with senile plaques. In the current study, an extensive accumulation of $\alpha\Delta C^{csp}$–APP immunoreactivity in neurons and glia in some cases of AD was not associated with senile plaques. This suggests that caspase activation occurs in multiple cellular components as discrete elements recruited by the amyloid burden in AD or in association with local pathologic events.

A role for glial cells in Alzheimer's disease pathology is supported by studies that describe increased Fas antigen (CD95) expression in astrocytes and in a

subpopulation of GFAP positive cells of Alzheimer's disease brains (Nishimira et al., 1995). Kitamura et al. (1997) have also shown an up-regulation of the tumor-suppressor protein p53 protein in glial cells of Alzheimer's disease subjects.

The major argument for apoptotic cell death in Alzheimer's disease is based primarily on an elevation of the number of cells with DNA fragmentation in Alzheimer's disease brains relative to age-matched controls (Su et al., 2001; Lassman et al., 1995; Lucassen et al., 1997; Smale et al., 1995; Stadelmann et al., 1999; Troncoso et al., 1996). There are, however, reservations about the notion that cells with DNA fragmentation are actually apoptotic. Neurons with DNA fragmentation in Alzheimer's disease do not show the classical morphological features of apoptosis, namely, chromatin condensation and nuclear fragmentation (Stadelmann et al. 1999, Perry et al., 1998). In our study, consistent with a role for caspase-3 activation in Alzheimer's disease pathology, $\alpha\Delta C^{csp}$–APP immunoreactivity colocalized with a subset of TUNEL positive pyramidal neurons in IFG and STG of Alzheimer's disease brains.

In the present study, we did not detect active caspase-3 in Alzheimer's disease brains, although we found weak active caspase-3 like-immunoreactivity around plaques and some neuronal cell bodies in both Alzheimer's disease and age-matched control as described by Su et al. (2001). This may be due to the fact that active caspase-3 has a shorter half-life than caspase-cleaved proteolytic fragments such as $\alpha\Delta C^{csp}$ –APP (Gervais et al., 1999).

In two studies, active caspase-3 immunoreactivity has been recently reported in AD brains (Stadelmann et al., 1999; Su et al., 1994). However, the number of active caspase-3 positive cells was not consistent in these two studies. Stadelmann et al. (1999) reported an exceptionally low number of active caspase-3 positive cells in sections from Alzheimer's disease and DS brains. Furthermore, a lack of colocalization of active caspase-3 with hyperphosphorylated tau was also found. In contrast, Su et al. (2001), using the same antibody (CM1) that recognizes the p18 kDa component of active caspase-3 enzyme, have reported a significantly elevated number of active caspase-3 positive cells in Alzheimer's disease brains colocalized with hyperphosphorylated tau. The explanation for these discrepancies is beyond the scope of the present study. However, differences in tissue processing (paraffin embedding versus post-fixed free-

floating fresh frozen tissue) and counting methods may have contributed to these discrepant findings. Furthermore, Zheng et al. (2000) have recently reported a lack of specificity of the CM1 antibody for active caspase-3 enzyme as a result of cross-reactivity with active caspase-6. These findings suggest that the presence of active caspase-3 in neurodegenerative pathologies such as Alzheimer's disease remain to be convincingly shown.

Our study provides evidence of caspase-dependent proteolytic events during aging and AD pathology. We concluded that an accumulation of caspase-3 cleaved APP proteolytic fragments occurs in multiple cellular components in Alzheimer's disease. This suggests that caspase activation may contribute to cell death in Alzheimer's disease. However, whether activation of caspases initiates cell death in Alzheimer's disease remains to be determined.

3.6. Acknowledments

We wish to thank Francois Gervais (Merck-Frosst Centre for Therapeutic Research) for kindly providing the $\alpha\Delta C^{csp}$-APP antibody and Kevin Clark (Merck-Frosst Centre for Therapeutic Research) for assistance with the figures. We are also grateful to A.C. Cuello (McGill University) for providing the $A\beta_{(1-12)}$ antibody. We are particularly indebted to the Sun Health Research Institute for providing us with Alzheimer's and aged-matched control brain sections for immunohistochemical analysis. C. Ayala-Grosso is a fellow of Consejo de Desarrollo Científico y Humanístico de la Universidad Central de Venezuela.

Figure 3.1. Immunoprecipitation of the caspase-cleaved amyloid precursor protein ($\alpha\Delta C^{csp}$-APP) proteolytic fragment from human brain. Tissue extracts of Parietal cortex from age-matched controls and Alzheimer's disease patients were incubated 24 h at 4°C with the $\alpha\Delta C^{csp}$-APP polyclonal antibody and protein A. Proteins immunoprecipitated were separated by sodium dodecyl-sulfate-polyacrylamide gel electrophoresis, transferred to nitrocellulose, and probed with the holo-amyloid precursor protein 22C11 monoclonal antibody. A prominent band at 116 kDa was detected in an Alzheimer's disease brain extract.

FIGURE 3.1

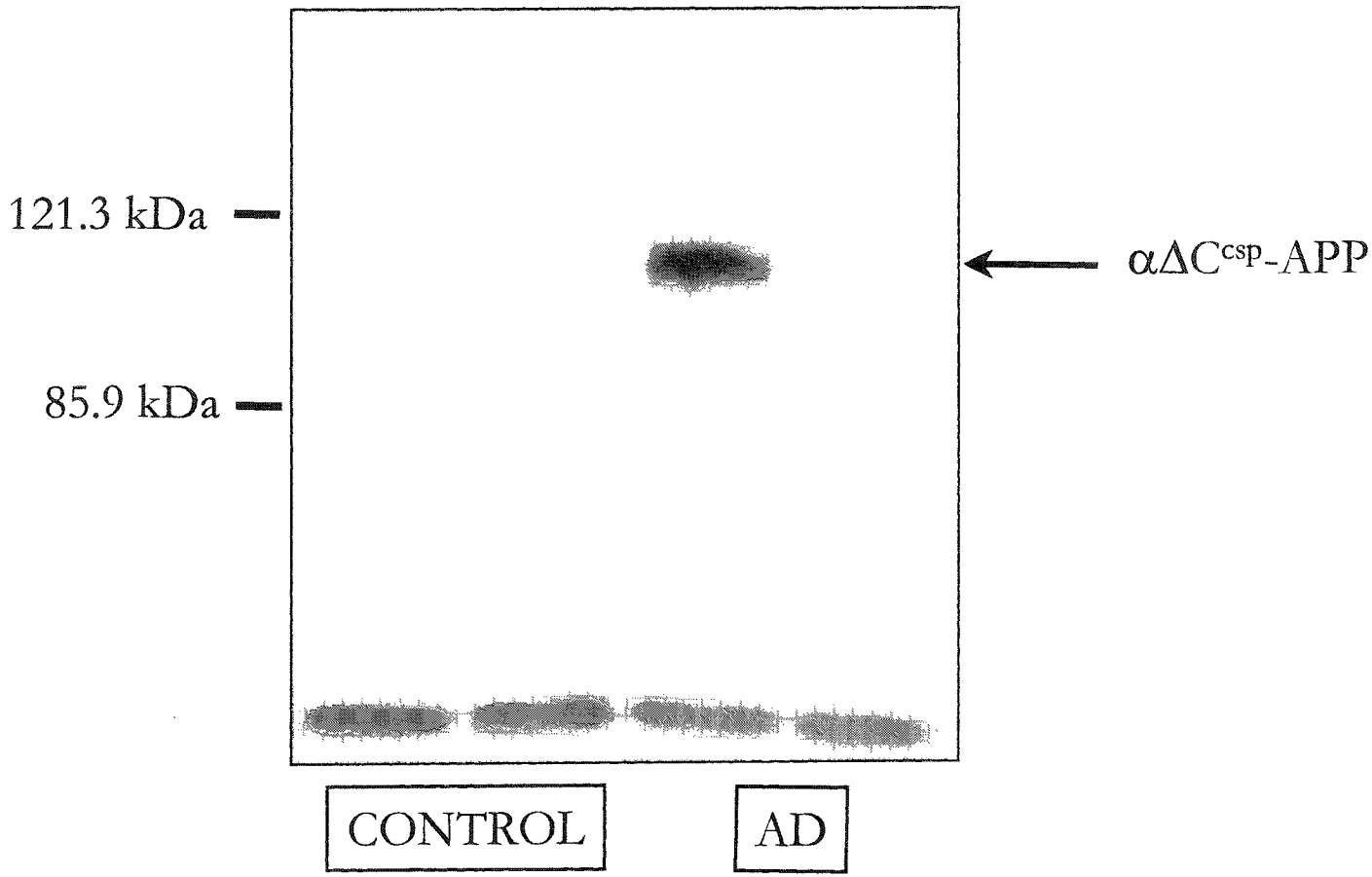

Fig 3.2. In age-matched control brains, small ($\alpha\Delta C^{csp}$-APPsp, 3 μm, circle) and medium ($\alpha\Delta C^{csp}$-APPmp, 6 μm, arrow) sized immunoreactive particulate elements were detected in a sparsely distributed fashion in the neuropile of all laminae of the frontal cortex (A), and in some diffuse amyloid plaques (B). In Alzheimer's disease brains, pyramidal neurons were detected with the $\alpha\Delta C^{csp}$-APP antibody (C, arrow), and in some cases $\alpha\Delta C^{csp}$-APP immunopositives pyramidal neurons were found colocalized with intracellular Aβ (D, arrow). Scale bar = 50 μm

FIGURE 3.2

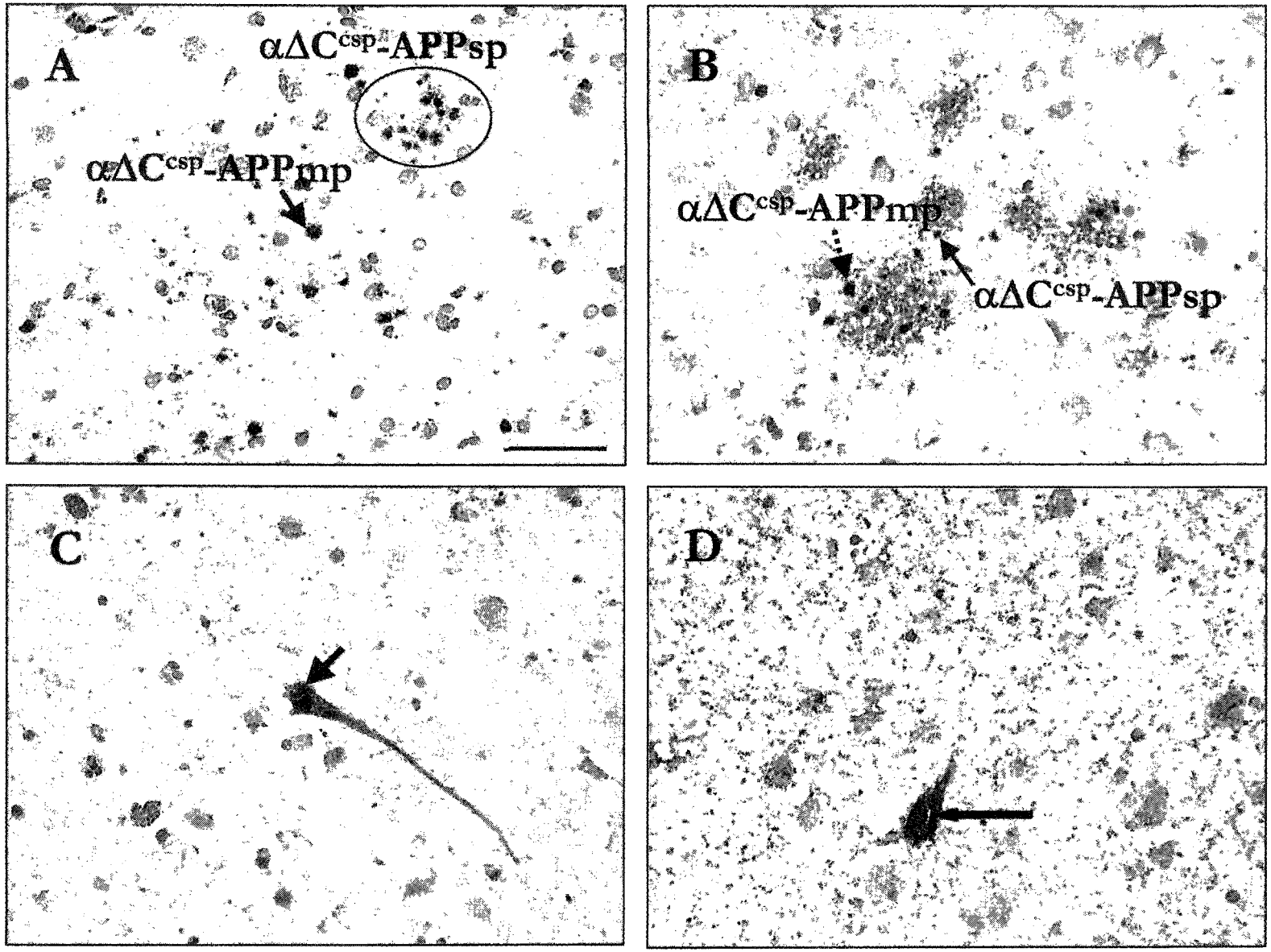

Figure 3.3 In Alzheimer's disease brains, $\alpha\Delta C^{csp}$-APP immunoreactivity was found in the cytoplasm of multipolar neurons (circle) or astroglia (arrow) (A). $\alpha\Delta C^{csp}$-APP immunoreactive medium and small particulate elements were associated with remnant nuclei (B, broken arrows) and dystrophic neurites, respectively (B, arrow). $\alpha\Delta C^{csp}$-APP immunoreactive small particulates were also found in the middle and/or the periphery of diffuse plaques (B, C, D, circles) and in dense-core senile plaques (C, arrow). $\alpha\Delta C^{csp}$-APP immunoreactivity was also associated with and in the cytoplasm of neuronal cells as a component of granulovacuolar deposits (D, arrow). Scale bar = 50 μm

FIGURE 3.3

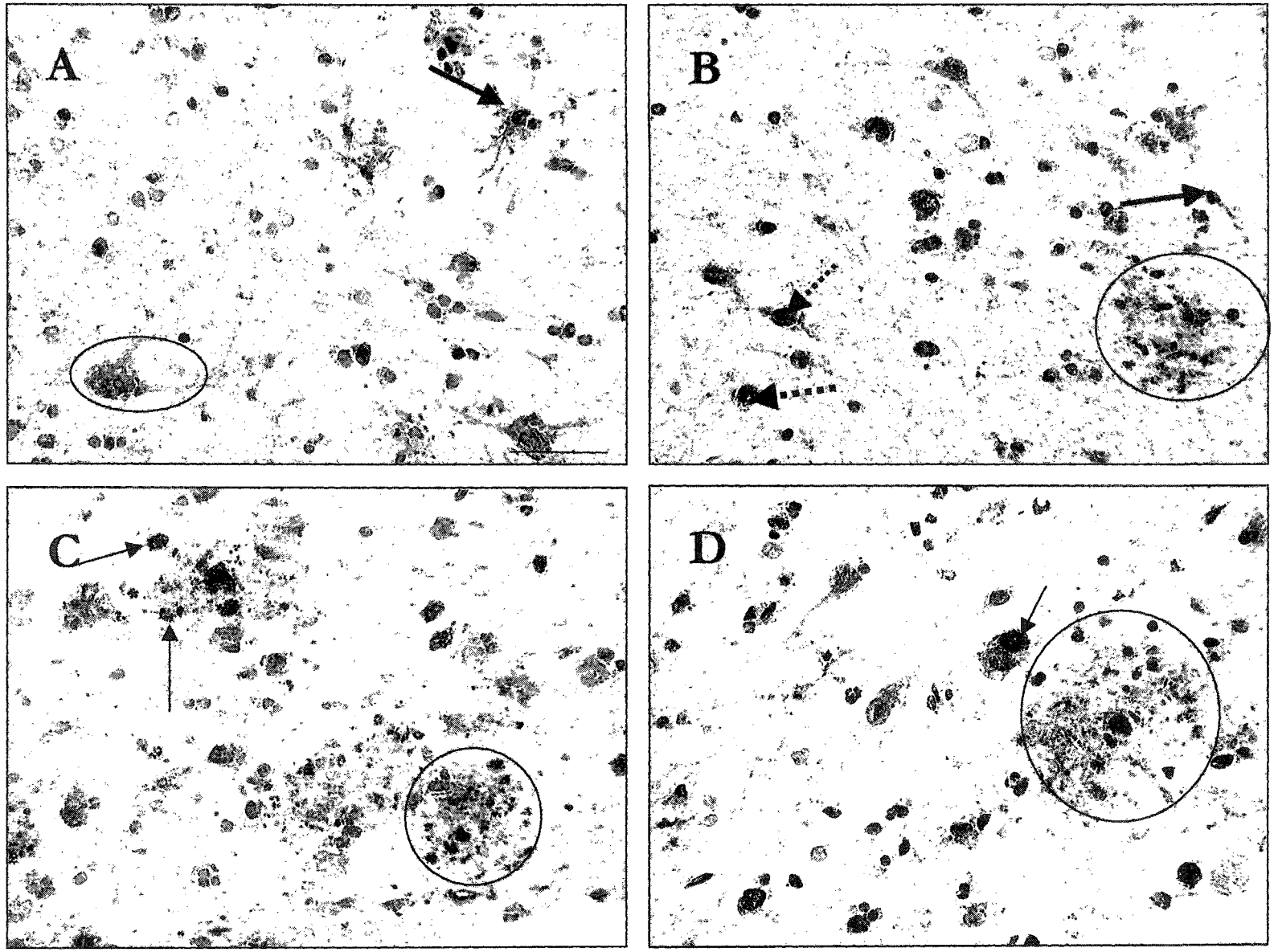

Figure 3.4. In Alzheimer's disease brains, $\alpha\Delta C^{csp}$-APP immunoreactivity was detected in pyramidal neurons of the temporal cortex associated with some dense-core senile plaques (A, arrow), as well as in neurons (C, arrow) and GFAP positive cells (D, arrows) unassociated with senile plaques. $\alpha\Delta C^{csp}$-APPsp and $\alpha\Delta C^{csp}$-APPmp immunoreactivities were the main components found in mature non dense-core senile plaques (B, arrows). Scale bar = 50 μm

FIGURE 3.4

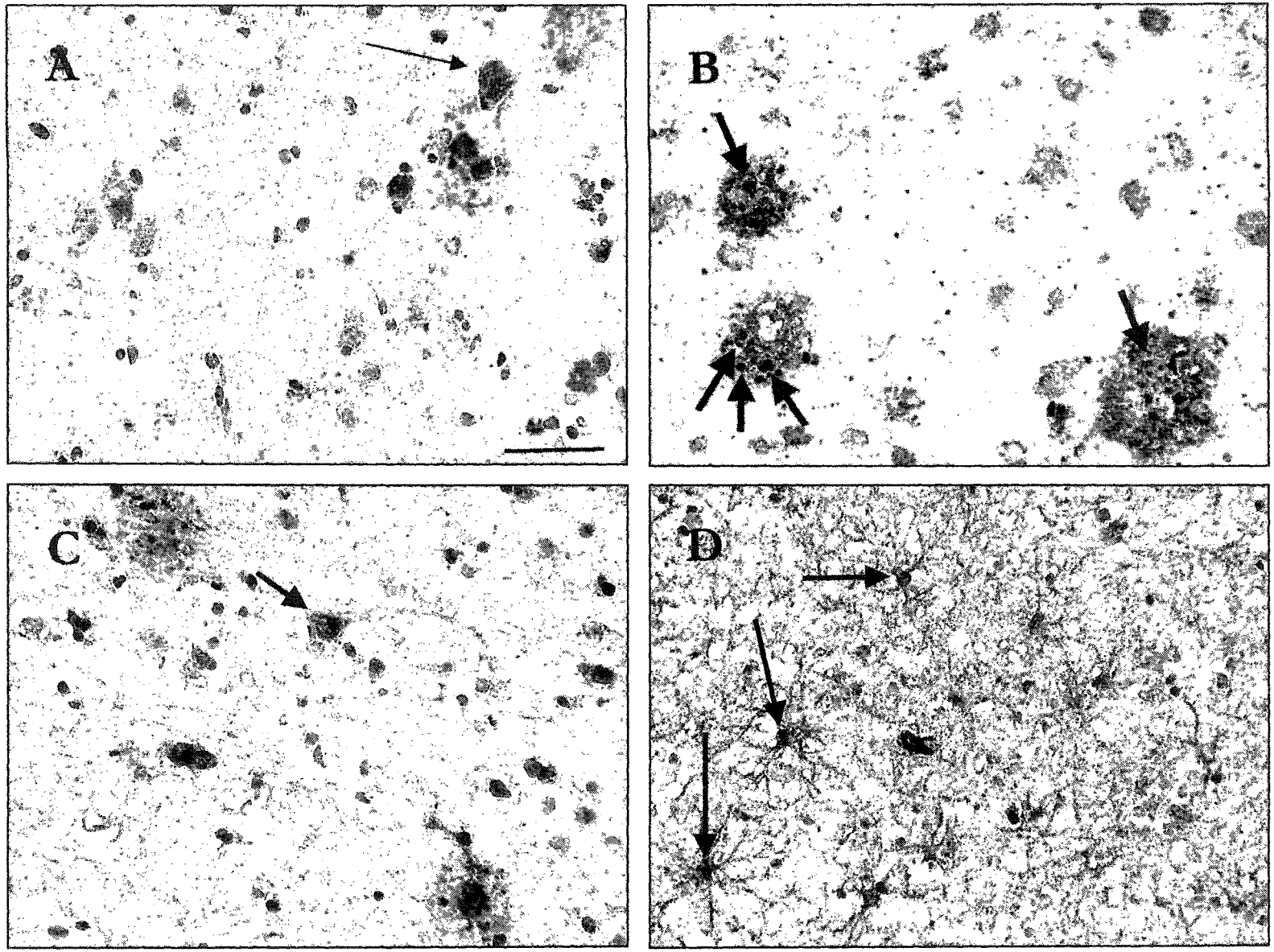

Figure 3.5. Counts (mean ± SEM) of senile plaques and $\alpha\Delta C^{csp}$-APP immunoreactive elements in the inferior frontal gyrus and superior temporal gyrus of age-matched control (n = 12) and Alzheimer's disease (n = 14) brains. Densities of senile plaques associated ($\alpha\Delta C^{csp}$-APPpl^{+}) or unassociated ($\alpha\Delta C^{csp}$-APPpl^{-}) with $\alpha\Delta C^{csp}$-APP immunoreactive profiles are shown in Fig 5A. Seniles plaques were significantly elevated in Alzheimer's disease with respect to age-matched control brains ($F = 71.97$, $df = 1$, $^{*}P < 0.0001$). In Alzheimer's disease brains, senile plaques unassociated with $\alpha\Delta C^{csp}$-APP were significantly higher with respect to senile plaques associated with $\alpha\Delta C^{csp}$-APP ($F = 13.41$, $df = 1$, $^{**}P = 0.001$). Counts of $\alpha\Delta C^{csp}$-APPn, $\alpha\Delta C^{csp}$-APPmp, and $\alpha\Delta C^{csp}$-APPsp immunoreactive profiles are shown in Fig 5B. Overall, there was an elevated number of $\alpha\Delta C^{csp}$-APP immunoreactive profiles in Alzheimer's disease with respect to age-matched control brains ($F = 40.57$, $df = 1$, $^{*}P < 0.0001$). A significant association between $\alpha\Delta C^{csp}$-APP immunoreactive profiles with Alzheimer's disease was determined ($F = 14.89$, $df = 2$, $P = 0.0001$).

FIGURE 3.5A

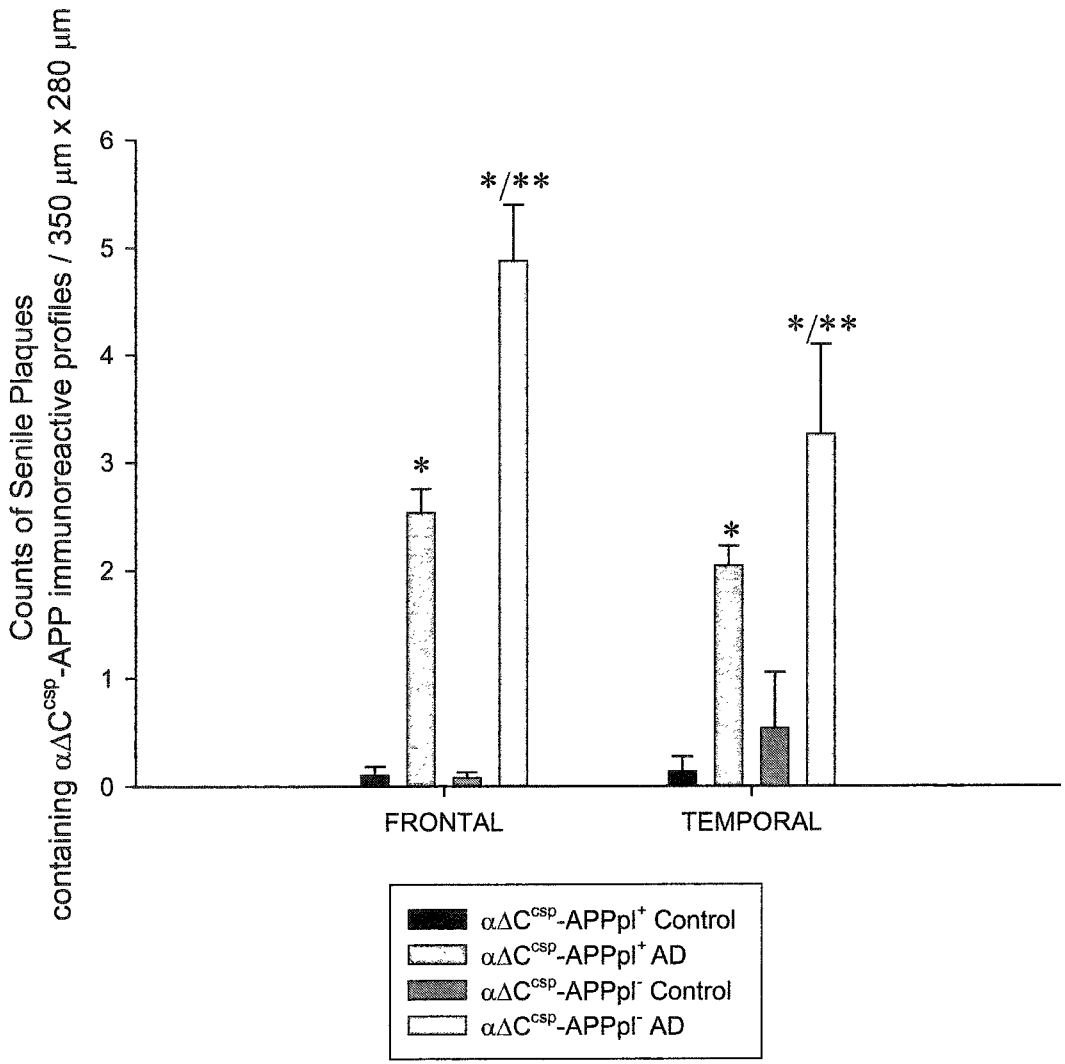
Counts of Senile Plaques
containing αΔC^csp-APP immunoreactive profiles / 350 µm x 280 µm
0
1
2
3
4
5
6
*
*/**
*
*/**
FRONTAL
TEMPORAL
αΔC^csp-APPpl+ Control
αΔC^csp-APPpl+ AD
αΔC^csp-APPpl- Control
αΔC^csp-APPpl- AD

FIGURE 3.5B

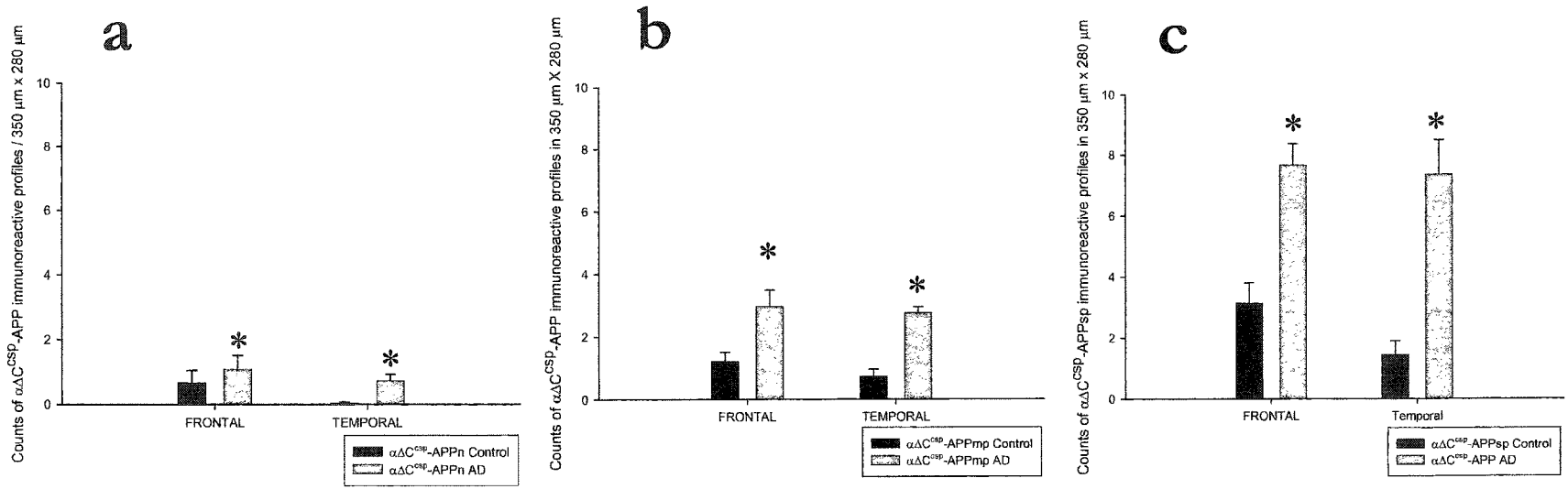
a
Counts of αΔC^CSP-APP immunoreactive profiles / 350 µm x 280 µm
10
8
6
4
2
0
FRONTAL
TEMPORAL
αΔC^CSP-APPn Control
αΔC^CSP-APPn AD
b
Counts of αΔC^CSP-APP immunoreactive profiles in 350 µm X 280 µm
FRONTAL
TEMPORAL
αΔC^CSP-APPmp Control
αΔC^CSP-APPmp AD
c
Counts of αΔC^CSP-APPsp immunoreactive profiles in 350 µm x 280 µm
FRONTAL
Temporal
αΔC^CSP-APPsp Control
αΔC^CSP-APP AD

Figure 3.6. In age-matched control brains, we rarely found TUNEL-positive cells (A) Scale bar = 50 μm. In contrast, in Alzheimer's disease brains we found a significant higher number of TUNEL-positive cells (B, C, D, arrows). We found $\alpha\Delta C^{csp}$-APP immunoreactivity in a subset of pyramidal neurons of the temporal cortex colocalized with TUNEL-positive labeling (B, C, D, circles). Chromatin condensation can be seen in a neuron (D, circle, broken arrow). Scale bar in D = 50 μm

FIGURE 3.6

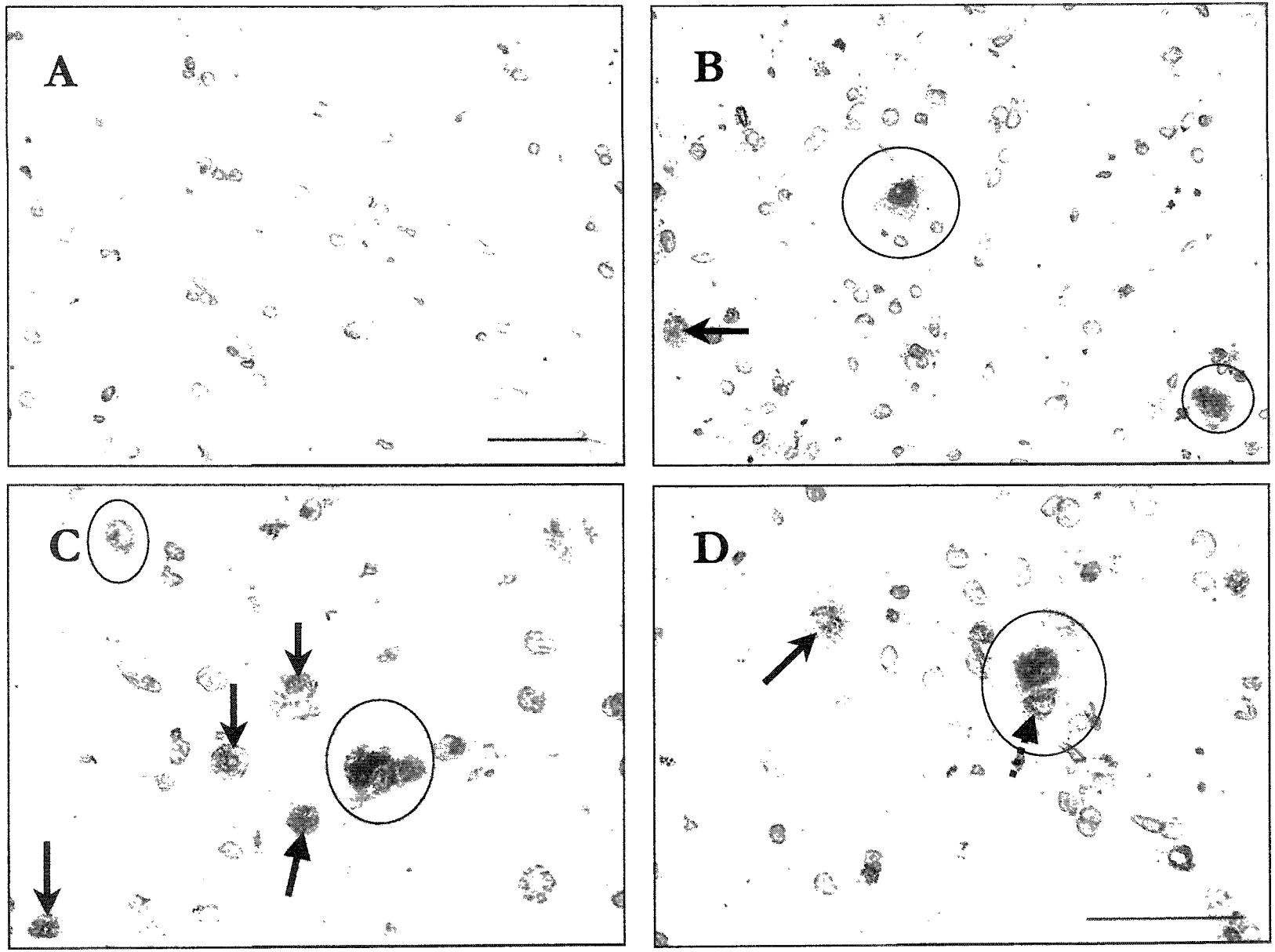

Connecting Text

The previous study provided evidence that the caspase-3 cleaved APP proteolytic fragment accumulates in Alzheimer's disease brain tissues. We observed a variety of immunoreactive elements associated with neurons and astroglial cells as well as in extracellular deposits ressembling dystrophic neurites associated with senile plaques or spare in the neuropil suggesting discrete events of programmed cell death. We inferred that activation of caspases may occurs in cell bodies as well as in synaptic compartments as a consequence of stimuli triggering activation of caspase cascade. Thus, using a caspase-3 cleaved spectrin neo-epitope antibody we decided to investigate whether spectrin, a cytoskeletal protein, was differentially accumulated in Alzheimer's disease brains.

Chapter 4

Caspase-3 activation in SMI-32 immunoreactive cortical pyramidal neurons is an early event underlying corticocortical disconnection in Alzheimer's disease

Carlos Ayala-Grosso[1], John Tam[2], Sophie Roy[2], Steven Xanthoudakis[2], Donald W Nicholson[2] and George S Robertson[3]

[1]Department of Pharmacology, McGill University, McIntyre Medical Sciences Building, 3655 Promenade Sir-William-Osler, Montreal H3G 1Y6, Canada

[2]Department of Biochemistry and Molecular Biology, Merck Frosst Centre for Therapeutic Research C.P./ P.O. Box 1005, Pointe Claire, Dorval, Quebec, Canada H9R 4P8

[3]Department of Psychiatry and Pharmacology, Sir Charles Tupper Medical Building, 5850 College Street, Halifax, Nova Scotia, B3H 1X5, Canada

4.1 Abstract

Corticocortical disconnection in Alzheimer's disease occurs by the progressive impairment and eventual loss of a small subset of pyramidal neurons in layers III and V of association areas of the neocortex that exhibit large somatic size, extensive dendritic arborization and high contents of nonphosphorylated neurofilaments of medium and high molecular weight that can be identified using a monoclonal SMI-32 antibody. It is thought that the accumulation of amyloid Aβ and neurofibrillary tangles may provoke metabolic disturbances that result in dysfunction of these SMI-32 immunoreactive neurons. The recent detection of increased levels of caspase-3 cleaved fodrin in fontal, temporal and parietal association areas in Alzheimer's disease brains suggests that programmed cell death may contribute to the destruction of SMI-32 positive neurons. In the present study, we utilized an antibody that selectively recognizes the 120 kDa breakdown product of αIIspectrin (fodrin) generated by caspase-3 to determine whether this protease is activated in vulnerable pyramidal neurons located in layers III and V of Alzheimer's disease brains. Consistent with the preferentialy impairment of SMI-32 neurons in Alzheimer's disease, neurons immunoreactive for caspase-3 cleaved αIIspectrin were located predominantly in layers III and V of the inferior frontal and superior temporal cortices of patients with Alzheimer's disease but not age-matched controls. Pyramidal neurons immunoreactive for caspase-3 cleaved αIIspectrin invariably displayed SMI-32 immunoreactivity suggesting that caspase-3 activation is an early pathological event in Alzheimer's disease. These findings suggest that caspase-3 activation is an early pathological event that may be responsible for the loss of a subset of pyramidal neurons that comprise coticocortical projections.

4.2. Introduction

Alzheimer's disease is the most common cause of dementia in the elderly and affects more than 12 million individuals worldwide (Cummings and Cole, 2002). Disease progression is characterized by a global decline of cognitive function that is accompanied by brain atrophy that spreads from the temporal and limbic cortices into frontal and occipital brain regions but spares sensorimotor cortices (Deweer et al., 1995; Juottonen et al., 1998; Janke et al., 2001; Scahill et al; 2002; Thompson et al., 2003). In Alzheimer's disease, brain atrophy may result from either a shrinkage or loss of neurons, axons and dendrites (for review McEwen, 1997; Uylings and Brabander, 2002). Neuronal shrinkage, as determined by morphometric analysis of neurons in the basal forebrain and neocortex, is correlated with cognitive decline in Alzheimer's disease (Rinne et al., 1987; Vogels et al., 1990; Salehi et al., 1994; Regeur et al., 1994). However, a reduction in the number of pyramidal neurons also occurs in Alzheimer's disease (Shefer, 1973; Colon, 1973). It has been estimated that there is about a 45% loss of large pyramidal neurons in the superior temporal and mid-frontal gyri in patients that have died with advanced Alzheimer's disease (Terry et al., 1981; Brun and Englund, 1981; Mann et al., 1985; Hubbard and Anderson, 1985; West et al. 1994; Gomez-Isla et al., 1997). Taken together, these findings indicate that pyramidal neurons in association cortical areas are highly vulnerable in Alzheimer's disease.

The precise causes of neuronal death in Alzheimer's disease are not clear. Early studies on the role of programmed cell death in Alzheimer's disease consisted largely of the *in situ* detection of fragmented DNA by terminal deoxynucleotidyl transferase-mediated deoxyuridine tryphosphate nick end-labeling (TUNEL) (Smale et al., 1995; Troncoso et al 1996; Su et al., 2001). Despite the fact that these studies detected a large numbers of neurons with DNA fragmentation, only a few of these cells displayed the morphological characteristics of apoptosis such as membrane blebbing and chromatin condensation or labeling for the c-jun/activating protein-1 (apoptosis-specific protein) (Lassman et al., 1995; Troncoso et al., 1996; Lucassen et al., 1997; Stadelmann et al., 1999). Although some investigators have reported the co-localization of neurofibrillary tangles and active caspase-3 in Alzheimer's disease brains (Su et al., 1994; Rohn et al.,

2001), the exceptionally small number of neurons that display active caspase-3 in Down syndrome autopsied brains as well as the lack of co-localization between neurofibrillary tangles and putative apoptotic markers such as DNA fragmentation and active caspase-3 has cast doubt on a principal role for caspase activation in neuronal death in Alzheimer's disease (Lassman et al., 1995; Su et al., 1997; Bancher et al., 1997; Stadelmann et al., 1998; Selznick et al., 1999; Ayala-Grosso et al., 2002).

Accumulation of caspase-3 generated proteolytic fragments of cytoskeletal proteins such as actin, αII-spectrin (fodrin), and tau (Yang et al., 1998; Rohn et al, 2001; 2002; 2003) or amyloid precursor protein (APP) (Gervais et al., 1999; Lu et al., 2000; Ayala-Grosso et al., 2002; Su et al., 2002) have been proposed as surrogate markers of programmed cell death in Alzheimer's disease. In the present study, we have utilized antibodies that selectively recognize the N-terminus *neo* epitope generated by caspase-3 from αII-spectrin ($\alpha\Delta N^{caspase}$-αIIspectrin), to determine whether this proteolytic event occurs in specific populations of neurons in the cerebral cortices of Alzheimer's disease and age-matched control autopsied brains. Consistent with a role for caspase-3 activation in Alzheimer's disease pathology, we observed a larger number of $\alpha\Delta N^{caspase}$–αIIspectrin immunoreactive neurons in the inferior frontal gyrus and superior temporal gyrus of subjects with Alzheimer's disease pathology than age-matched controls. Furthermore, $\alpha\Delta N^{caspase}$-αIIspectrin immunoreactivity was colocalized with a subset of non-phosphorylated neurofilament (SMI-32) bearing-pyramidal neurons in lamina III and V in the inferior frontal gyrus and superior temporal gyrus of autopsied Alzheimer's disease brains. We found a significant reduction in the choline acetyl transferase activity in these brain regions of Alzheimer's disease patients indicative of a loss of cholinergic efferents in these association areas of the neocortex. Localization of $\alpha\Delta N^{caspase}$–αIIspectrin immunoreactivity in SMI-32 immunopositive neurons suggests that activation of caspase-3 is an early pathological event in Alzheimer's disease that precedes the interstitial accumulation of amyloid Aβ or intracellular deposition of phosphorylated neurofilaments and likely tau protein in pyramidals neurons responsible of cortico-cortical projections from association areas of the brain.

4.3. Materiales and methods

4.3.1 Antibodies

The antibody directed against the epitope SVEALI ($\alpha\Delta N^{caspase}$–αIIspectrin) found in the 120 kDa proteolytic fragment of caspase-3 cleaved αIIspectrin was generated following procedures described by Bahr et al. (1995) and Rohn et al. (2001). This antibody was used at a dilution of 1/200. Monoclonal antibodies directed against neurofilaments of medium and high molecular (SMI-32) (Stenberger, Mar. USA) or amyloid $A\beta_{(1-12)}$ (kindly provided by A.C. Cuello (McGill University, Montreal, Canada) were used at concentrations of 1/1000 and 1/2000, respectively. MAB1622 (Chemicon, CA, USA) a monoclonal antibody that recognizes the full-length non erythroid αIIspectrin cytoskeletal protein, as well as the 150 kDa and 120 kDa proteolytic fragments of this protein generated by caspase-3 was used at a concentration of 1/1000. An enhanced Vectastain ABC Elite or ABC alkaline phosphatase kit was used from Vector Laboratories (Burlingame, CA) to visualize, $\alpha\Delta N^{caspase}$–αIIspectrin imunoreactivity, SMI-32 positive cells and $A\beta_{(1-12)}$ positive senile plaques. All other chemicals were of reagent grade and obtained commercially.

4.3.2. Human brain tissue

Brain tissues from the inferior frontal gyrus (IFG), superior temporal gyrus (STG) and superior parietal gyrus (SPG) were obtained at autopsy from 12 subjects: 6 clinically diagnosed and identified histopathologically as having Alzheimer's disease (average age ± SEM = 84.6 ± 1.12 years, postmortem index mean 2.18 ± 0.14 h) and 6 age-matched non-demented control subjects (78.66 ± 1.68 years; postmortem index 2.48 ± 0.13 h). Braak and Braak (1991) staging was based on Gallyas (1971), silver-pyridin Campbell-Switzer (1987) and Thioflavine S staining methods. The human brain tissue used in this study was provided by the Sun Health Research Institute, (Sun City, AZ). A demographic summary of these cases is presented in Table 4.1.

4.3.3. Characterization of the caspase-3 cleaved αIIspectrin *neo*-epitope antibody using a rat and human cell-free system

To validate the selectivity of the $\alpha\Delta N^{caspase}$-αIIspectrin antibody, a series of *in vitro* experiments were undertaken beginning with assessment of the ability of this antibody to recognize caspase-3 cleaved proteolytic fragments of fodrin after digestion with recombinant caspase-3 in a cell-free system. Human superior parietal cortex, rat cortex or rat dorsal hippocampus were homogenized in extraction buffer (50 mM Tris pH 7.5, 2 mM EDTA, 1% NP-40) and centrifuged at 13000x g for 10 min at 4°C. The resulting supernatants were used as brain extracts. The ratio of wet brain tissue/extraction buffer was exactly 1:10. Protein concentrations in extracts from tissue homogenates were determined by bincichonic acid microprotein assays (Pierce Inc., Rockford, Il, USA) with bovine serum albumin as a standard. Tissue extracts (200μg of protein) were incubated in a reaction buffer (50 mM HEPES, pH 7.4, 100 mM NaCl, 1 mM EDTA, 10% glycerol, 0.1% CHAPS, 10 mM DTT) and incubated with or without 118 nM of active recombinant caspase-3 for 2.5 h at 37°C.

Protein balanced samples were prepared for sodium dodecyl sulfate-polyacrylamide gel electrophoresis (SDS-PAGE) in six-fold loading buffer containing 0.25 M Tris (pH 6.8), 0.2 M DTT, 8% SDS, 0.02% bromophenol blue, and 20% glycerol in distilled H_2O. Samples were heated for 5 min at 95°C. Forty-five micrograms of protein per lane were routinely resolved by SDS-PAGE on 6% or 4-20% tris/glycine gels for 2 h at 110 V.

Following electrophoresis, separated proteins were laterally transferred to nitrocellulose membranes (0.45 μm) in a transfer buffer containing 0.192 M glycine and 0.025M Tris (pH 8.3) with 10% methanol at a constant voltage (100 V) for 1 h at 4°C. Ponceau Red (Sigma, St Louis, Mo, USA) staining was used to confirm successful transfer of protein, and to ensure that an equal amount of protein was loaded in each lane. Blots containing protein from human superior parietal cortex, rat cortex or rat dorsal hippocampus were blocked for 1 h at room temperature (RT) in 5% non-fat milk in TBS and incubated with the $\alpha\Delta N^{caspase}$-αIIspectrin antibody (1/200 dilution) in 5% non-fat

milk for 2 h at RT. Matched tissue extracts treated with recombinant caspase-3 were run in parallel and subsequently incubated at the same conditions as before with MAB1622 (1/1000 dilution). After incubation, blots were washed with 2 to 3 times with Tris buffer solution for 10 min. The blots were subsequently incubated for 1 h at room temperature with 5% non-fat milk containing a horseradish peroxidase-conjugated goat anti-mouse IgG, goat anti-rabbit IgG (each diluted 1/5000). Enhanced chemiluminiscence (Supersignal, Pierce) reagents were used to visualize immunolabeling on Kodak Biomax ML film.

4.3.4. Immunoprecipitation of caspase-3 cleaved αIIspectrin from Human Brain

Tissue samples of the superior parietal gyrus (SPG) from at least 4 age-matched controls and 4 Alzheimer's disease cases were homogenized in lysis buffer containing 50 mM Tris-HCl pH 7.4 (Gibco), 1% nonidet-40 (Sigma), 2 mM EDTA (Gibco), a minicomplete protease inhibitor cocktail (Roche) and 1 mM caspase-3 inhibitor. The homogenates were centrifuged at 16000x g (4°C) for 20 min. The supernatant was removed and precleared with protein A sepharose (Amersham) at 4°C for 1 h. Precleared extracts were incubated at 4°C in a circular rotator with $\alpha\Delta N^{caspase}$–αIIspectrin antibody and protein A. Next, the samples were washed at least 4 times with lysis buffer. Samples were electrophoresed on a 6% Tris-glycine gel (Novex) for 120 min (110 V) and electrically transferred to a nitrocellulose membrane (0.45 μm pore size) overnight. Blots were then incubated for 2h with the αIIspectrin monoclonal antibody MAB1622 (diluted 1/1000 in 5% non-fat milk) and incubated with anti-mouse~horseradish peroxidase (Amersham), the immunoreactivity was detected with luminol (ECL, Amersham).

4.3.5. Immunohistochemistry

Autopsied brain tissues were snap frozen and cryostat sectioned at 10 μm of thickness, mounted on superfrost slides and stored at –80°C until staining. Tissue sections were post fixed in 4% paraformaldehyde buffered with sodium phosphate (0.1 M, pH 7.4) at 4°C for 5 min, then treated with 0.3% hydrogen peroxide in 100% methanol for 15 min at RT, and permeabilized with PBS (0.01 M) containing 0.1% Triton X-100 at RT for 30 min. Nonspecific sites were blocked with 15% normal goat serum or normal horse serum

or normal rabbit serum for 30 min. Slides were then incubated with the primary antibody at 4°C overnight. Biotinylated secondary antibodies (Vector Labs) at a dilution of 1/200 were applied for 1 h at RT and immunoreactivity detected using diaminobenzidine (DAB) brown or alkaline phosphatase (AP) with DAB and AP substrate kits (Vector). No specific staining was detected on slides lacking the primary antibody. Slides from cases diagnosed with AD as well as age-matched controls were routinely stained side by side in a single and double labeling paradigm using the same batch of antibodies.

We examined immunohistochemical labeling in cortical layers containing plaques and $\alpha\Delta N^{caspase}$–αIIspectrin immunoreactivity from 1-3 sections/brain sample. All histological and immunohistochemical images were acquired from a Zeiss Axioplan 2 microscope equipped with an Axiophoto 2 system adapted to a Sony 3 CCD DXC-950 color video camera. The video signal was routed via a Sony camera adaptor CMA-D2 into a microcomputer. Images were analyzed by a custom designed program implemented in Northern Eclipse, an image analysis system produced by Empix Imaging, Inc. (Mississauga, Ontario, Canada). Quantification of positive labeling was performed on longitudinal bands following a linear sampling pattern using a micrometer scale in the ocular as an external calibrator. Each determination represented the mean ± SEM of 10 measurements per brain section performed on different regions of the frontal and temporal cortices. The number of $\alpha\Delta N^{caspase}$–αIIspectrin and SMI-32 immunopositive cells as well as cells that displayed both of these immunoreactivities was counted over an area of 350 µm x 280 µm.

4.3.6. Choline-Acetyl Transferase (ChAT) enzymatic activity assay

Tissue extracts were stored at -70°C until assayed. ChAT activity was determined using a modified version of the method of Fonnum (1975). Briefly, 20 µl of tissue extracts were incubated in a 0.05 M sodium phosphate buffer (pH 7.4) containing 0.01 M disodium EDTA, 0.01 M choline chloride, 0.3 M sodium chloride and 0.001 M eserine sulfate. The assay was initiated by the timed addition of 10 µl of ^{14}C-acetyl CoA (NEN NEC-313; 12.5 mCi/mmol; 0.1 mM). Tubes were incubated at 37 °C in a metabolic incubator under gentle shaking for a 20 min period. The reaction was terminated by the

timed addition of 500 µl of 3-heptanone containing 10 mg/ml sodium tetraphenylboron. Samples were then vortexed and placed on ice. Tubes were centrifuged for 1 min. in a Fisher Micro-centrifuge, and 200 µl of the supernatant were counted in 5 ml Ecolume using a liquid scintillation counter. Blanks were obtained in the absence of choline substrate and data expressed in µmoles ^{14}C-ACh formed / mg protein/ min.

4.3.7. Statistical Analysis

Analysis of variance (ANOVA) with a mixed design (two factor-within subjects, one factor-between subjects) was carried out to compare the mean values for ChAT activities or the optical density of bands corresponding to caspase-cleaved spectrin proteolytic fragments in the superior temporal and superior parietal cortices from age-matched and Alzheimer's disease autopsied brains. A statistical test was considered significant at $P < 0.05$. Data analyses were performed using the SPSS statistical package (Version 10.0, 1998).

TABLE 4.1

Age-matched Control and Alzheimer's disease Case Demographic Information

Patient	Age	Sex	PMI (h)	ApoE	Braak Index	Neuropathological Diagnosis
C1-9710	79	M	2.00	3/3	I	Control
C2-9714	76	M	2.50	3/3	I	Control
C3-9717	78	M	2.66	3/3	I	Control
C4-9639	73	F	2.50	3/3	I	Control
C5-9702	81	M	2.75	3/3	I	Control
C6-9613	85	F	2.75	3/3	II	Control/spasmodic dysphonia
AD1-9605	87	F	2.00	3/3	V	Alzheimer's disease
AD2-9609	75	M	2.50	3/3	V	Alzheimer's disease/Cerebral amyloid angiopathy
AD3-9707	87	F	2.50	2/2	V	Alzheimer's disease
AD4-9725	88	M	1.75	3/3	V	Alzheimer's disease
AD5-9733	85	M	2.33	3/3	V	Alzheimer's disease
AD6-9828	84	F	2.00	3/3	VI	Alzheimer's disease

PMI: Postmortem interval in hours; ApoE: Apolipoprotein genetic load: Nd: Not determined

4.4. Results

4.4.1. Cases Demographics

Table 4.1 shows characteristics of the sample population by diagnostic group. The age-matched controls and Alzheimer's disease individuals were similar in age, ApoE genetic load and postmortem interval.

4.4.2 Characterization of the caspase-3 cleaved αIIspectrin *neo*-epitope antibody using a rat cell-free system

To validate the specificity of the $\alpha\Delta N^{caspase}$-αIIspectrin antibody, a series of *in vitro* experiments were undertaken to test the ability of this antibody to recognize caspase-3 cleaved proteolytic fragments of fodrin after digestion with recombinant caspase-3 in a cell-free system. Rat cortex and dorsal hippocampus tissue extracts were incubated with or without caspase-3 for 2 h at 37 °C as described in the Methods. As expected, the $\alpha\Delta N^{caspase}$-αIIspectrin antibody recognized the secondary caspase-3 cleaved αIIspectrin proteolytic fragment of 120 kDa (Fig. 4.1A, lanes 2, 6, 7), but neither the full-length fodrin (240 kDa) nor the initial cleavage product of αIIspectrin (150 kDa). In the cerebral cortex, the antibody also detected two additional fragments of 110 and 85 kDa. Based on the molecular weights described by Wang et al. (2001), the 110 and 85 kDa fragments likely represent caspase-3 generated breakdown products of βIIspectrin.

Matched tissue extracts treated with recombinant caspase-3 were run in parallel and subsequently probed with MAB1622, a monoclonal antibody that recognizes full-length αIIspectrin, as well as the 150 and 120 kDa proteolytic fragments of this structural protein generated by caspase-3. Incubation with recombinant caspase-3 resulted in accumulation of the 150 and 120 kDa bands (Fig. 4.1B, lanes 2, 4, 6 and 7). These findings indicate that the $\alpha\Delta N^{caspase}$-αIIspectrin polyclonal antibody recognizes primarily the 120 kDa fragment generated by caspase-3 cleavage of αIIspectrin.

4.4.3. Characterization of the caspase-3 cleaved αIIspectrin *neo*-epitope antibody using a human cell-free system

Extracts from the superior parietal cortex of age-matched control (Fig. 4.2A, lanes 1, 4, 5) and Alzheimer's disease (lanes 2, 3, 6, 7) were incubated without active caspase-3 (lanes 1-3) or with active caspase-3 (lanes 4-7) as described in the Methods. In the absence of active enzyme (Figure 4.2A; lanes 1, 2, 3) undetectable to low levels of labeling were found in the tissue samples from AD and age-matched control brains.

In tissue extracts treated with active caspase-3, the $\alpha\Delta N^{caspase}$-αIIspectrin antibody recognized mainly the expected secondary 120 kDa proteolytic fragment of caspase-3 cleaved αIIspectrin (Fig. 2A, lanes 4 - 7). As expected, neither the full-length 240 kDa form nor the initial 150 kDa caspase-3 generated fragments of fodrin were detected. The $\alpha\Delta N^{caspase}$-αIIspectrin antibody recognized by immunoprecipitation a single 120 kDa band in extracts from the parietal cortex of age-matched control (1 of 4 subjects) and Alzheimer's disease (2 of 4 subjects) (Fig. 4.2B). These results suggest that during senescence, and more importantly during progression of Alzheimer's disease pathology, activation of caspase-3 occurs with a subsequent accumulation of the 120 kDa proteolytic fragment of caspase-3 cleaved αIIspectrin.

4.4.4. $\alpha\Delta N^{caspase}$-αII spectrin immunoreactivity as a marker for apoptosis in Alzheimer's disease and senescence

In age-matched control brains, we rarely found neuronal somas and neuritic threads immunoreactive for $\alpha\Delta N^{caspase}$-αII spectrin (Fig. 4.3A). No staining was observed in the absence of the primary antibody (results not shown) supporting the specificity of the $\alpha\Delta N^{caspase}$-αII spectrin antibody. In Alzheimer's disease brains, tissue sections from the IFG and STG stained with the $\alpha\Delta N^{caspase}$-αII spectrin antibody showed extensive labeling of neuronal cell somas, neuropil threads, apical dendrites and processes of various lengths (Fig. 4.3B-D). $\alpha\Delta N^{caspase}$-αIIspectrin immunoreactive elements were sparsely distributed in layers I to VI of the IFG and STG. Large pyramidal neurons in layers III to VI were prominently labeled. Cells counts revealed that the number of $\alpha\Delta N^{caspase}$-αIIspectrin

positive neurons were greater in both STG and IFG tissue sections from Alzheimer's disease than age-matched control brains [$F(1,10)=9.40$, $p<0.05$] (Fig. 4.4). We rarely observed $\alpha\Delta N^{caspase}$-αIIspectrin immunoreactive elements associated with diffuse senile plaques in age-matched control (Fig. 4.6A) or diffuse and core-dense senile plaques in Alzheimer's disease brains (Fig. 4.6B-D).

4.4.5. Co-localization of $\alpha\Delta N^{caspase}$-αIIspectrin and SMI-32 immunoreactivity in AD brains

In age-matched control brains, the majority of neurons immunoreactive for SMI-32 in the IFG and STG were large pyramidal neurons, distributed primarily in layers III-IV and V-VI with the occasional large multipolar cell observed in layer III (Fig. 4.5A). In Alzheimer's disease brains, we found a similar pattern of SMI-32 immunoreactivity with labeling predominantly located in pyramidal neurons of layer III and IV in the cerebral cortex (Fig. 4.5B-D). We assessed the extent of cellular co-localization between $\alpha\Delta N^{caspase}$-αIIspectrin and SMI-32 immunoreactivities in layer III of the inferior frontal and superior temporal gyri. $\alpha\Delta N^{caspase}$–αIIspectrin immunopositive cells were always located in SMI-32 immunoreactive cells. Approximately 35% of the total number of SMI-32 immunopositive pyramidal neurons in layer III of Alzheimer's disease brains contained $\alpha\Delta N^{caspase}$–αIIspectrin immunoreactivity. The number of SMI-32 immunoposituive neurons in layer III of age-matched controls (IFG, 37.3 ± 4.5; STG, 35.0 ± 5.1) and AD (IFG, 37.0 ± 6.5; STG, 34.0 ± 5.3) patients were the same. The co-localization of $\alpha\Delta N^{caspase}$–αIIspectrin immunoreactivity in SMI-32 immunoreactive pyramidal neurons indicates that activation of caspase-3 occurs before neurofilament phosphorylation which in turn results in the loss of SMI-32 immunoreactivity.

In Alzheimer's disease brain sections stained with the SMI-32 antibody, we observed rounded "pale spots" devoid of SMI-32ir in layer III (Fig. 4.5D) where presumable senile plaques had disorganized and compressed the columnar pattern of pyramidal neurons. Previous reports by Su et al. (1996; 1998) showed that these "pale spots" represent areas of hyperphosphorylated neurofilaments where the epitope recognized by the SMI-32 antibody is occluded. In "pale spots" lacking SMI-32

immunoreactivity, $\alpha\Delta N^{caspase}$—αIIspectrin immunoreactivity was either absent or weakly detected. These findings indicate active caspase-3 was not present in cells with hyperphosphorylated neurofilaments.

$\alpha\Delta N^{caspase}$—αIIspectrin immunoreactivity in pyramidal neurons (Fig. 4.6B) and neuritic threads (Fig. 4.6C) were rarely associated with either diffuse or dense-core plaques (Fig. 4.6B-D). Furthermore, dystrophic neurites immunoreactive $\alpha\Delta N^{caspase}$—αIIspectrin did not co-localize with MC-1 immunoreactive neuritic threads (results not shown). These results suggest that caspase-3 activation is an early event in the evolution of Alzheimer's disease pathology that may be independent of amyloid Aβ deposition and the hyper-phosphorylation of cytoskeletal proteins.

4.4.6. ChAT activity in homogenate tissue extracts from the inferior parietal and superior temporal cortex of Alzheimer's disease and age-matched control brains

ChAT activity was assessed in the inferior parietal and superior temporal cortices of age-matched controls and Alzheimer's disease patients. ChAT activities in the inferior frontal and superior temporal gyri were the same for both the Alzheimer's disease and age-matched control brains. Consistent with the neuropathological classification of the control and Alzheimer's disease groups by the Braak and Braak index as reported in Table 1, severe Alzheimer's disease cases demonstrated a severe reduction in ChAT activity in both cortices [$F(1,8)=34.36$, $p<0.01$] (Fig. 4.7).

4.5. Discussion

Caspase-3 activation has been shown to occur in association with microglial and neuronal cell bodies, dystrophic neurites and senile plaques in Alzheimer's disease brains providing a mechanistic link between programmed cell death and gliosis (Yang et al., 1998), amyloidosis (Gervais et al., 1999; Su et al., 2002; Ayala-Grosso et al., 2002), or neurofibrillary tangles formation (Rohn et al., 2001; 2002; 2003). However, a temporal order of events underlying cell loss in Alzheimer's disease pathology has not yet been established. In the present study, caspase activation was measured using an antibody that selectively recognizes the 120 kDa fragment of αIIspectrin generated by caspase-3

cleavage of this structural protein. Consistent with a previous report (Rohn et al., 2001), we observed an increase in the number of neurons that displayed $\alpha\Delta N^{caspase}$–αIIspectrin immunoreactivity in the inferior frontal, superior temporal and parietal gyri of Alzheimer's disease relative to age-matched control autopsied brains. In layers III and V of these cortical regions, caspase-3 cleaved spectrin immunoreactivity co-localized exclusively with a subset of pyramidal neurons enriched with non-phosphorylated neurofilaments identified with the SMI-32 antibody. SMI-32 immunoreactive pyramidal neurons comprise long corticocortical projections whose functional impairment is thought to contribute to dementia in Alzheimer's disease (Hof et al., 1990; Hof and Morrison, 1990; Bussiere et al., 2003). The detection of caspase-3 cleaved spectrin within these neurons suggests that activation of this protease is responsible for the disruption and eventual loss of corticocortical projections in Alzheimer's disease. Identification of caspase activation in discrete populations of neurons in association areas of the cerebral cortex also implicates programmed cell death in the initial progression of corticocortical disconnection in Alzheimer's disease.

Using the $\alpha\Delta N^{caspase}$–αIIspectrin polyclonal antibody, we were able to immunoprecipitate from human parietal cortex of Alzheimer's disease cases fragments with the predicted molecular weight of the proteolytic products of caspase-cleaved αIIspectrin as established by Wang et al. (1998). This result supports the specificity of the $\alpha\Delta N^{caspase}$–αIIspectrin antibody and is in agreement with previous *in vitro* findings where activation of caspase-3 by apoptotic triggers resulted in the generation of fragments of spectrin ranging from 120 to 55 kDa in size (Rohn et al., 2001).

In addition to a 120 kDa fragment of spectrin, we also detected the accumulation of 110 and 85 kDa proteolytic fragments with the $\alpha\Delta N^{caspase}$–αIIspectrin antibody in Alzheimer's disease brains. Several possibilities may account for these observations: *i*) alternative caspase-3 cleavage sites in spectrin, *ii*) multiple spectrin isoforms, and *iii*) differential turnover of caspase-generated spectrin fragments in Alzheimer's disease. In contrast to our results, Rohn et al. (2001) detected only a 55 kDa fragment of fodrin in Alzheimer's disease brain. Differences in the AD patient populations examined in the present study and the report by Rohn et al. (2001) may account for this discrepancy.

Accumulation of the breakdown products for βIIspectrin in a subset of senile plaques or αIIspectrin in neuronal processes in Alzheimer's disease but not in age-matched control cases suggests that abnormalities in spectrin structure or function may play a key role in the formation or deposition of amyloid plaques. It is tempting to speculate that an abnormal processing or altered expression and distribution of spectrin in the aging brain could initiate a cascade of events leading to the disruption of the membrane-specific domains (Sihag and Cataldo, 1996). In agreement with this suggestion, previous studies have reported the existence of antibodies in sera of Alzheimer's disease patients which recognize spectrin specific antigens from crude human brain extracts (Vasquez et al., 1996; Fernandez-Shaw et al., 1997).

$\alpha\Delta N^{caspase}$-αII spectrin immunoreactivity was more intense in the soma of pyramidal neurons from intermediate and deep cortical layers, in keeping with a prevalent distribution of senile plaques in layers III to VI of these association areas of the cortex. In the present study, we did observe rarely overlap between $\alpha\Delta N^{caspase}$-αII spectrin immunoreactive dystrophic neurites and $A\beta_{(1-12)}$ immunopositive dense-core senile plaques. These observations are suggestive of that caspase-3 activation may occur in parallel with amyloidosis or the progressive accumulation of microtubules and neurofilaments resulting from the hyperphosphorylation process.

Accumulation of caspase-3 generated proteolytic fragments in glia (Yang et al., 1998) as well as neuronal compartments in the present study suggests that caspase activation may occur as a consequence of multiple stimuli. These findings are in agreement with a previous report where caspase-3 cleaved amyloid precursor protein proteolytic fragments were co-localized with 23% of dense-core senile plaques (Ayala-Grosso et al., 2002). $\alpha\Delta N^{caspase}$-αII spectrin immunoreactivity was detected in dystrophic neurites sparsely distributed in the neuropil as well as long, distorted, swollen dendrites usually continuous with normal appearing processes. These evidences are indicative of local neurotoxic processes disrupting interconnection between layers of the cortex.

Our data indicate that caspase-3 activation may represent an early event in cellular dysfunction in AD. We propose that caspase-3 activation is a primary event that

may occur prior to phosphorylation of neurofilaments and likely neurofibrillary tangles formation. In support of our hypothesis, subpopulations of caspase-cleaved spectrin immunoreactive cell bodies have been reported to be present in the prefrontal cortex of aged dogs, an animal species that develops extensive Aβ deposition but not neurofibrillary tangles (Rohn et al., 2001). Furthermore, in the human tau isoform transgenic mouse, a tauopathy-induced animal model, overexpression of tau protein leads to conformational changes and hyperphosphorylation of tau, as well as widespread axonopathy accompanied by the accumulation of neurofilaments and microtubules in the brain gray matter as well as the spinal cord. However, surprisingly no sign of cell death was detectable in this mouse (Sppitaels et al., 1999). These results indicate that neurofibrillary tangles alone may not be the primary trigger of neuronal apoptosis in Alzheimer's disease.

Pyramidal neurons enriched in SMI-32 immunopositive neurofilaments connecting the superior temporal and prefrontal cortices of the association neorcortex are selectively and severely affected in dementia (Hof et al., 1990). Glutamate receptors (GluRs) are differentially expressed among different corticocortical circuits and their expression in these pathways is reduced by the aging process (Hof et al., 2002). The decreases in glutamate receptor expression that occurs as a consequence of aging has been hypothesized to create an imbalance in glutamatergic transmission in discrete efferents from the neocortex that could result in the loss of subsets of neocortical neuronal populations. Using autoradiography, immunocytochemistry or in situ hybridization, several studies have revealed considerable alterations in the distribution and density of several GluRs in the cerebral cortex of Alzheimer's disease brains (Armstrong et al., 1994; Gazzaley et al., 1997; Ikonomovic et al., 2000; Sze et al., 2001; Magnusson et al., 2000). Lower levels of GluR2 may render pyramidal neurons particularly prone to calcium-mediated toxicity. In agreement with this proposal, knockdown experiments in rats and gerbils with GluR2 antisense oligonucleotide resulted in neuronal cell death of pyramidal neurons and enhanced the injurious effects of brief ischemic episodes (Tanaka et al., 2000). Similarly, long-term antagonism of NMDA receptor may trigger irreversible neurodegeneration affecting neurons in cerebrocortical and limbic regions (Farber et al., 2002). These findings suggest that chronic reductions in glutamatergic

neurotransmission may promote cortico-cortical pathway dysfunction leading to cell death independent of amyloid Aβ deposition.

It has been proposed that the accumulation of senile plaques and neurofibrillary tangles are the primary triggers of caspase activation and subsequent cell death in Alzheimer's disease. In contrast, our data lead us to propose that caspase activation may occur as an early event initiated by metabolic decline that precedes phosphorylation of neurofilaments and likely microtubules associated with the protein tau.

4.6. Acknowledgements

We are grateful to A.C. Cuello (McGill University) for providing the amyloid $A\beta_{(1-12)}$ antibody. We are particularly indebted to the Sun Health Research Institute for providing us with Alzheimer's and aged-matched control brain sections for immunohistochemical analysis. C. Ayala-Grosso is a fellow of Consejo de Desarrollo Científico y Humanístico de la Universidad Central de Venezuela.

Figure 4.1. Characterization of the caspase-3 cleaved αIIspectrin *neo*-epitope antibody using a rat cell-free system. Rat cortex and dorsal hippocampus tissue extracts were incubated with (lanes 2, 6 and 7) or without (lanes 1, 3, and 5) caspase-3 for 2 h at 37 °C as described in the Methods. A) The $\alpha\Delta N^{caspase}$-αIIspectrin antibody recognized mainly a caspase-3 generated product of αIIspectrin 120 kDa in mass in the cerebral cortex and dorsal hippocampus. In addition, fragments of 110 and 85 kDa were detected by the $\alpha\Delta N^{caspase}$-αIIspectrin antibody in the cerebral cortex. B) Matched tissue extracts treated with recombinant caspase-3 were run in parallel and subsequently probed with the MAB1622 monoclonal antibody. After incubation with recombinant caspase-3, accumulation of a 150 kDa band was evident (lanes 2, 4, 6 and 7). In contrast with the results shown in panel A, the MAB1622 antibody recognizes mainly caspase-3 generated proteolytic fragments of 150 kDa and 120 kDa in size.

FIGURE 4.1

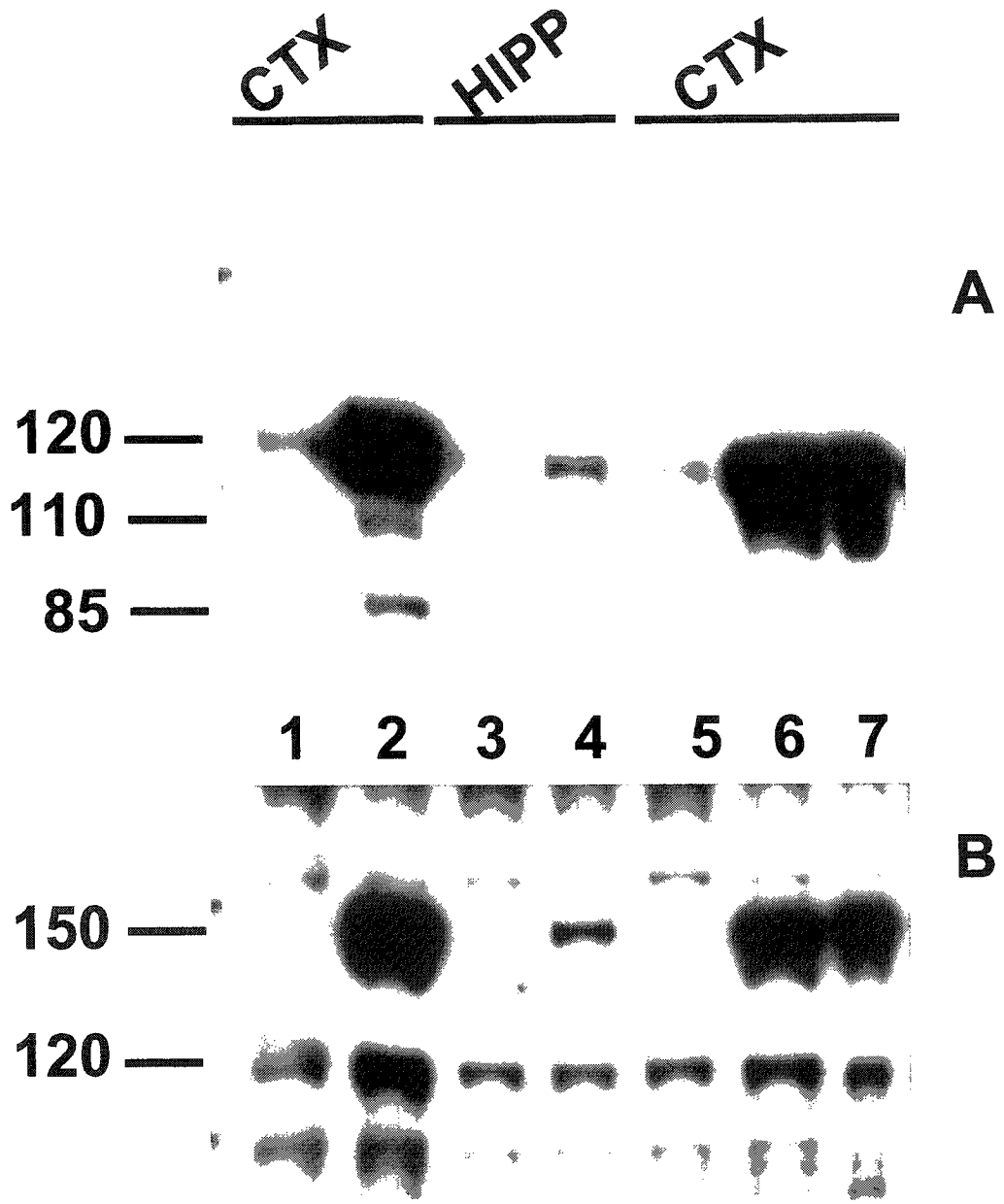

Figure 4.2. Characterization of the caspase-3 cleaved αIIspectrin *neo*-epitope antibody using a human cell-free system. (A) Extracts of superior parietal cortex from age-matched control (lanes 1, 4,5) and Alzheimer's disease (lanes 2, 3, 6, 7) brains were incubated with (lanes 2, 6 and 7) or without (lanes 1, 3, and 5) caspase-3 for 2 h at 37 °C as described in the Methods. The $\alpha\Delta N^{caspase}$-αIIspectrin antibody recognized mainly a caspase-3 cleaved αIIspectrin proteolytic fragment of 120 kDa in the cerebral cortex. Minor fragments of 110, 85 and 55 kDa were also detected with the $\alpha\Delta N^{caspase}$-αIIspectrin antibody after incubation of the extract with active caspase-3. (B) Immunoprecipitation of caspase-3 cleaved αIIspectrin ($\alpha\Delta N^{caapase}$-αIIspectrin) proteolytic fragments from human brain. Tissue extracts from the parietal cortex of age-matched controls and Alzheimer's disease subjects were incubated for 24 h at 4°C with the $\alpha\Delta N^{caspase}$-αIIspectrin polyclonal antibody and protein A. Immunoprecipitated proteins were separated by sodium dodecyl-sulfate-polyacrylamide gel electrophoresis, transferred to nitrocellulose, and probed with the MAB1622 monoclonal antibody. A prominent band at 120 kDa was detected in age-matched control (1 of 4 subjects) and Alzheimer's disease (2 of 4 subjects) brain extracts. Additional bands of 110 kDa and 85 kDa were also detected with the $\alpha\Delta N^{caspase}$-αII-spectrin polyclonal antibody in age-matched control and Alzheimer's disease brains. Since the 120 kDa band was the prominent band in AD subjects, this fragment was likely the predominant product responsible for $\alpha\Delta N^{caspase}$-αII-spectrin immunoreactivity in Alzheimer's disease brain.

FIGURE 4.2

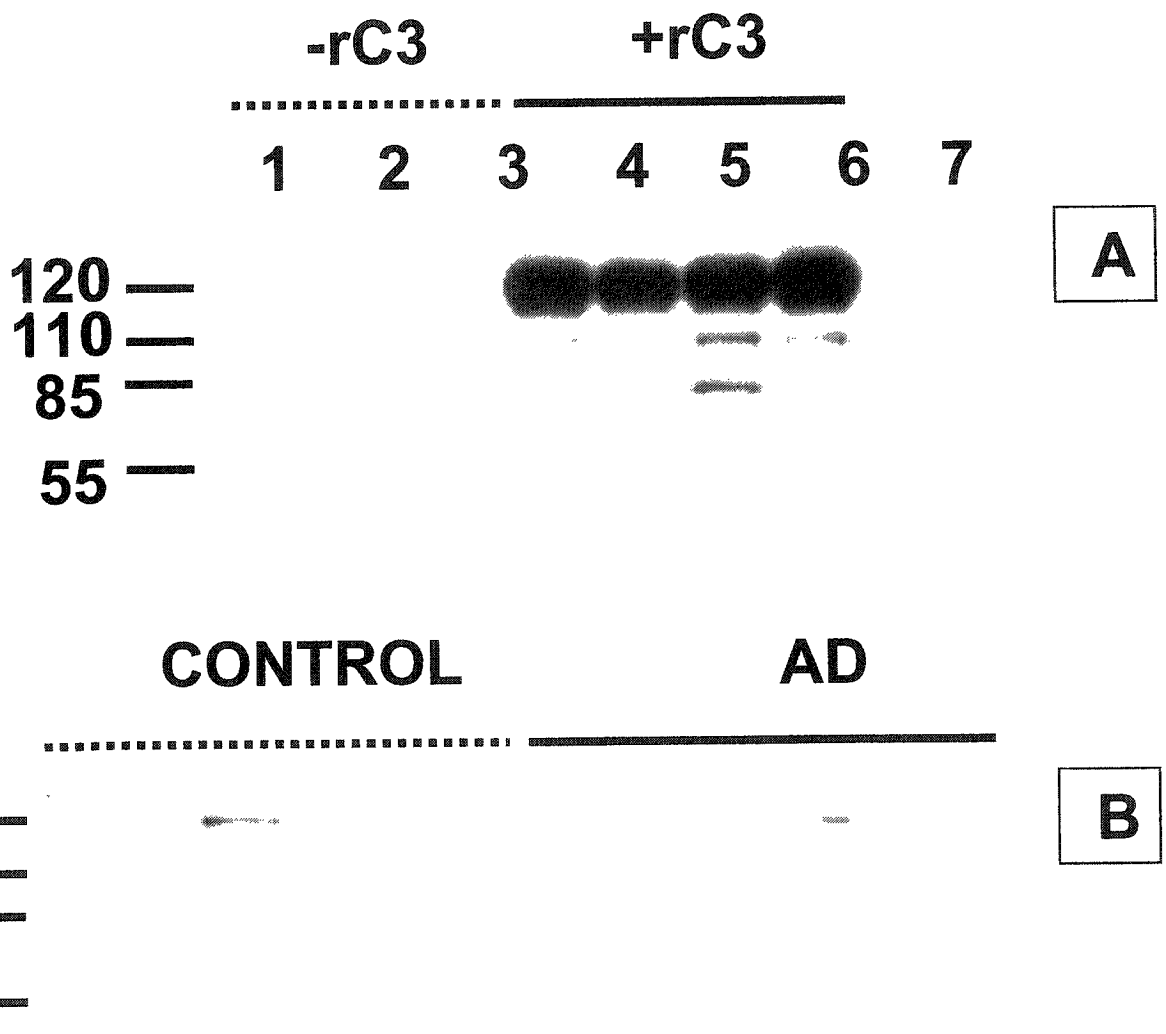

Figure 4.3. Immunohistochemical detection of caspase-3 generated fragments of αIIspectrin in tissue sections from the inferior frontal and superior temporal cortices of age-matched control and Alzheimer's disease brains. In age-matched control brains (A), neuronal somas and neuropil threads immunopositive for $\alpha\Delta N^{caspase}$-αII spectrin were rarely detected. In Alzheimer's disease brains (B, C, D), prominent labeling of large pyramidal neurons from layers III and VI was observed. $\alpha\Delta N^{caspase}$-αIIspectrin immunoreactive elements, such as neuritic threads (short arrows, B), dystrophic neurites (C, circle), and neuronal processes of a various lengths (long arrow, B; arrows, C and D), were sparsely distributed in layers I to VI of the IFG and STG. Neuronal cell bodies in deep cortical layers such as Meynert cells at the border of layer VI (D) were stained with the $\alpha\Delta N^{caspase}$-αII spectrin antibody.

FIGURE 4.3

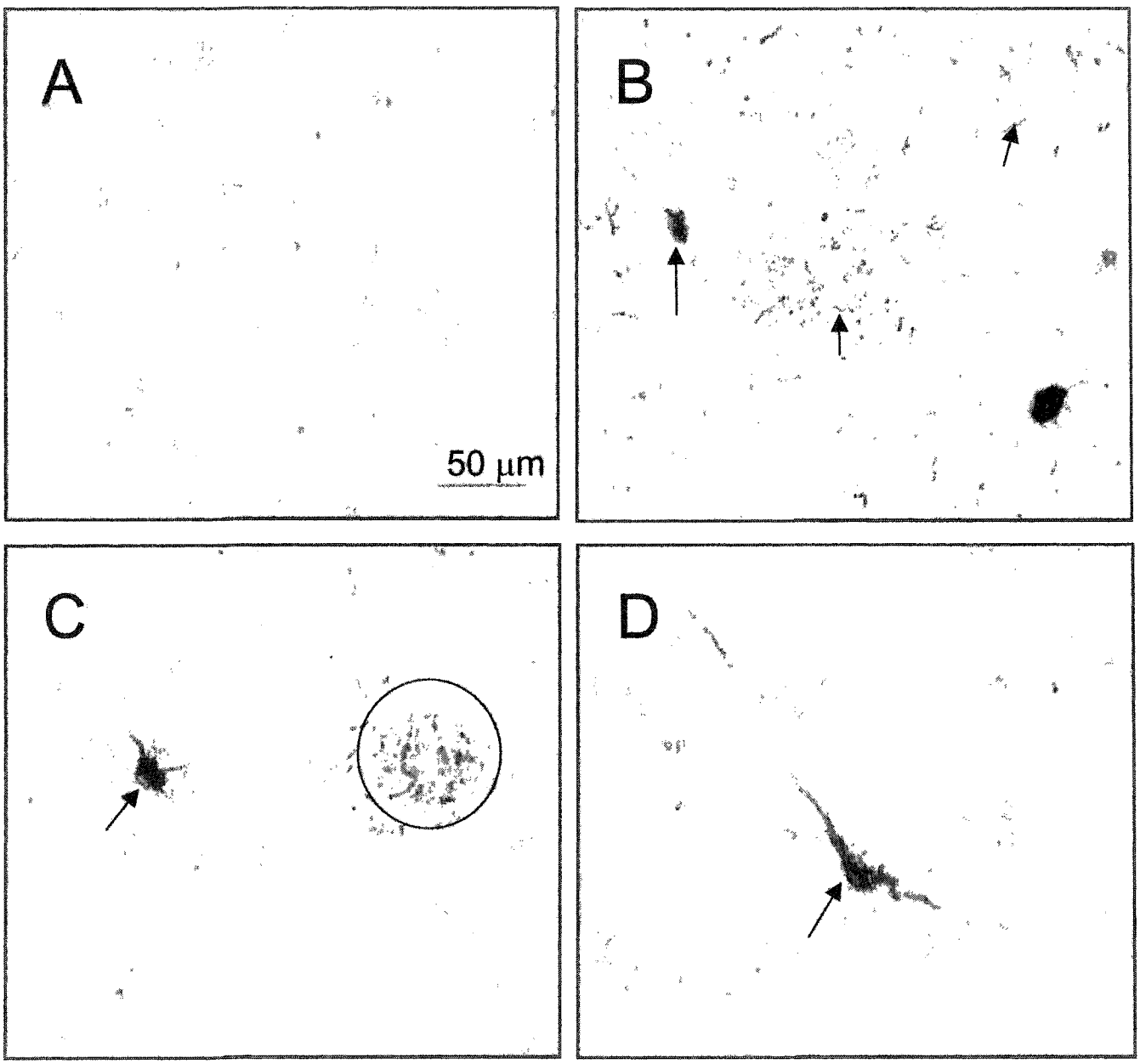

Figure 4.4. Counts of $\alpha\Delta N^{caspase}$-αIIspectrin positive neurons in the superior temporal and inferior frontal gyri of Alzheimer's disease and age-matched control brains. There were significantly more $\alpha\Delta N^{caspase}$-αIIspectrin positive neurons in both these cortical regions in AD than control brains [$F(1,10)=9.40$, $p<0.05$].

FIGURE 4.4

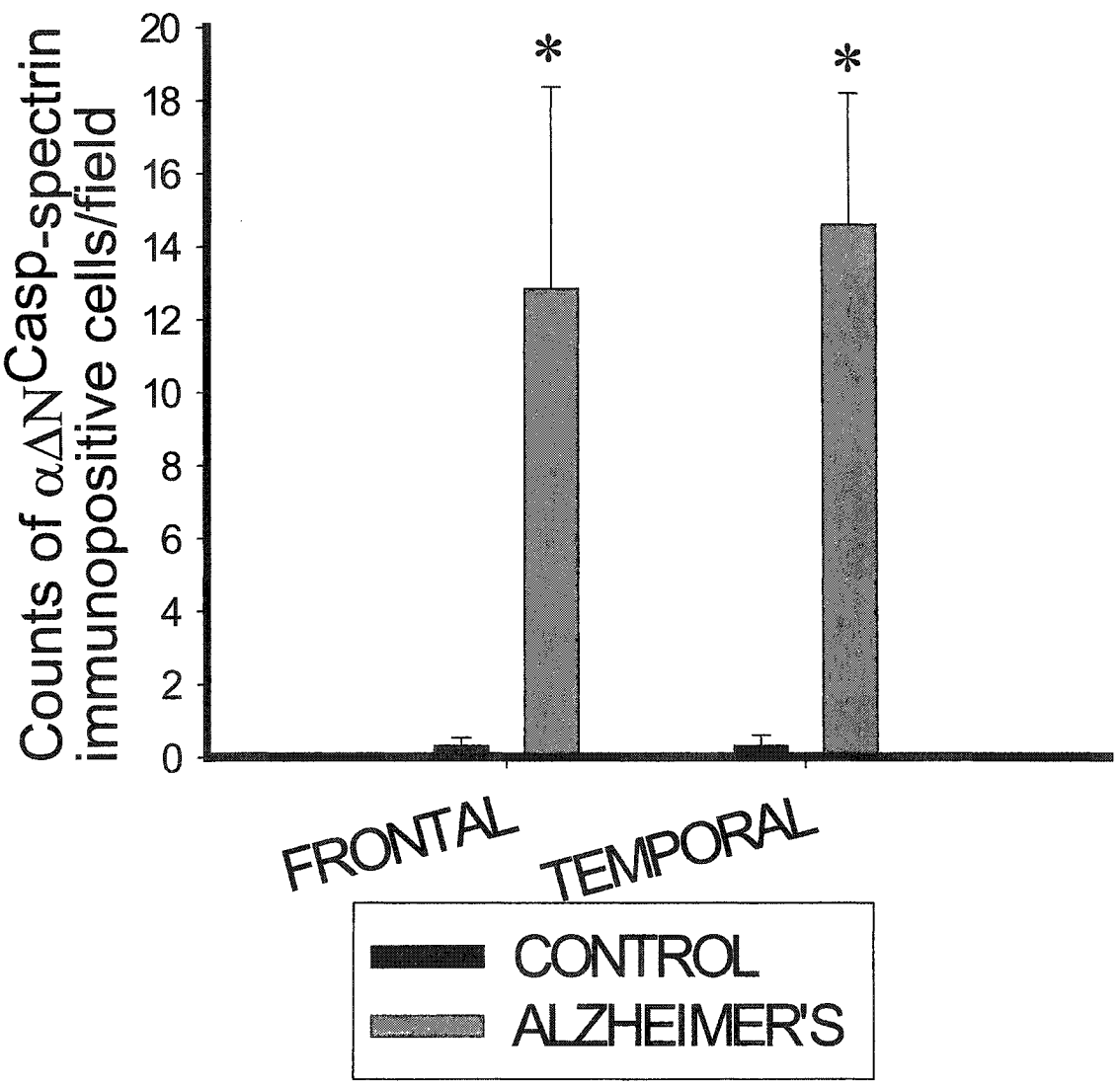
Counts of αΔNCasp-spectrin immunopositive cells/field
20
18
16
14
12
10
8
6
4
2
0
*
*
FRONTAL
TEMPORAL
CONTROL
ALZHEIMER'S

Figure 4.5. Caspase-3 cleaved αIIspectrin and SMI-32 immunoreactivities in normal and Alzheimer's disease brains. In age-matched control brains (A), the majority of SMI-32-ir neurons (dark blue) in the inferior frontal and superior temporal cortices were large pyramidal neurons distributed primarily in deep layers III-IV and superficial layers V-VI. A few large multipolar cells were observed in layer III. In AD brains (B), a comparable pattern of SMI-32 immunoreactive pyramidal neurons was detected. Quantification revealed that there were a similar number of SMI-32ir cell bodies in layer III of age-matched controls (IFG, 37.3 ± 4.45; STG, 35.0 ± 5.14) and Alzheimer's disease (IFG, 37.0 ± 6.47; STG, 34.0 ± 5.26) brains. In Alzheimer's disease brains, immunoreactivity for $\alpha\Delta N^{caspase}$-αIIspectrin (dark brown) was co-localized with SMI-32 immunoreactive pyramidal neurons in layer III indicating that caspase-3 activation occurred in neurons enriched in nophosphorylated neurofilaments of medium and high molecular weight. (C, D, circles). Disorganized and compressed neuropile appeared as areas devoid of SMI-32ir or "pale spots" (5D) suggestive of seniles plaques. These pale spots did not contain $\alpha\Delta N^{caspase}$-αIIspectrin positive neurons.

FIGURE 4.5

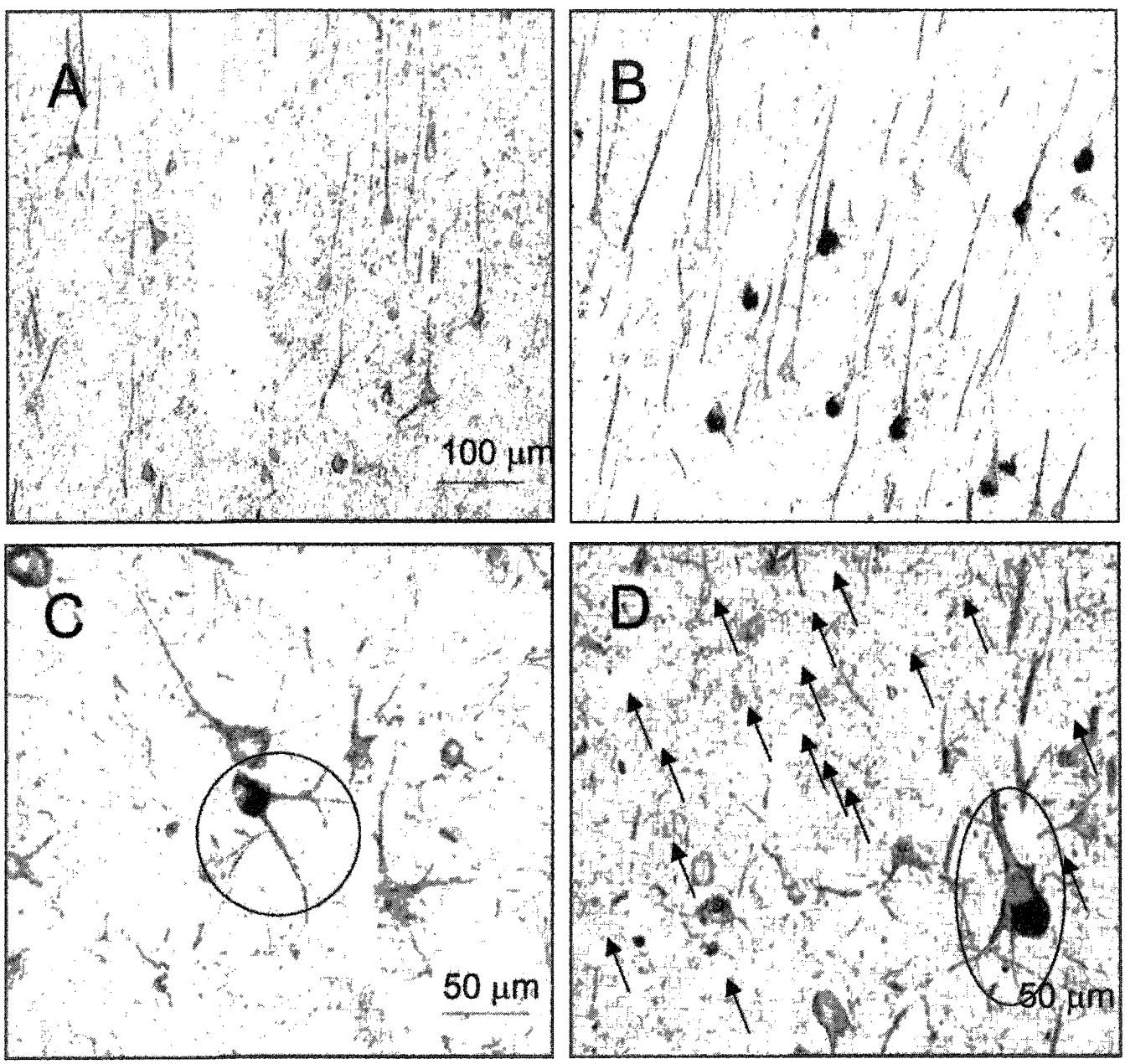

Figure 4.6. Localization of $\alpha\Delta N^{caspase}$—αIIspectrin (dark brown) and amyloid $A\beta_{(1-12)}$ (red) immunoreactivities in age-matched control (A) and Alzheimer's disease brain sections (B, C, D) from inferior frontal gyrus. Caspase-3 cleaved—αIIspectrin immunoreactivity was rarely detected and seldom associated with diffuse senile plaques in age-matched control brains (A). In Alzheimer's disease brains, $\alpha\Delta N^{caspase}$—αIIspectrin immunoreactive pyramidal neurons (B, circles) and neuritic threads (C, D) were infrequently associated with diffuse (B and C) and dense-core (D) plaques.

FIGURE 4.6

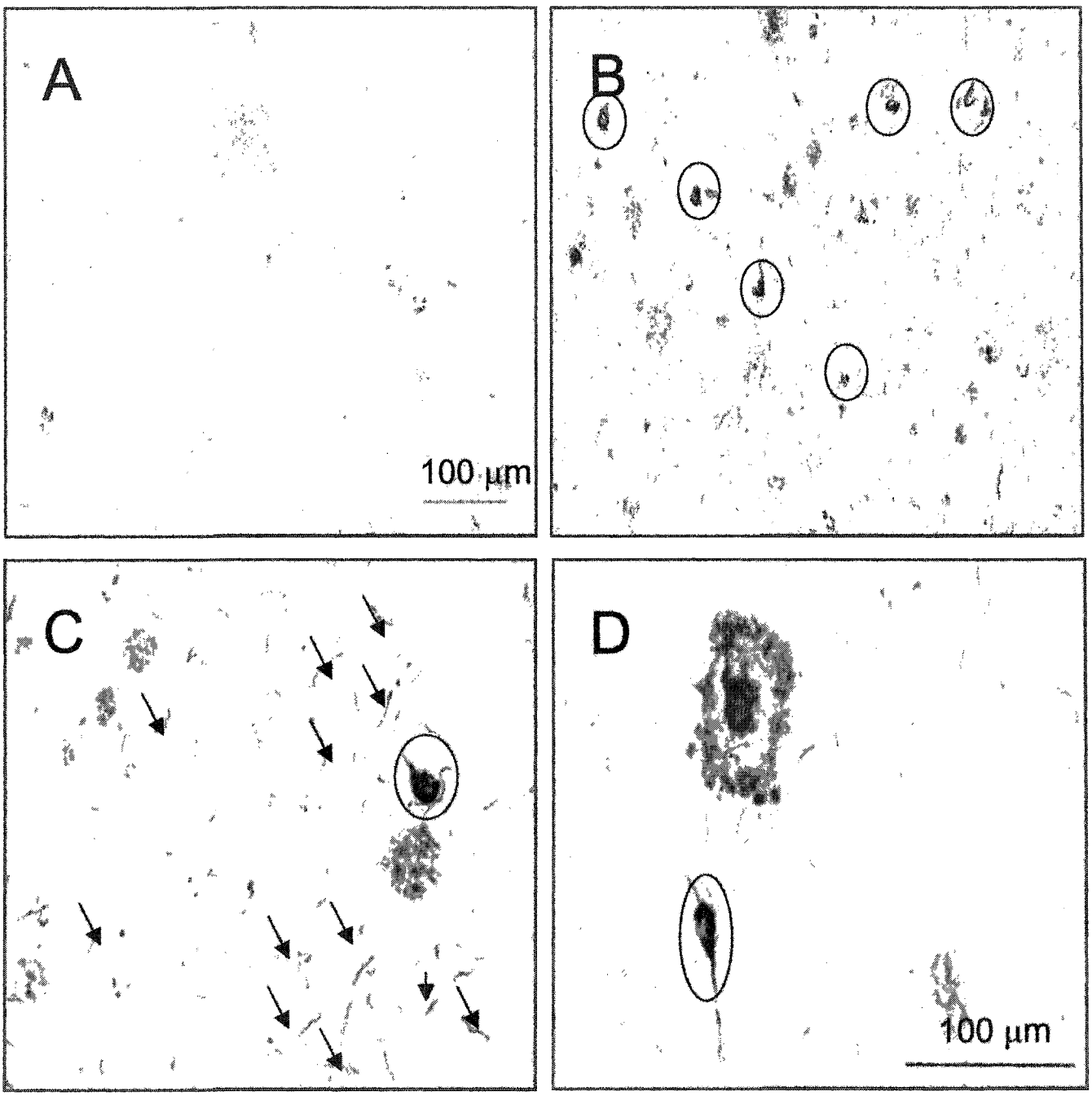

Figure 4.7. ChAT activity in the inferior parietal and superior temporal cortices of Alzheimer's disease (n=6) and age-matched controls (n=6). No differences in ChAT activity were found between lobes of Alzheimer's disease and age-matched controls. ChAT activities in both cortices of Alzheimer's disease patients were reduced to 17% of those values detected in age-matched controls [$F(1,8)=34.36$, $P<0.01$].

FIGURE 4.7

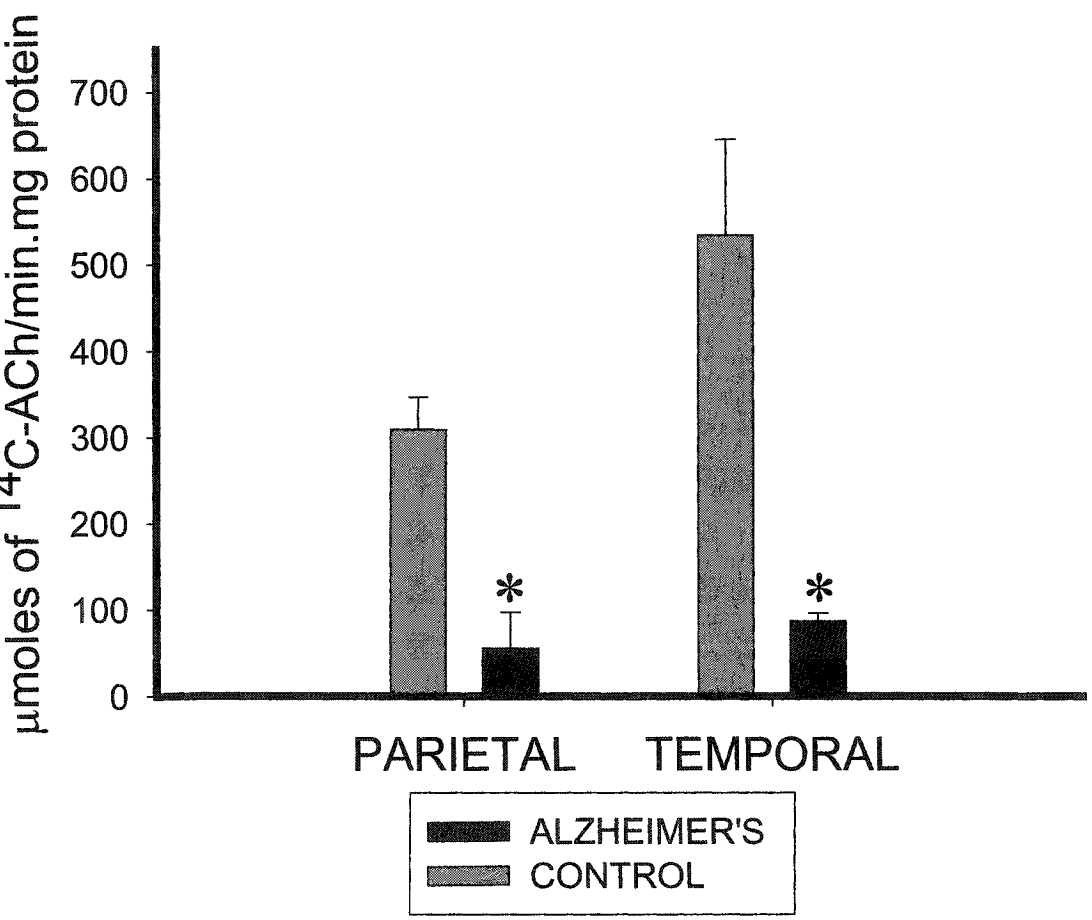
µmoles of ^{14}C-ACh/min.mg protein
700
600
500
400
300
200
100
0
*
*
PARIETAL
TEMPORAL
ALZHEIMER'S
CONTROL

Connecting Text

Results from our previous study shown that caspase-3 cleaved spectrin was located in a subset of pyramidal neurons of layer 3 and 6 from association cortices extremely vulnerable in Alzheimer's disease.

We observed that accumulation of caspase-3 cleaved spectrin occurred partially associated with amyloidosis and neurofibrillary pathology. These findings were suggestive that activation of caspases in Alzheimer's disease may also occur independently of amyloidogenesis or neurofibrillary tangles. Thus, we decided to explore the role of caspase-3 in a rat model of septo-hippocampal denervation as a result of axotomy of the fimbria-fornix pathway.

Chapter 5

Effects of Fimbria-Fornix Transection on Calpain and Choline Acetyl Transferase Activities in the Septohippocampal Pathway

C. Ayala-Grosso[1]§, J. Tam[2], S. Xanthoudakis[2], Y. Bureau[3], S, Roy[2], D.W. Nicholson[2] and G.S. Robertson[4*]

Department of Pharmacology and Therapeutics[1], McGill University, McIntyre Medical Sciences Building, 3655 Promenade Sir-William-Osler, Montreal H3G 1Y6, Canada. Department of Biochemistry and Molecular Biology[2], Department of Pharmacology[3], Merck Frosst Centre for Therapeutic Research, Pointe-Claire, Dorval H9R 4P8, Quebec, Canada. Department of Psychiatry and Pharmacology[4], Sir Charles Tupper Medical Building, 5850 College Street, Halifax, Nova Scotia B3H 1X5, Canada

5.1. Abstract

The ability of fimbria-fornix bilateral axotomy to elicit calpain- and caspase-3 activation in the rat septohippocampal pathway was determined using antibodies that selectively recognize either calpain- or caspase-cleavage products of the cytoskeletal protein αII-spectrin. Radioenzymatically determined choline acetyl transferase (ChAT) activity was elevated in the septum at day 5, but reduced in the dorsal hippocampus at days 3, 5 and 7 after axotomy. Prominent accumulation of calpain-, but not caspase-3-, cleaved spectrin proteolytic fragments was observed in both the septum and dorsal hippocampus 1-7 days after axotomy. ChAT-positive neuronal cell bodies in the septum also displayed calpain-cleaved -spectrin indicating that calpain activation occurred in cholinergic septal neurons as a consequence of transection of the septohippocampal pathway. Calpain-cleaved αII-spectrin immunoreactivity was observed in cholinergic fibers coursing through the fimbria fornix, but not in pyramidal neurons of the dorsal hippocampus, suggesting that degenerating cholinergic nerve terminals were the source of calpain activity in the dorsal hippocampus following axotomy. Accumulation of calpain-cleaved -spectrin proteolytic fragments in the dorsal hippocampus and septum at day 5 after axotomy was reduced by intracerebroventricular administration of two structurally distinct calpain inhibitors. Calpain inhibition partially reduced the elevation of ChAT activity in the septum produced by transection but failed to decrease the loss of ChAT activity in the dorsal hippocampus following axotomy. These findings suggest that calpain activation contributes to the cholinergic cell body response and hippocampal axonal cytoskeletal degradation produced by transection of the septohippocampal pathway.

Keywords: axotomy, neurodegeneration, rodents, cholinergic, spectrin, apoptosis

5.2. Introduction

Considerable attention has been devoted to elucidation of the molecular mechanisms responsible for neuronal cell death in acute and chronic neurodegenerative disorders such as motor neuron disease, Huntington's disease, Parkinson's disease and Alzheimer's disease (Cotman and Anderson, 1995; Sawa, 1999; Behl, 2000; Heintz and Zoghbi, 2000; Hugon et al., 2000; Honig & Rosemberg, 2000; Shimohama, 2000; Terry, 2000; Yuan and Yankner, 2000; Raff et al., 2002). The accumulative effects of neuronal loss appear to be more relevant for clinical deficits that occur in late stages of these diseases. In contrast, synaptic loss resulting in local and global disconnection within the telencephalon may account for cognitive deficits that occur at earlier stages of chronic neurodegenerative disorders (Masliah et al., 1990; DeKosky et al., 1990; 1996; Terry, 2000). For instance, neuropathological studies have shown that synaptic loss in the hippocampus and the tempo-parietal cortex are the most prominent features of early stages of Alzheimer's disease (Hyman et al., 1990; Arriagada et al., 1992).

Dysfunction of the cholinergic septohippocampal system has been thought to underlie many of the cognitive deficits observed in Alzheimer's disease (Hyman et al., 1984) and aged rats that are behaviorally impaired (Gage et al., 1984). Interest in this cholinergic pathway has been increased by neuropathological studies implicating loss of basal forebrain cholinergic neurons in cognitive decline in Alzheimer's disease and other degenerative dementing disorders (Bartus et al., 1985).

The septum and the hippocampus are interconnected primarily by the fimbria, fornix, and supracallosal stria (Raisman, 1966; Mosko et al., 1973; Meibach & Siegel, 1977; Crutcher et al.,1981; McKinney et al.,1983; Gage et al.,1983; Amaral et al., 1985). Quantitatively, 60%, 30%, and 10% of the total content of choline acetyl transferase (ChAT) activity in the hippocampus are contributed by the fimbria-fornix, supracallosal and ventral pathways, respectively (Storm-Mathisen and Blackstad, 1964).

Historically, the loss of septal cholinergic and non-cholinergic neurons after fimbria-fornix transection has been assessed by measurement of Nissl-stained cell bodies as well as acetylcholinesterase and ChAT-immunopositive neurons in the medial septum (Gage et al., 1986; Hefti, 1986; Williams et al., 1986; Kromer, 1983; Frotscher, 1988;

Sofroniew and Isacson, 1988; O'Brien et al., 1990; Naumann et al., 1992; 1994). It has been hypothesized that disconnection of medial septal cholinergic neurons from the hippocampus eventually results in the death of these cells (Gage *et al.*, 1989). However, the short-term up-regulation of cholinergic markers produced by administration of nerve growth factor (NGF) (Hagg et al., 1988), or recombinant human brain derived neurotrophic factor (rhBDNF) (Knusell et al., 1992) as well as the spontaneous recovery of ChAT enzymatic activity (Gage et al.,1986; Naumann et al.,1994) suggest that axotomized neurons in the septal complex may not actually die following transection of the fimbria-fornix, but rather become refractory to histological detection (Peterson et al., 1990; Sofroniew et al. 1990; Naumann et al. 1992; Sofroniew et al. 1993; Hage et al. 1996).

However, conflicting results concerning the relative roles of caspase and calpain activation in septo-hippocampal denervation or excitotoxicity (Seubert et al., 1988; Ginsberg et al., 1999; Anguelova et al., 2000; Kolasa and Harrell, 2000; Cowan et al., 2001; Ginsberg and Martin, 2002), cortical brain injury produced by fluid-percussion (Pike et al.,1998; 2001; Singleton et al., 2002; Stone et al., 2002) and middle cerebral artery occlusion (Nath *et al.*, 2000) have motivated us to evaluate whether these proteases contribute to the loss of ChAT activity following axotomy of the septohippocampal pathway.

In the present study, we have evaluated the role of caspase-3 and calpain activation in a model of cholinergic septohippocampal disconnection produced by transection of the fimbria-fornix pathway with a microknife. Using antibodies that recognize multiple caspase-3 and calpain-generated αII-spectrin proteolytic fragments or specific *neo*-epitopes sequences in αII-spectrin generated by caspase-3 and calpain-mediated cleavage of this protein, we have found that calpain, but not caspase-3, is predominantly activated by transection of the fimbria-fornix pathway. Axotomized cholinergic cell bodies located in the septum showed a transient increase in radioenzymatically and histochemically determined ChAT activity. In contrast, a reduction of ChAT activity and immunopositive terminals in the rostral pole of the dorsal hippocampus was evident after axotomy. These alterations in ChAT activity and immunoreactivity were paralleled by accumulation of calpain-generated -spectrin

proteolytic fragments in the septum and hippocampus. In the septum, elevated ChAT activity was partially reduced by administration of calpain inhibitors, but despite the fact that accumulation of calpain-cleaved spectrin fragments in the septum and dorsal hippocampus was prevented by calpain inhibition, the decline in ChAT activity in the dorsal hippocampus was not reversed.

5.3. Material and experimental methods

5.3.1 Bilateral fimbria-fornix axotomy

A retractable tungsten wire blade released by a model 120 microknife device from Kopf (Tujunga, Cal. USA) was used to transect the fimbria-fornix pathway in rats. Adult male (250-275 *g*) Sprague-Dawley rats (Charles River, USA) were anesthetized with ketamine/xylazine (75/5 mg/kg, i.p.) and mounted in a stereotaxic frame (Stoelting Co, IL. USA) secured by ear and incisor bars positioned –3.5 mm ventral from interaural zero. A midline cranial incision was made, the soft tissues were reflected, and a bilateral craneotomy 1.0 mm in diameter performed –1.6 mm from bregma and ± 0.6 mm from midline (ML) according to the Atlas of Paxinos and Watson (1997). Fimbria-fornix axotomy was produced by gradually lowering the microknife introduced at these coordinates to a position –5.5 mm from the skull surface. Transection of fibers was produced by moving the extended blade (2.5 mm in length) of the microknife up and down 2-3 times a distance of 2 mm. The blade was then retracted, the microknife slowly withdrawn and the skin wound sutured. Sham-injured animals underwent identical surgical procedures but did not receive axotomy. Appropriate pre- and post-injury management was maintained to insure that compliance was made with all guidelines set forth by the Merck Frosst Research Center Animal Care Committee.

5.3.2. Brain tissue preparation

At the appropriate time-points, eight to twelve axotomized or sham-injured animals were euthanized by decapitation under deep anesthesia (Somnotol, 120 mg/kg, i.p., sodium

pentobarbital, MTC pharmaceuticals, Cambridge, On., Canada). To dissect the septum and the rostral pole of the dorsal hippocampus, the brain was dissected on ice, rinsed in ice cold 0.05 M Tris~HCl buffer (Gibco) containing 0.002 M ethylenediaminetetraacetic acid (EDTA, Gibco), and 0.001 M L-883,826 (caspase-3 inhibitor). Hemispheres were separated and the corpus callosum sectioned longitudinally to expose the septum. Then a vertical cut was performed at the end of the septum, followed by horizontal cut between anterior comisuras. The hippocampi were isolated from the cerebral cortex and orientated rostrocaudally side by side to be sectioned in four segments that were snap frozen in liquid nitrogen. Samples were stored at –80 °C until analysis. On the day of analysis, samples were homogenized in an Eppendorf tube with a Teflon Konter pestle with 0.15 ml of ice-cold TNE detergent lysis buffer (0.05 M Tris, 0.002 M EDTA, 1% nonidet-40, 0.001 M L-883,326) containing a miniprotease cocktail inhibitor (Roche) and then maintained on ice for 30 min and finally centrifuged at 14000*g* for 25 min at 4 °C.

5.3.3. Immunoblot analyses of septal and dorsal hippocampal tissues

Protein concentrations of supernatant from tissue homogenates were determined by bincichonic acid microprotein assays (Pierce Inc., Rockford, Il, USA) with bovine serum albumin as a standard. Protein balanced samples were prepared for sodium dodecyl sulfate-polyacrylamide gel electrophoresis (SDS-PAGE) in six-fold loading buffer containing 0.25 M Tris (pH 6.8), 0.2 M dithiothreitol (DTT), 8% sodium dodecyl sulfate (SDS), 0.02% bromophenol blue, and 20% glycerol in distilled H_2O. Samples were heated for 5 min at 95°C. Forty-five micrograms of protein per lane were routinely resolved by SDS-PAGE on 6% or 4-20% tris/glycine gels for 2 h at 110 V. Following electrophoresis, separated proteins were laterally transferred to nitrocellulose membranes (0.45 μm) in a transfer buffer containing 0.192 M glycine and 0.025M Tris (pH 8.3) with 10% methanol at a constant voltage (100 V) for 1 h at 4°C. Blots were blocked for 1 h at ambient temperature in 5% non-fat milk in TBS. Ponceau Red (Sigma, St Louis, Mo, USA) was used to stain membranes to confirm successful transfer of protein and to ensure that an equal amount of protein was loaded in each lane.

Immunoblots containing septal or dorsal hippocampal protein were probed with an αII-spectrin monoclonal antibody (MAB1622, Chemicon, Temecula, Cal, USA) that detects intact non-erythoid αII-spectrin (280 kDa) as well as 150, 145, and 120 kDa fragments of αII-spectrin (Figure 5.1). A proteolytic fragment of 150 kDa is initially produced by calpain- or caspase-3 mediated cleavage of αII-spectrin (Nath *et al.*, 1996; Wang *et al.*, 1998). The calpain-generated 150 kDa product is further cleaved by calpain to yield a 145 kDa fragment (Harris *et al.*, 1988; Nath *et al.*, 1996a, b) or caspase-3 to yield a specific product of 120 kDa (Nath *et al.*, 1996; Wang *et al.*, 1998). To further confirm the specificity of calpain-cleaved -spectrin proteolytic fragments, two additional antibodies against αII-spectrin (FG6090, Affinity Research Products Limited, Mamhead Castle, Mamhead, Exeter, UK) that recognize the holoprotein, calpain- and caspase-3 generated fragments, as well as the calpain-cleaved 145 kDa proteolytic fragment were used. An affinity purified antibody raised in goats using the C-termini *neo*-epitope CQQQEVY generated by calpain ($\alpha\Delta C^{calpain}$-αII-spectrin) was custom prepared by Chemicon (Temecula, CA, USA) according to the method published by Robert-Lewis *et al.*, (1994) (Figure 5.1). To characterize the caspase-3 cleaved -spectrin 120 kDa fragment, a custom generated, affinity purified, antibody raised in rabbits against the N-termini *neo*-epitope SVEALI exposed by caspase (Figure 5.1) ($\alpha\Delta N^{caspase}$-αII-spectrin) was prepared according to the method described by Rohn *et al.*, (2001).

Following 2 h of incubation at room temperature with MAB1622 (1/1000 dilution), FG6090 (1/3000 dilution), $\alpha\Delta C^{calpain}$-αII-spectrin (1/250 dilution) or $\alpha\Delta N^{caspase}$-αII-spectrin (1/200 dilution) in 5% non-fat milk, blots were subsequently incubated for 1 h at room temperature with 5% non-fat milk containing a horseradish peroxidase-conjugated goat anti-mouse IgG, rabbit anti-goat IgG or anti-rabbit IgG (each diluted 1/5000). Enhanced chemiluminiscence (Supersignal, Pierce) reagents were used to visualize immunolabeling on Kodak Biomax ML film.

5.3.4. Immunohistochemistry

Sham-operated and fimbria-fornix lesioned animals were examined at day 5 (n=3) and 7 (n=3) following surgery. These animals were transcardially perfused under deep

anesthesia (Somnotol, 120 mg/kg, ip, sodium pentobarbital, MTC pharmaceuticals, Cambridge, On, Canada) with saline (0.9%) followed by phosphate buffer (0.1M) containing 4% paraformaldehyde according to the method described by Cote *et al.*, (1993). Brains were removed from the skull, postfixed for 3 h in 4% paraformaldehyde in phosphate buffer (0.1M). Perfused brain tissues were maintained at 4°C in phosphate buffered saline (PBS, 0.01 mM) containing 10% sucrose until sectioning. Sections 10 µm thick were cut using a cryostat, mounted on superfrost slides and stored at –80 °C until staining. Tissue sections were washed with PBS then treated with 0.3% hydrogen peroxide in 100% methanol for 15 min at room temperature (RT), and permeabilized with PBS containing 0.1% Triton X-100 at RT for 30 min.

Nonspecific sites were blocked by incubation with 15% normal serum from the species where the secondary was raised for 30 min. Slides were then incubated with either $\alpha\Delta C^{calpain}$-αII-spectrin or choline acetyl tranferase antibodies at 4 °C overnight. Biotinylated secondary antibodies (Vector Labs) at a dilution of 1/200 were applied for 1 h at RT and immunoreactivity detected using diaminobenzidine (DAB) brown substrate kits (Vector). Fluorescence immunodetection was obtained using Alexa fluor 488 donkey anti-goat or Alexa fluor 594 donkey anti-goat antibodies (diluted 1/250) (Molecular Probes, Inc. Eugene, Or. USA). No specific staining was detected on slides lacking the primary antibody. Slides from sham-operated and axotomized animals were routinely stained side by side in a single and double labeling paradigm using the same batch of antibodies.

We examined immunohistochemical labeling of the septum and the dorsal hippocampus in 2-3 sections/brain sample. All histological and immunohistochemical images were acquired from a Zeiss Axioplan 2 microscope equipped with a Sony 3 CCD DXC-950 color video camera routed via a Sony camera adaptor CMA-D2 to a computer.

5.3.5. Choline-Acetyl Transferase (ChAT) enzymatic activity assay

Tissue extracts were stored at -70 °C until assayed. ChAT activity was determined using a modified version of the method of Fonnum (1975). Briefly, 20 µl of tissue extracts were incubated in a 0.05 M sodium phosphate buffer (pH 7.4) containing 0.01 M

disodium EDTA, 0.01 M choline chloride, 0.3 M sodium chloride and 0.001 M eserine sulfate. The assay was initiated by the timed addition of 10 µl of ^{14}C-acetyl CoA (NEN NEC-313; 12.5 mCi/mmol; 0.1 mM). Tubes were incubated at 37 °C in a metabolic incubator under gentle shaking for a 20 min period. The reaction was terminated by the timed addition of 500 µl of 3-heptanone containing 10 mg/ml sodium tetraphenylboron. Samples were then vortexed and placed on ice. Tubes were centrifuged for 1 min. in a Fisher Micro-centrifuge, and 200 µl of the supernatant were counted in 5 ml Ecolume using a liquid scintillation counter. Blanks were obtained in the absence of choline substrate and data expressed in µmoles ^{14}C-ACh formed / mg protein / hr.

5.3.6. Intracerebroventricular administration of calpain inhibitors

Osmotic minipumps (Alza Corp) were loaded with 200 µl of vehicle (sterile saline containing 2% dimethyl sulfoxide and 10% cyclodextrin) (RBI, Natick. MA) or leupeptin (Sigma) (10 mg/ml, 0.25 mg/day) or MDL 28,170 (1 mg/ml, 0.025 mg/day) were primed overnight at 37°C. These pumps were implanted at the same time that axotomy was performed. The injection cannulae were implanted in the left lateral ventricle at the coordinates from bregma: AP -0.9 mm, ML 1.4 mm and DV -3.5 mm from the skull surface. All animals were euthanized 5 days after axotomy.

5.3.7 Statistical analysis

Analysis of variance (ANOVA) with a mixed design was carried out to compare the values for ChAT activities or the optical density of bands corresponding to calpain-cleaved -spectrin proteolytic fragments in the septum and the dorsal hippocampus of axotomized and sham-operated animals. Significant interactions were further analyzed using one-way ANOVAs, paired t-tests and post-hoc Tukey tests. If heterogeneity of variance was detected by the Levene's test, non-parametric equivalents to the parametric tests were performed (exact tests mentioned in results). All analyses were considered significant when $P<0.05$, and were conducted using the SPSS statistical package (Version 10.05, 1999).

5.4 Results

5.4.1 Effects of axotomy on choline acetyl transferase activity in the septum and dorsal hippocampus

A significant structure by time after axotomy interaction for ChAT activity after bilateral axotomy was detected [F(4,51)=13.75, $P<0.001$] (Figure 5.2). Differences for ChAT activity values in the septum and dorsal hippocampus became progressively more pronounced after axotomy with peak increases occurring at day 5. To further explore this interaction, we analyzed ChAT activity over time after axotomy separately for each structure. The Levene's test for heterogeneity of variance revealed that ChAT activities in the septum at different times after axotomy were heterogeneous. As a result, a non-parametric statistical analysis was performed to test for potential effects of axotomy on ChAT activity in the septum and dorsal hippocampus at various intervals after axotomy. The Kruskal-Wallis one-way ANOVA for ranked data revealed that ChAT activity levels in the septum and the dorsal hippocampus significantly changed over time after axotomy, [$\chi^2(4)=18.39$, $p<0.01$)] and [$\chi^2(4)=36.31$, $P<0.001$], respectively (Figure 5.2). Post-hoc Mann-Whitney U Tests were conducted with Bonferroni corrections to compare the sham group with each of the post-axotomy groups. For the septum, ChAT activity was elevated 1, 3 and 5 days after axotomy relative to the sham group (U=5 to 16, $P<0.01$ to 0.001). In contrast, ChAT activity in the dorsal hippocampus was reduced 3, 5 and 7 days after axotomy relative to sham animals (U=0 to 7, $P<0.001$).

Consistent with increased ChAT activity in the septum at day 5 after axotomy, ChAT immunoreactivity also appeared to be elevated in the septum at this time. Immunohistochemical detection of ChAT revealed densely labeled cholinergic fibers in the dorsolateral quadrant of the septum (Figure 5.3C). The decrease in ChAT activity observed in the dorsal hippocampus was accompanied by a loss of ChAT immunoreactive fibers coursing through the fimbria-fornix to the dorsal hippocampus and ChAT-positive terminals in the CA3 layer of the dorsal hippocampus (Figure 5.3D).

5.4.2. Effects of fimbria-fornix axotomy on proteolysis of αII-spectrin by calpain and caspase-3 in the septum and dorsal hippocampus

Axotomy of the fimbria-fornix resulted in the accumulation of the 145 and 150 kDa proteolytic fragments of αII-spectrin in the septum and dorsal hippocampus (Figure 5.4A and 5.4B). A significant 3-way interaction between structure, -spectrin fragment size and time after axotomy was observed [$F(4,43)=5.46$, $P<0.01$]. Specifically, it was found that differences between the optical density value (ODVs) for the 145 and 150 kDa fragments in the septum at day 1 and 7 after axotomy were larger relative to the differences observed for these fragments in the hippocampus at the same time points, [$t(9)=2.75$, $P<0.05$], and [$t(9)=4.79$, $P<0.01$], respectively. Excluding structure from the analysis revealed that there was a significant time after axotomy by fragment size interaction [$F(4,43)=21.38$, $P<0.001$]. As the delay after axotomy increased, a greater difference in optical density values (ODVs) was observed between the fragment subtypes. Main effects for structure, fragment subtype and time after axotomy were also observed, [$F(1,43)=4.39$, $P<0.05$], [$F(1,43)=113.38$), $P<0.001$], and [$F(4,43)=32.44$, $P<0.001$], respectively. When each one of these factors was considered alone, there was a significant trend for the 145 kDa fragment to be elevated to a greater extent than the 150kDa fragment. Over time, ODVs increased significantly to peak at day 3 after axotomy with decreases occurring thereafter which approached day one values. Mann-Whitney U tests showed that for the septum, but not the hippocampus, ODV were higher at day 1 after axotomy compared to the sham condition. This suggests that the calpain-generated 145and 150 kDa αII-spectrin proteolytic fragments increased more quickly after axotomy in the septum relative to the hippocampus [$U=18$, $P<0.05$; and $U=16$, $P<0.05$].

Low basal levels of the 120 kDa fragment generated by caspase-3-mediated cleavage of spectrin were detected in the septum and hippocampus (Figure 5.4A and 5.4B). ODVs for this band were not elevated in either of these structures by axotomy. These results were confirmed using an antibody that recognizes the caspase-3 N-terminal *neo*-epitope of spectrin ($\alpha\Delta N^{caspase}$-αII-spectrin) (data not shown).

To provide additional confirmation of calpain-mediated cleavage of αII-spectrin in the septum and hippocampus after axotomy, tissue samples from these areas of axotomized animals were analyzed using the FG6090 and calpain-cleaved αII-spectrin 145 kDa *neo*-epitope ($\alpha\Delta C^{calpain}$-αII-spectrin) antibodies. FG6090, recognizes the complete family of proteolytic fragments of spectrin generated by caspase-3- and calpain-mediated cleavage (150 kDa, 145 kDa and 120 kDa fragments) that are identical in mass to proteolytic fragments detected by the monoclonal antibody MAB1622 described in the Methods. Similar results were obtained in the septum and dorsal hippocampus with the FG6090 and MAB1622 antibodies (results not shown). The $\alpha\Delta C^{calpain}$-αII-spectrin antibody specifically recognizes the 145 kDa fragment generated by calpain-mediated cleavage of spectrin and does not recognize the holoprotein or proteolytic fragments generated from this protein. Using the $\alpha\Delta C^{calpain}$-αII-spectrin antibody, we observed an increase in the 145 kDa proteolytic fragment of -αII-spectrin in the dorsal hippocampus after axotomy [$F(4,23)=26.62$, $P<0.001$] (Figure 5.5). Post-hoc analyses showed that the sham group had significantly lower ODVs compared to animals examined 1, 3, 5 and 7 days after axotomy. This increase peaked at day 3 with a decline in levels of the 145 kDa fragment observed from day 5 to 7. Similar findings were observed in the septum (results not shown).

Accumulation of the 145 kDa fragment generated by calpain-mediated cleavage of αII-spectrin was also detected by immunohistochemistry. In sham-surgery animals, $\alpha\Delta C^{calpain}$-αII-spectrin immunoreactive cell bodies were not detected in the septum or the dorsal hippocampus (Figure 5.6A, C). In contrast, we observed numerous $\alpha\Delta C^{calpain}$-αII-spectrin immunoreactive cell bodies at day 5 and 7 after axotomy in the septum. Closer examination revealed that $\alpha\Delta C^{calpain}$-αII-spectrin immunoreactivity located in cell bodies of the septum was restricted to the cytosol and typically punctate in appearance (Figure 5.6B). In the dorsal hippocampus, $\alpha\Delta C^{calpain}$-αII-spectrin immunoreactivity was located in the blunt-ends of transected fibers (Figure 5.6D, circles) and was not detected in CA1-CA3 pyramidal neurons.

A partial overlap between ChAT and $\alpha\Delta C^{calpain}$-αII-spectrin immunoreactivities was observed in cell bodies of the septum at day 5 after axotomy suggesting calpain activation occurred in axotomized cholinergic cell bodies but was not restricted to this

cell type (Figure 5.7). The co-localization of ChAT and $\alpha\Delta C^{calpain}$-αII-spectrin immunoreactivities in the stumps of transected fibers in the dorsal hippocampus is indicative of an adaptive response of cholinergic neuronal cell bodies to axotomy. Our failure to detect $\alpha\Delta C^{calpain}$-αII-spectrin immunoreactivity in pyramidal neurons of the dorsal hippocampus after axotomy suggests that calpain activation in axotomized cholinergic fibers is solely responsible for the elevation of 150 and 145 kDa -αII-spectrin fragments detected in this structure following fimbria-fornix axotomy.

5.4.3 Inhibition of axotomy-induced calpain-mediated -αII-spectrin proteolysis by calpain inhibitors

The calpain inhibitors leupeptin and MDL 28,170 were used to determine whether inhibition of calpain activity prevents the accumulation of -αII-spectrin proteolytic fragments (145 and 150 kDa) in the septum (Figure 5.8A) and dorsal hippocampus (Figure 5.8B) and normalizes cholinergic function in these regions after axotomy. Intracerebroventricular infusions of vehicle, leupeptine and MDL 28,170 were performed on separate groups of rats immediately after axotomy. ChAT activity and accumulation of calpain-generated -αII-spectrin proteolytic fragments were examined at day 5 after axotomy. A significant fragment subtype by compound interaction was observed for ODVs, [$F(2,30)=11.82$, $P<0.001$] (Figure 5.8). To further characterize the basis for this interaction, a separate analysis was conducted excluding structure as a factor. Separate one-way ANOVAs were conducted for ODVs with respect to fragment types, taking into consideration inhibitor treatments. Inhibitor treatments had a significant effect on the 145 kDa and 150 kDa fragments levels, [$F(2,63)=18.63$, $P<0.001$], and [$F(2,63)=10.52$, $P<0.001$], respectively. Post-hoc analyses showed that for the 145 kDa fragment, ODVs were lower for the leupeptin compared to the vehicle and MDL 28,170 treated rats, which were not different from one another. For the 150 kDa fragment, ODVs were higher for the vehicle than leupeptin and MDL 28,170 groups that were not different from one another. Leupeptin and MDL 28,170 produced a 60 and 80% decrease, respectively, in the accumulation of calpain-cleaved αII-spectrin proteolytic fragments at day 5 after

axotomy relative to lesioned animals treated with vehicle when not taking fragment subtype into consideration.

The effects from the compounds were further explored by conducting one-way ANOVAs on the ODVs for each fragment size in the two structures separately. Significant differences were found for the 145 and 150 kDa fragments in the septum and for the 145 kDa fragment in the dorsal hippocampus, [$F(2,30)=6.32$, $P<0.01$], [[$F(2,30)=5.97$, $P<0.01$], and [$F(2,30)=14.00$, $P<0.001$], respectively. Post-hoc analyses revealed that in the septum, ODVs for the 145 kDA fragment were reduced in the leupeptin group compared to the vehicle group. In the case of the 150 kDa fragment, both leupeptin and MDL 28,170 reduced ODVs relative to the vehicle group. In the dorsal hippocampus, leupeptin reduced ODVs for the 145 kDa fragment relative to the MDL-28,170 and vehicle groups. Levene's test detected heterogeneity of variance when ODVs were analyzed for the 150 kDa fragment in the dorsal hippocampus. Square root transformations did not correct this problem. Non-parametric analyses did not detect any differences in ODVs for the 150 kDa fragment between the vehicle and drug treated groups in the dorsal hippocampus. Thus, it was concluded that calpain inhibition was effective in reducing both 145 and 150 kDa αII-spectrin fragment accumulation in the septum as well as the generation of the 145 kDa, but not the 150 kDa, fragment of αII-spectrin in the dorsal hippocampus after axotomy.

5.4.4. Effects of calpain inhibition on alteration in ChAT activity in the septum and dorsal hippocampus after axotomy

A two-way ANOVA was performed to examine the relationship between calpain inhibitor treatment and structure on ChAT levels. A significant interaction was found for these factors [$F(1,33)=6.05$, $P<0.01$] (Figure 5.9). To elucidate the nature of this interaction, one-way ANOVAs were conducted on the structures separately. A non-parametric test was used for these analyses because of heterogeneity of variance of the ChAT activity levels. A Kruskal-Wallis one-way test for ranked data detected differences in ChAT levels for the septum [$\chi^2(3)=9.87$, $P<0.05$] and the hippocampus [$\chi^2(3)=20.70$, $P<0.001$] that was dependent on treatment. Post-hoc analysis using the Mann Whitney U test with

Bonferroni corrections revealed that for the septum, ChAT levels were significantly higher for axotomized animals treated with vehicle compared to sham animals. No differences were detected between the calpain inhibitor treated groups and the sham group, suggesting that the calpain inhibitors normalized ChAT levels in the septum after axotomy. For the hippocampus, the sham group had higher ChAT levels compared to all other groups indicating that calpain inhibition failed to prevent the reduction in ChAT activity produced by axotomy.

5.5. Discusion

5.5.1 Changes in ChAT activity in the septum and hippocampus. Adaptive response in neuronal cell bodies and projection fibers to terminal fields

We observed that transection of the fimbria-fornix pathway produced a rapid but transient increase of ChAT activity in the septum that was paralleled by a rapid and sustained reduction of ChAT activity in the dorsal hippocampus. These biochemical changes were accompanied by an accumulation of calpain-cleaved non-erythroid αII-spectrin proteolytic fragments in axotomized septohippocampal cholinergic neurons.

The elevation of ChAT activity in the septum at day 5 and 7 after axotomy as well as the swelling of ChAT immunoreactive fibers in the dorsolateral quadrant of the septum implies a resistance of cholinergic somas to the injurious effects of axotomy at these early time points. These findings are somewhat in agreement with a report by Peterson *et al.*, (1990) and Naumann *et al.*, (1992) in which axotomy resulted in a minor loss of cholinergic neurons at short survival intervals. In the present study, we performed transections of the fimbria-fornix pathway at coordinates further away from cholinergic somas in the septum than the study by Peterson *et al.*, (1990). However, we did not detect a significant change in ChAT activity in the septum at 7 and 14 days after axotomy, despite the fact that these lesions produced a significant reduction of ChAT activity in the dorsal hippocampus (data not shown). Consequently, axotomy proximal to the cell bodies of cholinergic neurons may be more likely to produce neuronal cell death than distal axotomy.

Our results are in agreement with previous studies by Gage *et al.*, (1986) and Armstrong *et al.*, (1987) in which an accumulation of ChAT immunoreactivity was observed in the severed ends of cholinergic fibers that progressed in a time-dependent fashion towards the cell soma. These bulbous swellings are produced by passive accumulation of ChAT in the stumps of severed cholinergic fibers in transit to terminal fields of the fimbria-fornix pathway. Otherwise, we hypothesize that the elevation of ChAT activity and immunoreactivity in the septum following axotomy may represent an adaptive response of cholinergic cell bodies to terminal loss in the dorsal hippocampus. In support of this proposal, previous studies have reported elevation of ChAT activity in the septum accompanied by a reduction in ChAT activity in the dorsal hippocampus following intracerebroventricular administration of ethylcholine aziridinium mustard (AF64A), a specific irreversible choline uptake inhibitor (El Tamer *et al.*, 1993, Ayala-Grosso and Urbina, 1999) or bilateral transection (Hage et al., 1996).

Our observation that fimbria-fornix transection results in a transient elevation of ChAT activity in the septum is consistent with a number of reports indicating that septohippocampal neurons do not die following axotomy (Gage *et al.*, 1986; Peterson *et al.*, 1990; Sofroniew et al. 1990; Naumann et al. 1992; 1994; Sofroniew et al. 1993; Hage et al. 1996). Indeed, at least in young animals, septohippocampal neurons projection neurons may survive disconnection and are able to regenerate and reinnervate hippocampal tissue (Linke et al., 1995). These findings have led Frotscher *et al.*, (1996) to propose that septohippocampal neurons may have a unique ability to withstand the injurious effects of axotomy. In adult animals, only uninjured septohippocampal fibers may sprout following entorhinal cortical lesion (Cotman and Nadler, 1978; Frostcher et al., 1996). Axotomized septohippocampal neurons in adult animals can, however, be encouraged to sprout if growth factors are provided (Hefti, 1986; Hagg et al. 1988).

In contrast to the aspiration method, which is commonly used to produce fimbria-fornix transection, cutting septohippocampal axons with a microknife produces a discrete lesion located in a pre-selected coronal plane. This later experimental approach may therefore elicit a response that has not been observed previously with the classical aspiration method (Sofroniew & Isacson, 1988; Koliatsos *et al.*, 1993).

5.5.2 Changes in ChAT activity in the septum and hippocampus are associated with accumulation of calpain-cleaved non-erythroid αII-spectrin proteolytic fragments in axotomized animals

Our results also indicate that activation of the cysteine protease calpain, but not caspase-3, is primarily involved in the generation of αII-spectrin proteolytic fragments after axotomy of septohippocampal neurons. Using antibodies that recognize caspase-3 and calpain-cleaved spectrin products with identical molecular weights as predicted by Nath *et al.*, (2000) and Wang *et al.*, (1998), we found a prominent accumulation of calpain-(145 kDa), but not caspase-3- generated (120 kDa) breakdown spectrin products after axotomy. Furthermore, using additional antibodies that selectively recognize either the C-terminus neo-epitope in calpain-cleaved spectrin (145 kDa fragment) or caspase-3-cleaved spectrin (120 kDa fragment), we demonstrated that fimbria-fornix transection produced a preferential activation of calpain activity leading to proteolysis of the cytoskeletal protein αII-spectrin. Significantly greater accumulation of the calpain specific 145 kDa breakdown spectrin product than the 150 kDa proteolytic fragment in the septum and dorsal hippocampus indicates that calpain activity drove production of the 150 proteolytic fragment. In contrast, lack of accumulation of the caspase-3 specific 120 kDa fragment of spectrin indicates that caspase activation played a minor role in generation of the 150 kDa proteolytic fragment after axotomy. Consistent with this hypothesis, intracerebroventricular administration of calpain inhibitors such as leupeptin and MDL 28,170 reduced generation of the 150 kDa fragment of spectrin in the septum following transection of the septohippocampal pathway. The proposal that calpain activation may be part of an adaptive response of septohippocampal neurons to axotomy is supported by studies indicating that calpain activation is necessary for cytoskeletal disassembly and remodeling responsible for synaptic plasticity (Lynch & Baudry, 1984) and membrane resealing after neurite transection (Xie & Barrett, 1991: George et al, 1995).

Proteolysis of spectrin occurred too rapidly to be triggered by the complete structural deterioration of the septohippocampal pathway. For instance, ChAT activity was elevated in the septum from day 1 - 5 after axotomy. These increases in ChAT

activity were accompanied by a build-up of ChAT immunoreactivity in cholinergic neurons in the septum suggestive of an immediate and sustained response of cholinergic neurons to transection. Since loss of cholinergic inputs to the dorsal hippocampus may alter the activity of neuronal circuits that influence the activity of cholinergic cell bodies in the septum, this adaptive response might also involve alterations in the activity of projections from the hippocampus to the septum (Sarter *et al.*, 1990; Dragoi *et al.*, 1999; Buzsaki, 2002).

In the present study, we showed that calpain-mediated processing of αII-spectrin is a prominent event following septohippocampal disconnection. Calpain-mediated processing of αII-spectrin has been shown to be a more pronounced response to brain injury than caspase-3 activation following moderate lateral controlled cortical impact (Newcomb *et al.*, 1997; Pike *et al.*, 1998; 2001). However, the time course for the appearance of axotomy-induced αII-spectrin proteolytic fragments observed in the present study was delayed compared to the induction kinetics for calpain activation following traumatic brain injury in a rodent model (Pike e*t al.*, 2001; Seubert *et al.*, 1988). The delayed activation time course for calpain in septohippocampal neurons following axotomy versus cortical neurons after head trauma may be the result of differences in the severity of these types of injuries which influence the intensity of the intracellular signal transduction triggers for calpain activation such as calcium influx.

Axotomy produced a more rapid and sustained rise of calpain-generated proteolytic fragments in the septum than the dorsal hippocampus. This temporal sequence of events paralleled the more rapid alterations in ChAT activity levels observed in the septum compared to the dorsal hippocampus following fimbria-fornix axotomy. These findings suggest that calpain activation in the septum may participate in the signal transduction events that mediate the elevation of ChAT activity in the septum following axotomy. In support of this proposal, calpain inhibition by intracerebroventricular administration of small molecule inhibitors of this protease reduced the increase in septal ChAT activity produced by axotomy. However, calpain inhibition did not completely prevent the increase in ChAT activity in the septum following axotomy suggesting that either a degree of calpain inhibition necessary to completely reverse this response was not achieved or that other effectors are involved in this adaptive response.

Calpain activation in septohippocampal cell bodies may mediate the adaptive response to axotomy by the cleavage of multiple substrates in addition to spectrin such as membrane proteins, voltage-gated calcium channels, protein kinases (protein kinase C and calcium-calmodulin-dependent kinase II) and protein phosphatases, including calcineurin (Kwiatkowski & King, 1989; Saido *et al.*, 1994; Hell *et al.*, 1996; Chan & Mattson, 1999). In addition to cleavage of these substrates, calpain-mediated degradation of spectrin can lead to proteolysis of other cytoskeletal proteins such as integrin (Yan *et al.*, 2001), and NR2A and NR2B subunits of the NMDA receptor and the GluR1 subunit of AMPA receptors (Rong *et al.*, 2001). Calpain activation may also mediate cleavage of p35 to p25 and thereby trigger Cdk5 activity that results in hyperphosphorylation of the microtubule-associated protein tau. Tau hyperphosphorylation is thought to result in disruption of the neuronal cytoskeleton that may contribute to impairment of neural homeostasis in Alzheimer's disease (Patrick *et al.*, 1999). Activated Cdk5 can also phosphorylate the NR2A subunit of the NMDA receptor resulting in altered NMDA-regulated synaptic activity (Guttman *et al.*, 2002).

ChAT immunoreactive cell bodies in the septum were found to contain $\alpha\Delta^{calpain}$-αII-spectrin immunoreactivity demonstrating that cholinergic septohippocampal neurons were a source of elevated ChAT and calpain activities in this structure following fimbria-fornix transection. However, the cellular overlap between ChAT and $\alpha\Delta^{calpain}$-αII-spectrin immunopositive cell bodies in the septum was not complete indicating that after axotomy accumulation of calpain-cleaved spectrin proteolytic fragments occurs in non-cholinergic neurons. Calpain activation following septohippocampal transection may also occur in GABAergic neurons that comprise the second major neuronal cell type in the septum that projects to the dorsal hippocampus (Shute & Lewis, 1963; Lewis *et al.*, 1967; Kohler *et al.*, 1984; Freund & Antal, 1988; Gulyas *et al.*, 1991). Indeed, GABAergic septohippocampal neurons as well as GABAergic interneurons in the septum may be altered by deafferentation of septal cell bodies (Kermer et al., 1995; Heimrich *et al.*, 1996).

Following axotomy, loss of cholinergic terminals in the dorsal hippocampus was reflected by a significant reduction in ChAT activity and ChAT immunoreactivity. Loss of cholinergic terminals in the dorsal hippocampus was not prevented by administration

of calpain inhibitors, however, the potential benefit of this treatment on the cholinergic outcome at later time point was not explored in this study. In agreement with previous studies (Seubert *et al.*, 1988; Pike *et al.*, 2001), calpain inhibition prevented the accumulation of both the 145 and 150 kDa spectrin breakdown fragments indicating that generation of these fragments was driven by calpain activation. Inhibition of calpain activity reversed the elevation of ChAT activity in the septum produced by axotomy. The ability of calpain inhibitors to diminish the effects of axotomy on septohippocampal neurons is in agreement with the ability of calpain inhibitors to prevent -spectrin proteolysis and neuronal loss following electrolytic-induced lesions of the entorhinal lesion (Seubert *et al.*, 1988) and fluid percussion-induced cortical trauma (Pike *et al.*, 2001).

Accumulation of calpain-generated spectrin breakdown products (145 and 150 kDa proteolytic fragments) has been accepted as a specific signature of necrosis. In contrast, accumulation of breakdown products generated by caspase-3 mediated cleavage of spectrin (120 kDa proteolytic fragment) is thought to be indicative of neuronal apoptosis. In the present study, we did not observe an accumulation of caspase-3 generated proteolytic fragments after axotomy suggesting that septohippocampal neurons did not undergo apoptosis following this injury. Axotomy did, however, result in the loss of cholinergic terminals in the dorsal hippocampus that was accompanied by a profound elevation of calpain activity. Attenuation of the accumulation of calpain-generated spectrin proteolytic fragments in the dorsal hippocampus by calpain inhibitors such as leupeptin and MDL28,170 did not reduce the loss of cholinergic terminals in this structure suggesting that either a sufficient degree of calpain inhibition was not achieved to prevent synaptic terminal death or that other events are responsible for this degenerative process after axotomy.

In summary, we have shown that axotomy of the septohippocampal pathway by transection of this projection using a microknife triggers a marked increase in calpain-mediated cleavage of the structural protein αII-spectrin in the cholinergic cell bodies located in the septum and cholinergic terminals in the dorsal hippocampus. These increases in calpain activity were accompanied by an elevation of ChAT activity in the septum and a reduction in this enzymatic activity in the dorsal hippocampus.

Immunohistochemical colocalization of ChAT and calpain-cleaved spectrin suggested that activation of calpain in cholinergic cell bodies might be at least partially responsible for the elevation of ChAT activity in the septum after axotomy. This histochemical approach also revealed that calpain may also be responsible for the loss of cholinergic terminals in the dorsal hippocampus and subsequent decrease of ChAT activity in this structure produced by axotomy. Intracerebral administration of calpain inhibitors decreased the accumulation of calpain cleaved αII-spectrin fragments in the septum and to a lesser degree in the dorsal hippocampus. Taken together, these results suggest that calpain activation in cholinergic cell bodies and terminals may play a distinct role in these neuronal compartments following axotomy.

5.6. Acknowledgements

We wish to thank Kevin Clark (Merck-Frosst Centre for Therapeutic Research) for assistance with the figures. Carlos Ayala-Grosso is a fellow of Consejo de Desarrollo Científico y Humanístico de la Universidad Central de Venezuela (Caracas,Venezuela).

Figure 5.1. Caspase-3 and calpain cleavage sites in αII-spectrin. The molecular mass of αII-spectrin is about 280 kDa. Calpain and caspase-3 cleavage of spectrin results in the generation of two initial fragments of nearly identical size (150 kDa) that differ by 9 only amino acids (not shown). The calpain-generated 150 kDa product is further cleaved by calpain to yield a specific calpain product of 145 kDa (top). The indicated amino acid sequence was used to generate the calpain-cleaved spectrin antibody ($\alpha\Delta C^{calpain}$-αII-spectrin). The caspase-3 generated 150 kDa fragment is further cleaved by caspase-3 to yield a specific caspase-3 signature product of 120 kDa (bottom). The indicated sequence was used as immunogen to generate the caspase-3 cleaved spectrin antibody ($\alpha\Delta C^{caspase}$-αII-spectrin).

FIGURE 5.1

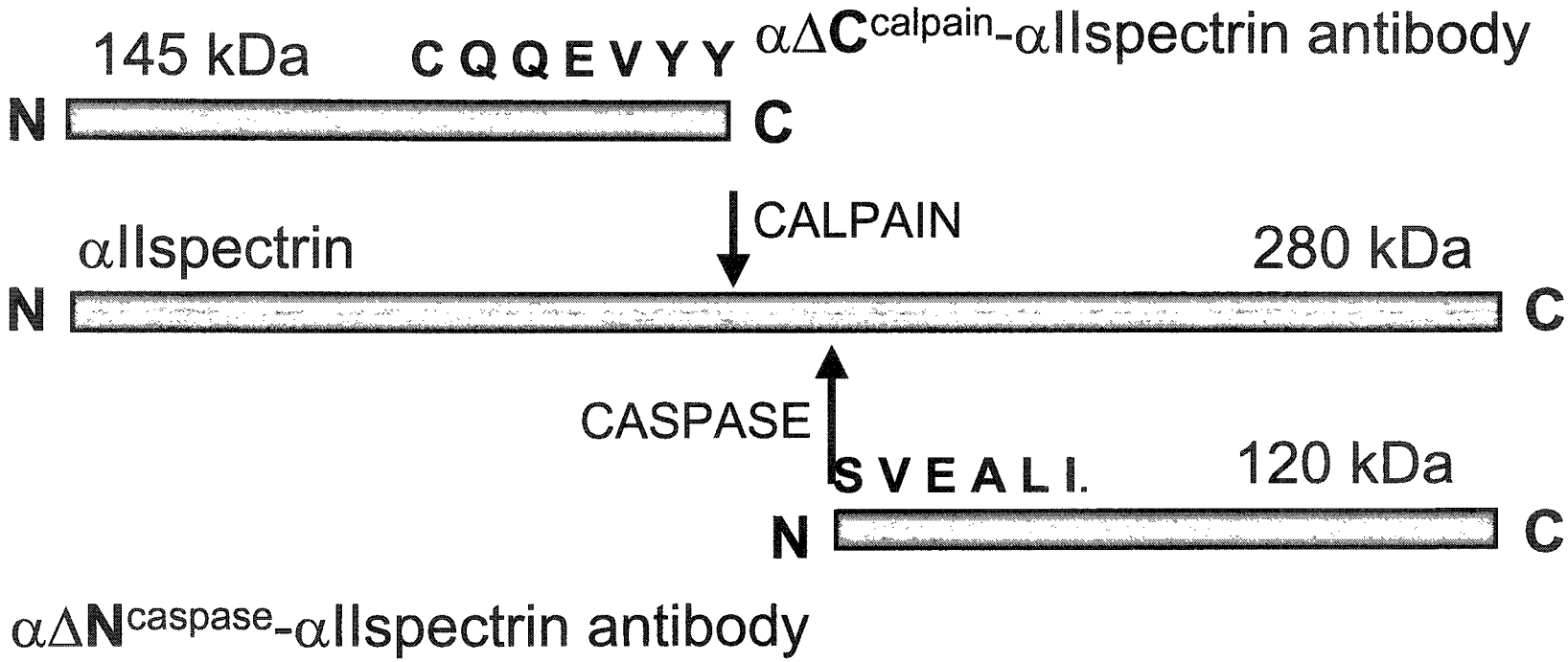
145 kDa
C Q Q E V Y Y
αΔC calpain-αIIspectrin antibody
N
C
αIIspectrin
CALPAIN
280 kDa
N
C
CASPASE
S V E A L I.
120 kDa
N
C
αΔN caspase-αIIspectrin antibody

Figure 5.2. Effects of fimbria-fornix transection on choline acetyl transferase (ChAT) activity in the septum and the dorsal hippocampus. Overall, the septum contained more choline acetyl transferase compared to the dorsal hippocampus. Axotomy elevated ChAT activity in the septum (filled circles) but reduced ChAT activity in the dorsal hippocampus (open circles). These changes in ChAT activity in the septum and the dorsal hippocampus became progressively more pronounced until five days post-axotomy. Values are the mean and S.E.M. of data from 10 animals per group at each time point. * $P<0.05$, ** $P<0.01$ relative to sham-surgery animals.

FIGURE 5.2

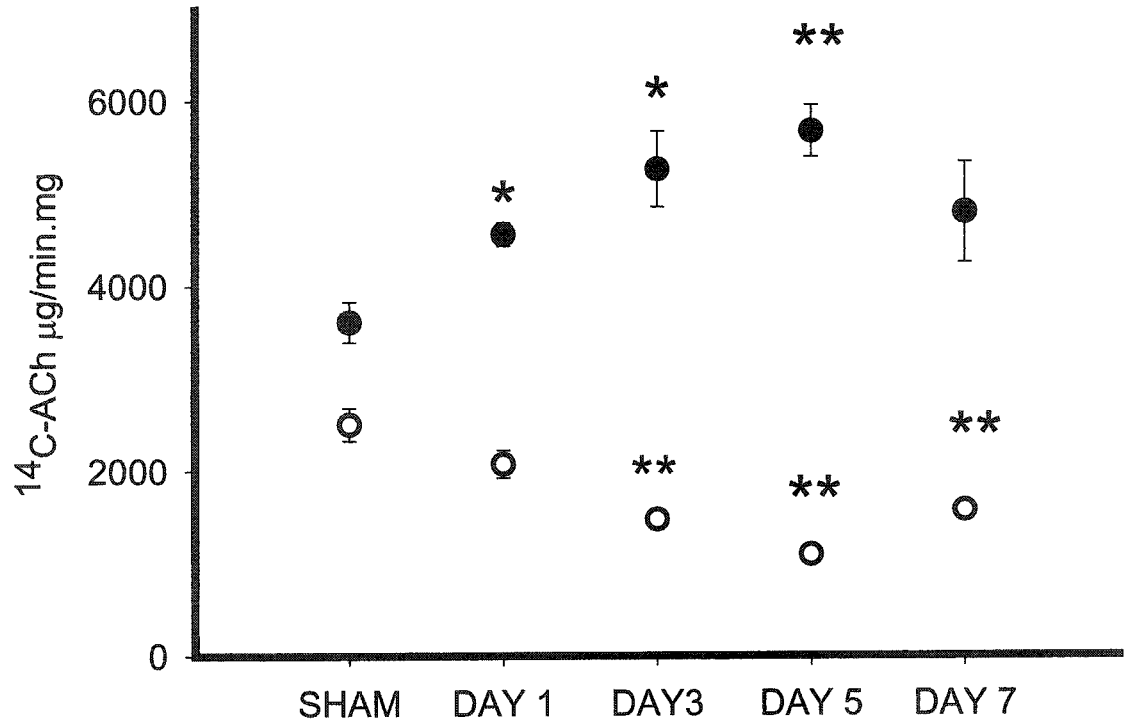

Figure 5.3. Effects of fimbria-fornix transection on choline acetyl transferase (ChAT) immunoreactivity in the septum and the dorsal hippocampus. In sham-operated animals (A, B) ChAT immunoreactive terminals were observed in fibers coursing the medial and lateral septum (A) and the fimbria (bottom right corner) and CA3 region of the dorsal hippocampus (upper left corner) in (B). Five days after axotomy, a significant reduction of ChAT immunoreactivity was observed in the fimbria (arrows identify remnant fibers in D) while almost complete lack of immunoreactive cholinergic terminals was observed in the CA3 sector (D). In contrast, numerous highly dense ChAT immunopositive fibers were present in the medial and lateral quadrant of the septum (C). Eventhough some chromatolysis and atrophy of cholinergic cell bodies was observed in the septum (results not shown, axotomy did not appear to produce a decrease in the number of ChAT immunoreactive cell bodies in the septum. These findings were typically observed in all sections (2-3) examined for 2-3 animals per time point. Scale bar = 50 μm (A, C), 100 μm (B, D).

FIGURE 5.3

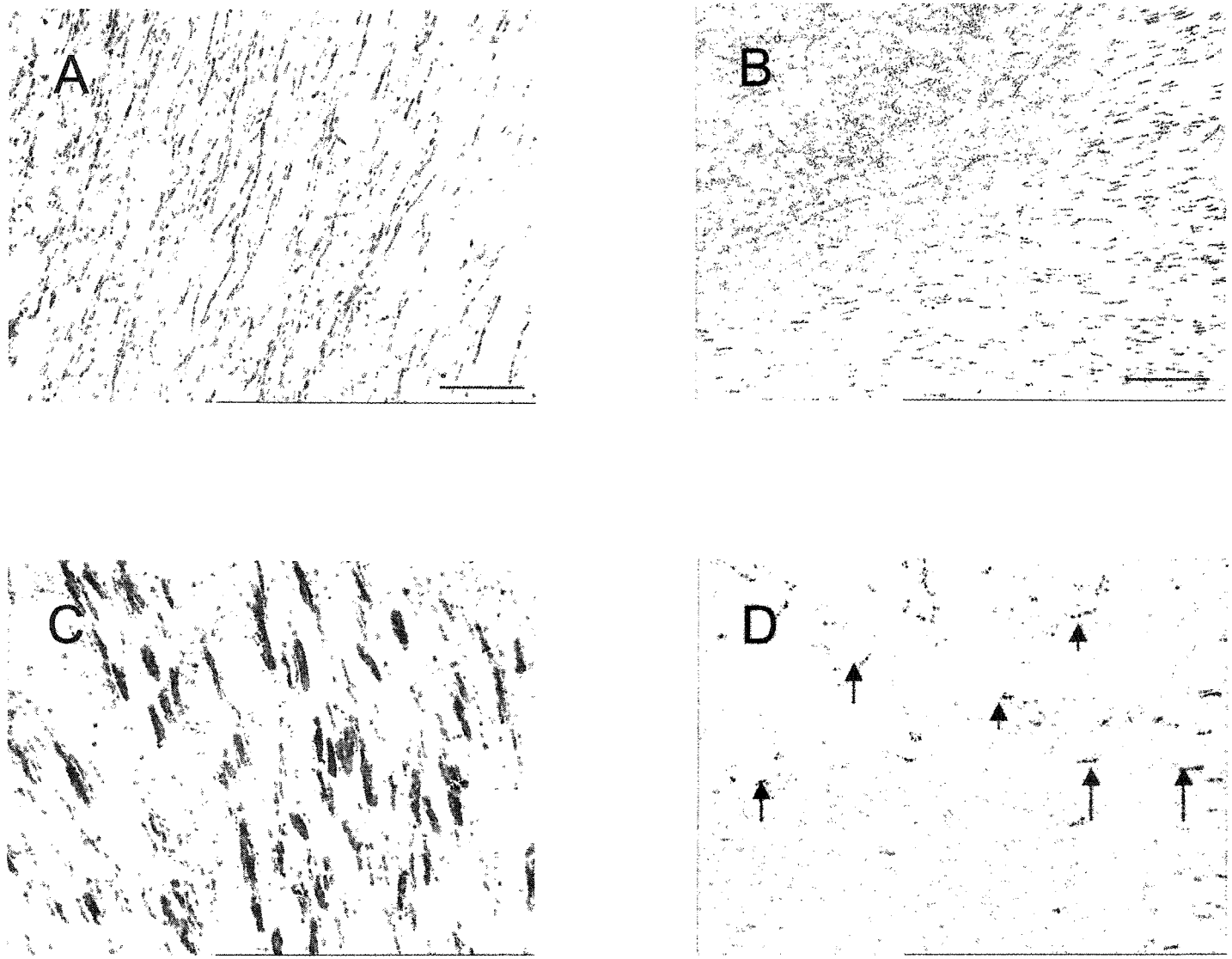

Figure 5.4. Effects of fimbria-fornix transection on the accumulation of 145 and 150 kDa spectrin fragments in the septum (A) and dorsal hippocampus (B). Axotomy produced a marked accumulation of the 150 kDa (filled circle) and 145 kDa (open circle) spectrin proteolytic fragments in the septum and dorsal hippocampus (n=8 for the sham-operated group and n=9-11 animals for each time point of the axotomized groups). Optical density values for both the 150 and 145 kDa fragments were elevated in the septum, but not the dorsal hippocampus, at day 1 after axotomy. Optical density values were elevated more for the 145 kDa spectrin fragment compared to the 150 kDa spectrin fragment at day 7. Blots at the bottom of panel A and B are representative of the time course observed in the septum and dorsal hippocampus. Each lane contains protein extracts from a separate animal. $*P<0.05$ relative to sham operated controls.

FIGURE 5.4A

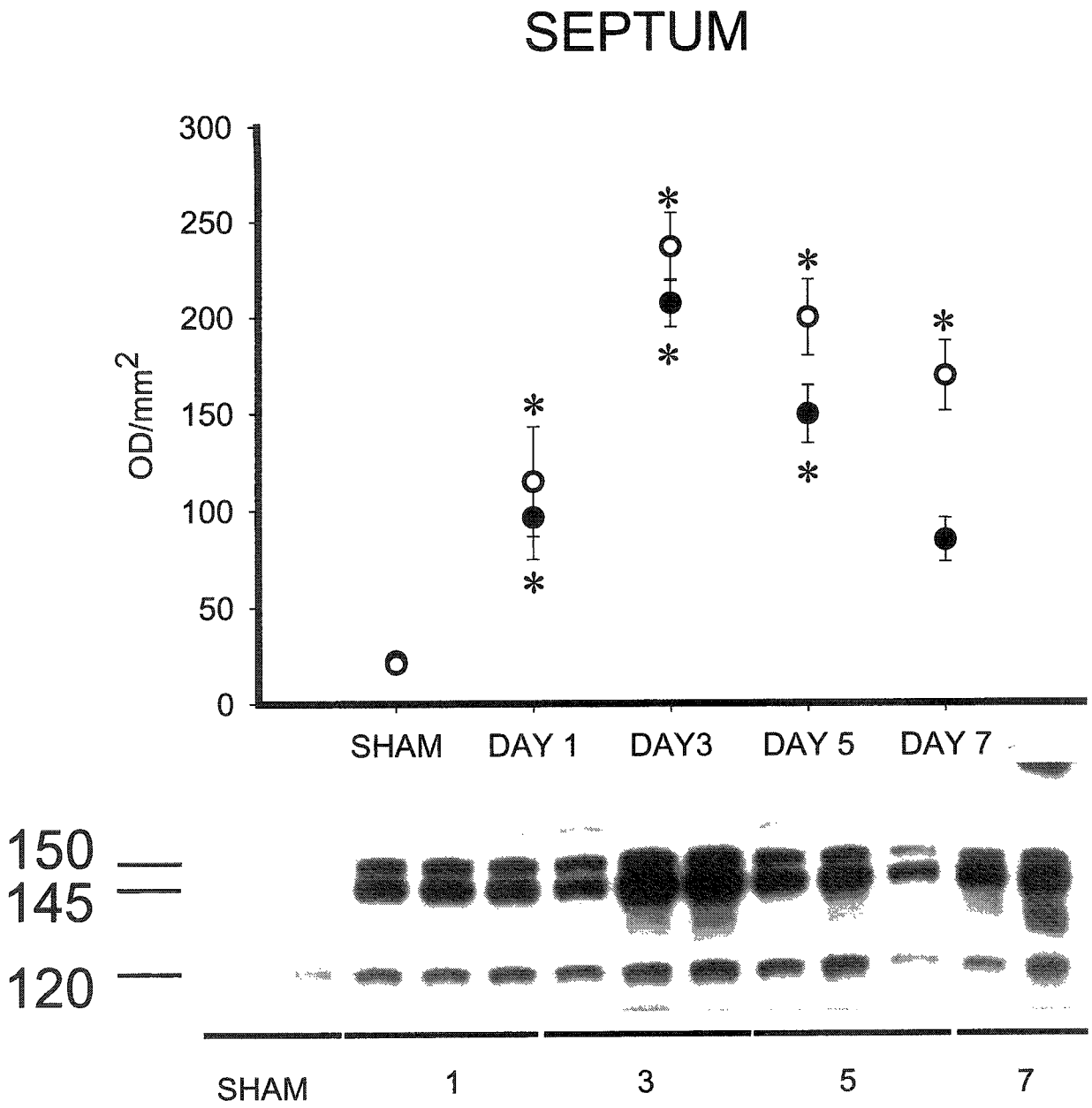
SEPTUM
300
250
200
150
100
50
0
OD/mm2
SHAM
DAY 1
DAY3
DAY 5
DAY 7
150
145
120
SHAM
1
3
5
7

FIGURE 5.4B

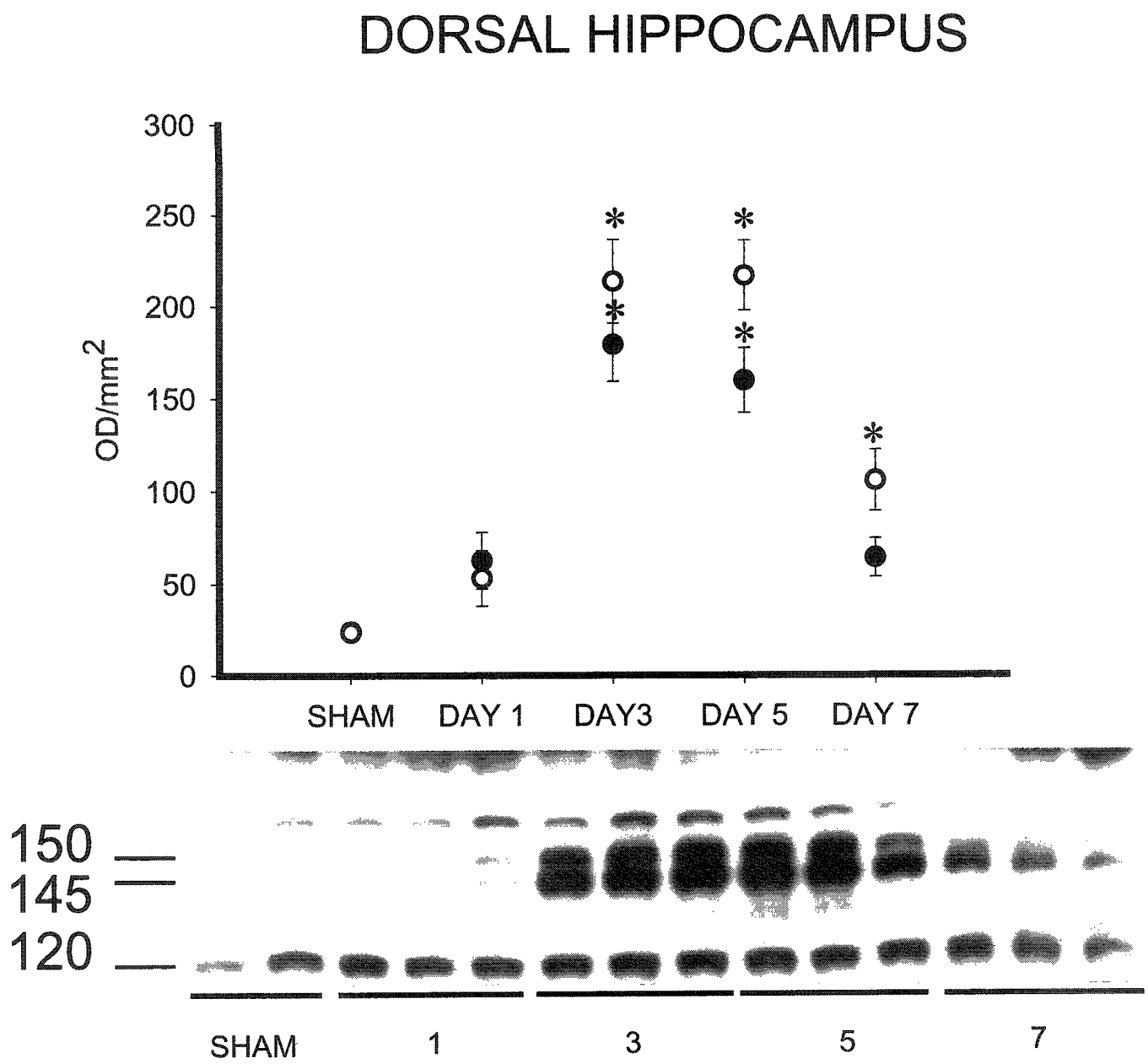
DORSAL HIPPOCAMPUS
300
250
200
150
100
50
0
OD/mm2
SHAM
DAY 1
DAY3
DAY 5
DAY 7
150
145
120
SHAM
1
3
5
7

Figure 5.5. Time course for elevation of calpain-generated 145 kDa proteolytic fragment of spectrin in the dorsal hippocampus after fimbria-fornix axotomy. Consistent with results obtained with the antibodies MAB1622 and FG6090, the $\alpha\Delta C^{calpain}$-αII-spectrin antibody detected a progressive accumulation of the calpain-generated spectrin 145 kDa proteolytic fragment at day 1, 3 (***$P < 0.001$) and 5 (**$P < 0.01$) after axotomy. Levels of the calpain-generated spectrin 145 kDa fragment were subsequently reduced to levels found in sham-operated animals at day 7 after axotomy. Values are the mean ± S.E.M. of data from at least 3 animals per time-point.

FIGURE 5.5

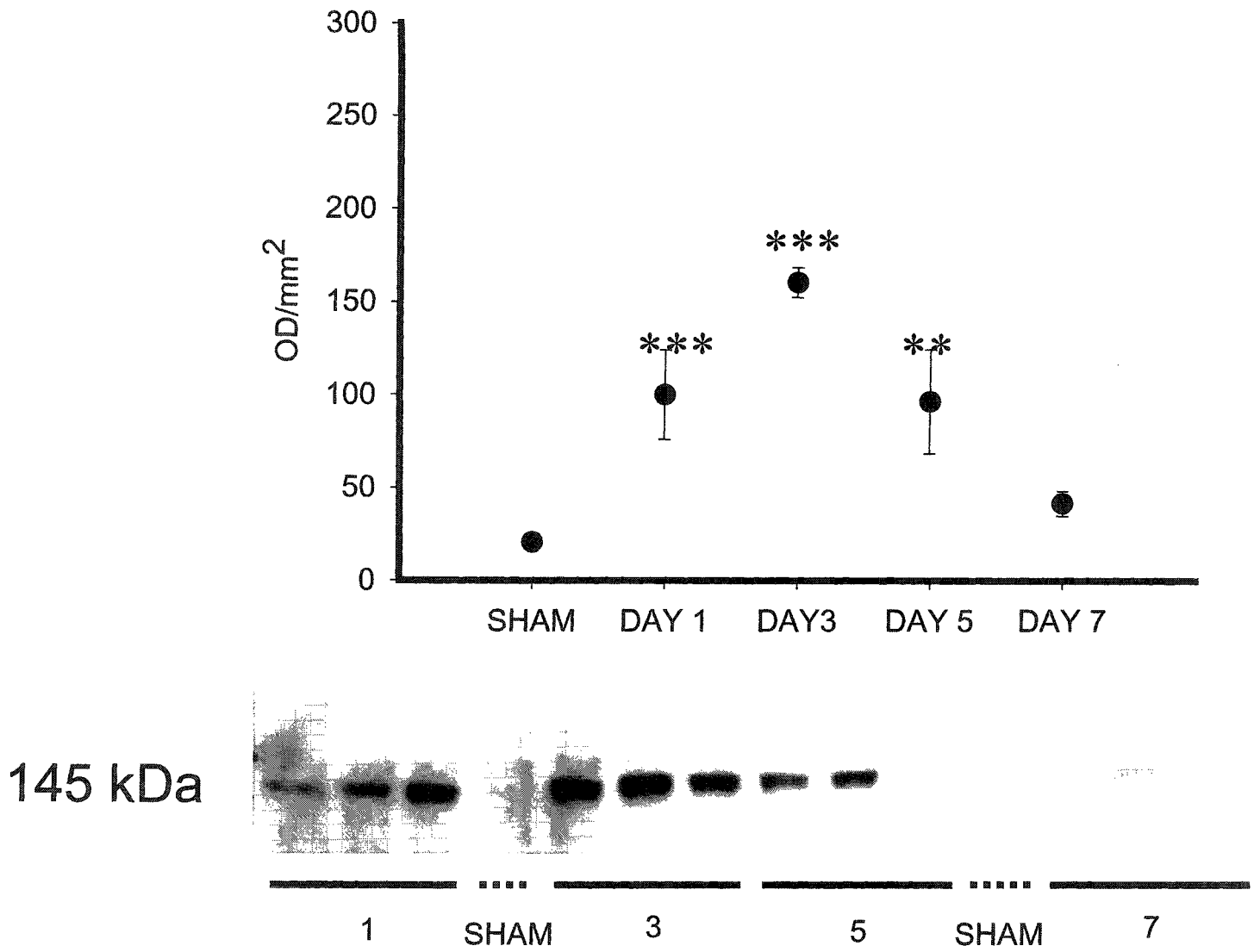
300
250
200
150
100
50
0
OD/mm2
***
***
**
SHAM
DAY 1
DAY3
DAY 5
DAY 7
145 kDa
1
SHAM
3
5
SHAM
7

Figure 5.6. Photomicrographies showing calpain-cleaved-αII-spectrin immunoreactive profiles in the septum (A, B) and dorsal hippocampus (C,D) of sham and axotomized animals five days after surgery. $\alpha\Delta C^{calpain}$-αII-spectrin immunoreactivity was not detected in sham operated animals (A and C). In the septum, $\alpha\Delta C^{calp}$-αII-spectrin immunopositive cell bodies were detected at day 5 after axotomy (B). Closer examination revealed that the $\alpha\Delta C^{calpain}$-αII-spectrin immunoreactivity was predominantly cytoplasmic and punctate in appearance (B, insert). After axotomy, $\alpha\Delta C^{calpain}$-αII-spectrin immunoreactive fibers were apparent in stumps of fimbria-fornix fibers (D, circles).

FIGURE 5.6

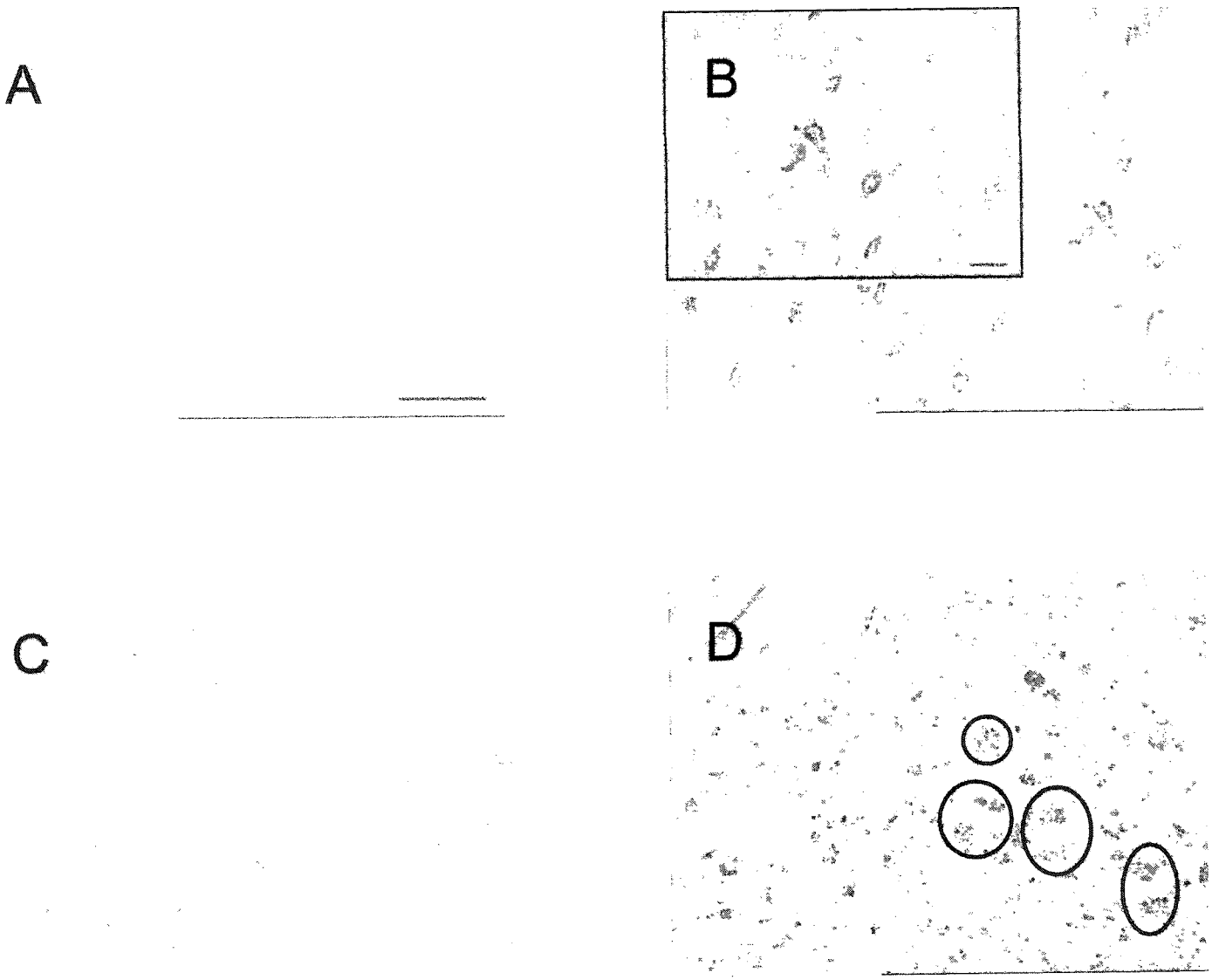

Figure 5.7. ChAT immunoreactive profiles partially co-localize with calpain-cleaved αII-spectrin immunoreactivity in the septum at day 5 after axotomy. Immunopositive cholinergic cell bodies were detected in sham operated animals (A) as well as animals at day 5 (B) and day 7 (C) after axotomy. Consistent with our immunoblotting results, $\alpha\Delta C^{calpain}$-αII-spectrin immunoreactivity was not detected in sham-operated animals (D). In contrast, numerous $\alpha\Delta C^{calpain}$-αII-spectrin immunopositive cell bodies were detected at day 5 (E, arrows) and day 7 after axotomy (F, arrows). Closer examination revealed that ChAT immunoreactivity was also observed in swollen fibers in the dorsolateral quadrant of the septum (B). Merging images for ChAT and $\alpha\Delta C^{calpain}$-αII-spectrin immunoreactivities for sham-operated animals (G) and animals examined at day 5 (H) and day 7 (I) axotomy revealed that some ChAT immunopositive cell bodies were double labeled with the $\alpha\Delta C^{calpain}$-αII-spectrin antibody (circles). Interestingly, ChAT immunoreactivity swollen fibers after axotomy in the septum did not appear to display $\alpha\Delta C^{calpain}$-αII-spectrin immunoreactivity.

FIGURE 5.7

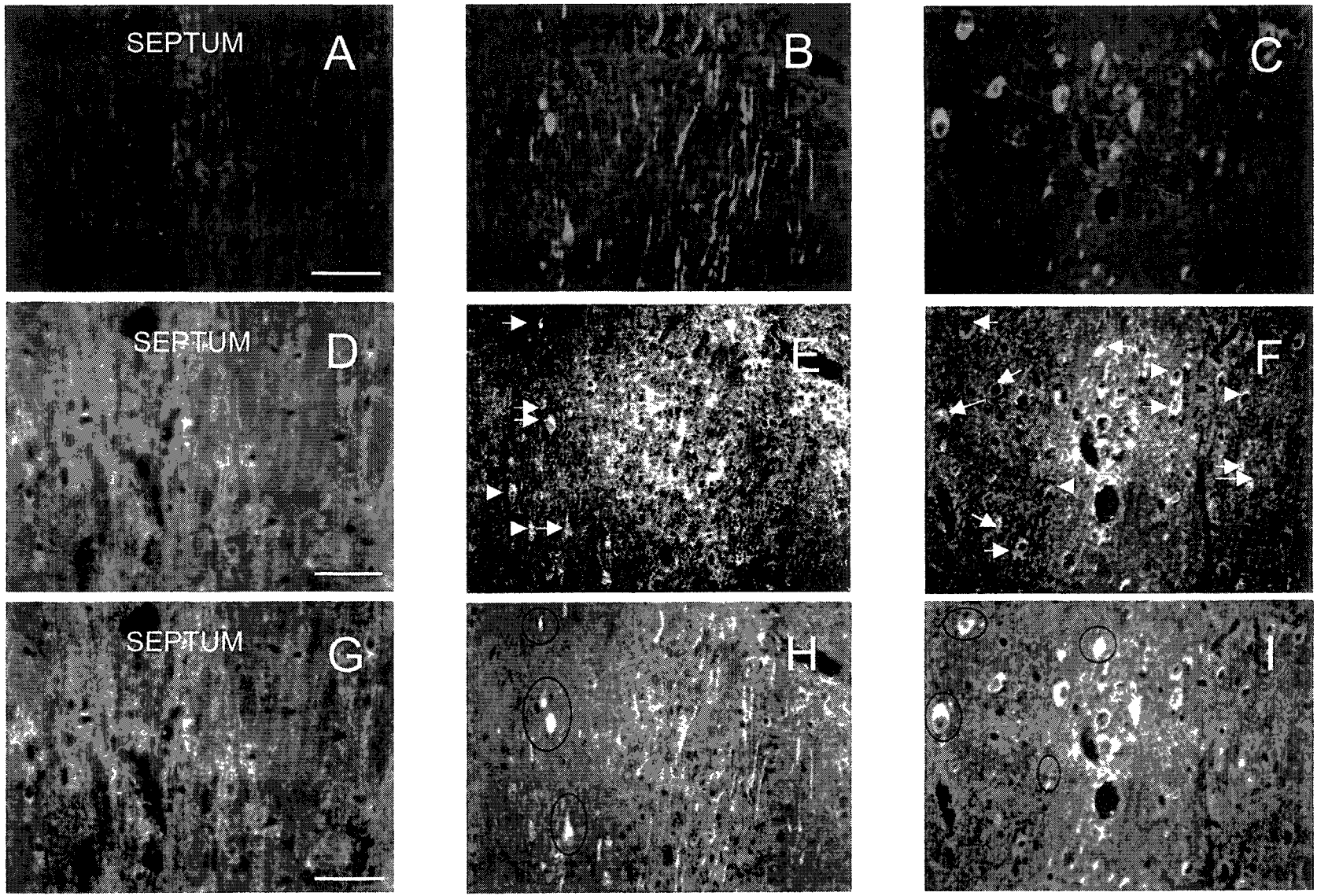

Figure 5.8. Effects of intracerebroventricular administration of vehicle, leupeptine or MDL 28,170 on accumulation of the 150 kDa (black bars) and 145 kDa (grey bar) spectrin proteolytic fragments in the septum (A) and dorsal hippocampal (B) after axotomy. Leupeptin and MDL 28,170 reduced the accumulation of the 150 kDa and 145 kDa fragments in the septum. In the dorsal hippocampus, accumulation of the 145 kDa band was reduced by leupeptine. Values are the mean and S.E.M. of data from 8-11 animals per group. * $P < 0.05$ with respect to axotomized vehicle-treated animals in post-hoc Tukey HSD test. Blots at the bottom of panel A and B are representative for the effects of vehicle, leupeptin and MDL 28,170 on the accumulation of the 145 and 150 kDa fragments of spectrin after axotomy in the septum and dorsal hippocampus.

FIGURE 5.8A

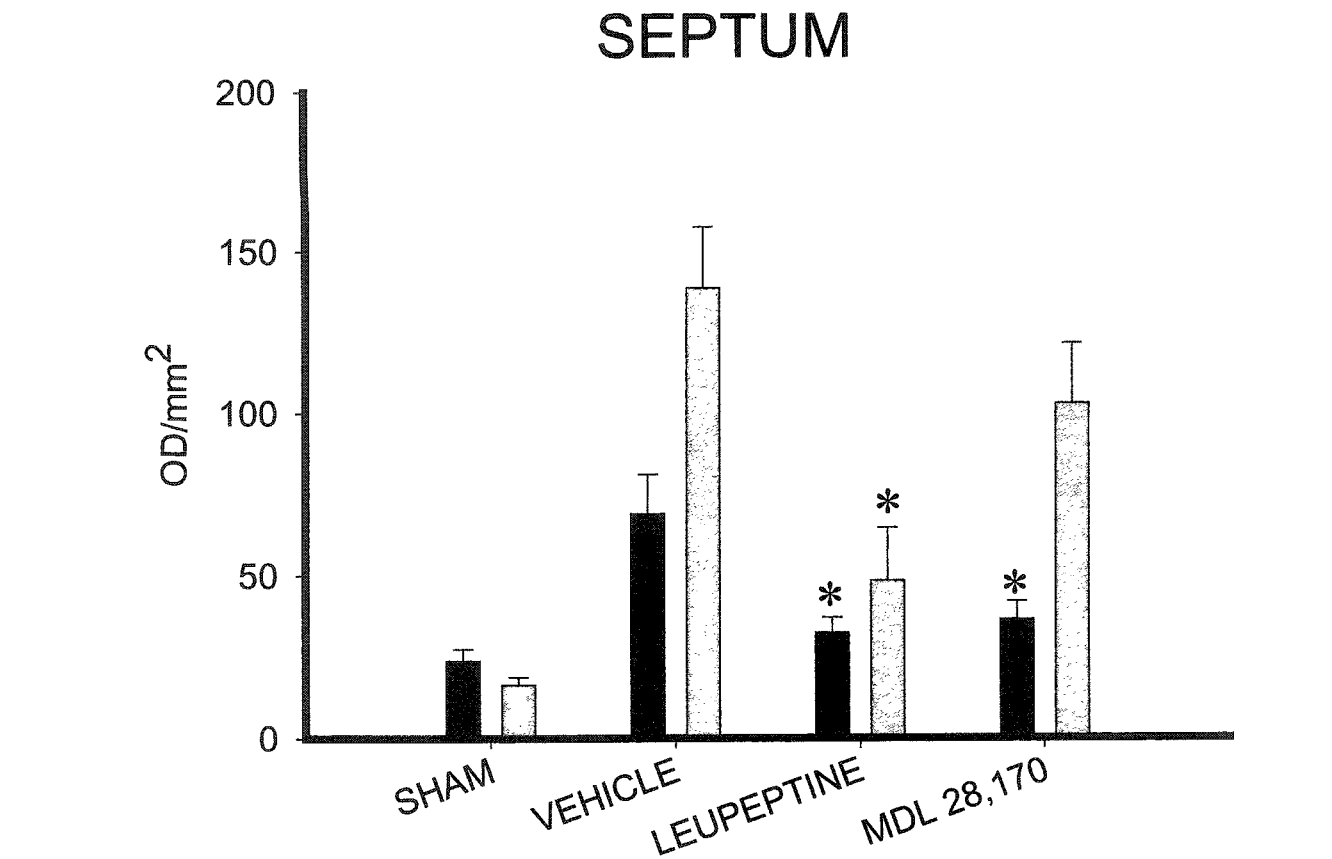
SEPTUM
200
150
100
50
0
OD/mm2
*
*
*
SHAM
VEHICLE
LEUPEPTINE
MDL 28,170

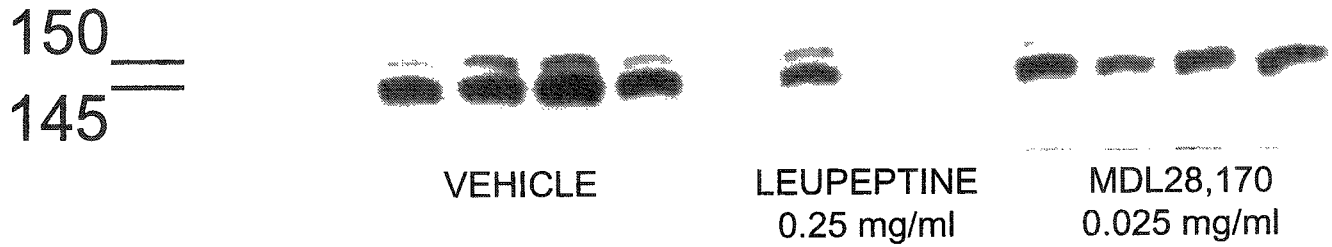
150
145
VEHICLE
LEUPEPTINE
0.25 mg/ml
MDL28,170
0.025 mg/ml

FIGURE 5.8B

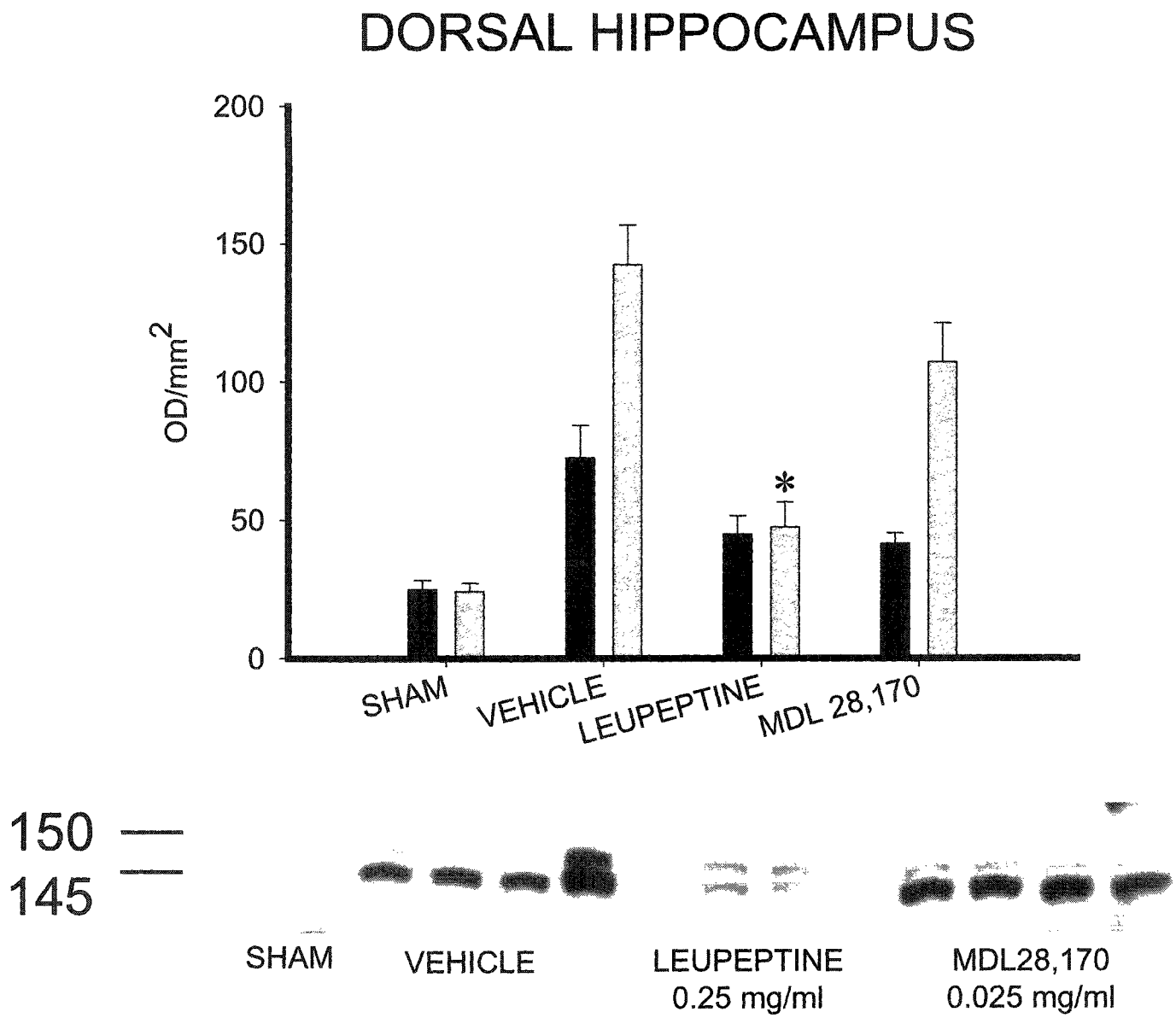
DORSAL HIPPOCAMPUS
200
150
100
50
0
OD/mm2
*
SHAM
VEHICLE
LEUPEPTINE
MDL 28,170
150
145
SHAM
VEHICLE
LEUPEPTINE
0.25 mg/ml
MDL28,170
0.025 mg/ml

Figure 5.9. Effects of leupeptine and MDL 28,170 on alterations in ChAT activities in the septum (filled circles) and dorsal hippocampus (open circles) produced by axotomy. Both leupeptin and MDL 28,170 partially reversed the increase in ChAT activity in the septum produced by axotomy. The decrease in ChAT activity that occurred in the dorsal hippocampus after axotomy was not reversed by either leupeptin or MDL 28,170. Values are the mean and S.E.M. of data from 8-11 animals per group. $*P<0.05$; $**P<0.01$ with respect to sham-operated animals.

FIGURE 5.9

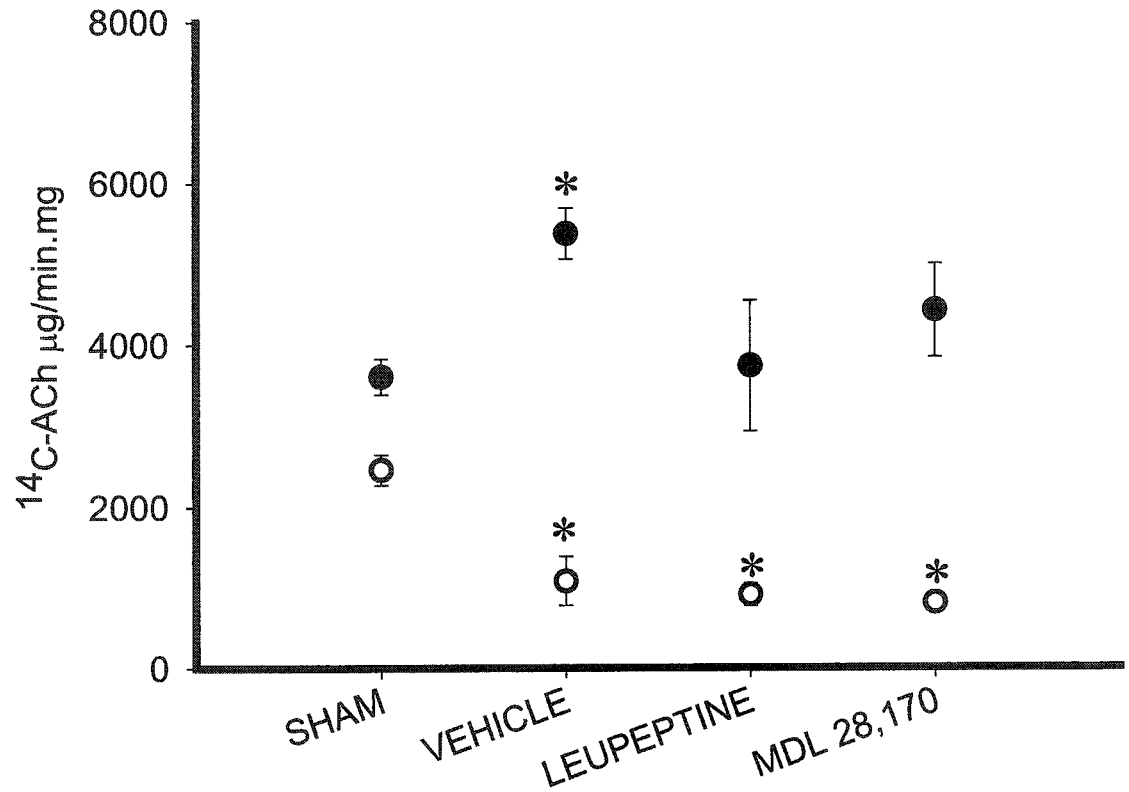
8000
6000
4000
2000
0
^{14}C-ACh µg/min.mg
SHAM
VEHICLE
LEUPEPTINE
MDL 28,170

Chapter 6

6. Discussion

In Alzheimer's disease, interstitial accumulation of amyloid Aβ (senile plaques) and intraneuronal filamentous deposits of microtubule associated protein Tau (neurofibrillary tangles) spread slowly from temporal and limbic into frontal and occipital cortices, sparing sensorimotor brain regions. Despite several lines of evidence suggesting that amyloidosis both precedes and promotes hyperphosphorylation of the microtubule associated protein Tau, a molecular mechanism that links amyloid burden and neurofibrillogenesis in Alzheimer's disease brain has not been clearly established (Nasslund, 2000; Lewis et al., 2001; Gotz et al., 2001; Mudher and Lovestone, 2002).

Brain atrophy as a result of neuropil compression, synaptic attrition and neuronal cell loss each represent a quantitative index of the severity of neuronal degeneration in Alzheimer's disease that have been correlated with memory and cognitive impairment during disease progression (Scahill et al. 2002; Thompson et al., 2003). At present, the threshold where cells become irreversibly locked into a physiological process leading to widespread metabolic decline and subsequent cell death is not yet clear. Results presented in this thesis suggest that in Alzheimer's disease brain the activation of programmed cell death as assessed by accumulation of caspase-3 cleaved APP proteolytic fragments in extracellular granular deposites, neuronal cell bodies and glial fibrillary acidic immunopositive cells associated with amyloidosis, may represent such a threshold event. In addition, the accumulation of caspase-3 cleaved spectrin (fodrin) proteolytic fragments was observed as an early event detected prior to the phosphorylation of neurofilaments in a subset of pyramidal cells from frontal and temporal association cortices responsible for cortico-cortical and corticofugal communication. The relative contribution of caspase-3 and calpain activation to the adaptive changes in basal forebrain cholinergic neurons resulting from septo-hippocampal transection was examined in a rat model of acute septo-hippocampal disconnection produced by axotomy of this pathway. In this model, axotomy-induced calpain, but not caspase-3, activation was partially

responsible for the adaptive response of basal forebrain cholinergic cell bodies to axonal injury.

Appearance of proteolytic fragments of APP and spectrin following caspase-3 activation in Alzheimer's disease brain appears to be partially dissociated in space and time from amyloid deposition and neurofibrillary tangles. Thus, while programmed cell death may contribute to chronic neuronal cell loss described in Alzheimer's disease, it is not solely responsible for this pathology. In an acute model of septo-hippocampal disconnection, calpain-cleaved spectrin proteolytic fragments accumulate in the septum and the hippocampus. It is noteworthy that calpain activation has also been observed in cortical neurons of Alzheimer's disease brain suggesting that this protease may also be responsible for adaptive changes in this disorder (Saito et al., 1993; Grynspan et al 1997; Bussiere et al 1999; Nixon, 2000).

There is a plethora of information concerning the abnormalities observed in *post mortem* Alzheimer's disease brain. Numerous *in vivo* and *in vitro* studies have attempted to establish a temporal order and molecular basis for theses abnormalities. In the following sections, I will develop an integrative view about how our findings might be interpreted within the context of these events. My goal is to validate a novel interpretation of the role of caspases in the cortical dysfunction that occurs during progression of Alzheimer's pathology, as well as the role of calpain activation in the cell body response to axotomy.

6.1 Identification of Programmed Cell Death in Alzheimer's Brain: Experimental and Theoretical Concepts

Historically, apoptosis was defined on the basis of morphological features such as membrane blebbing, shrinkage of the cell body, nuclear condensation and DNA fragmentation. However, recent advances in elucidation of the molecular processes involved in programmed cell death have extended this definition beyond strict morphological changes initially associated with the developmental apoptosis (Kerr et al., 1972; Nicotera et al., 1999).

Evidence for programmed cell death in the Alzheimer's disease brain derived from early studies consisting largely of the *in situ* detection of fragmented DNA by terminal deoxynucleotidyl transferase mediated deoxyuridine nick end-labeling (TUNEL) techniques. Several studies reported DNA fragmentation using the TUNEL technique in Alzheimer's disease that was absent in aged-matched control brain, suggesting that programmed cell death was the major pathway responsible for cell loss in this neurodegenerative disorder. However, conflicting results led to a critical evaluation of the TUNEL technique as a specific marker for programmed cell death. For instance, in human *post mortem* brain tissue, it was observed that neurons which have undergone necrotic cell death resulting from cerebral ischemia also display TUNEL-positive profiles suggesting that DNA fragmentation is a general marker of cell death rather than a specific feature of apoptosis.

One of the more worrisome aspects of the TUNEL techniques as markers of apoptosis is the large number of neurons detected following a necrotic insult, even though a high proportion of these neurons do not display morphological features of apoptosis. Therefore, if such high numbers of cells were committed to die, the brain would be depleted of cells in a very short period of time. However, if the progression of programmed cell death is considered to be prolonged and superimposed with the protracted time over which neuronal loss occurs in this chronic neurodegenerative disorder, only a small number of neurons would be expected to begin to undergo programmed cell death at any given time point. As a consequence, determination of the number of cells committed to death by TUNEL techniques do not seem to be an suitable indicator of the specific stage of programmed cell death but rather a reflection of the total number of cells that have succumbed to programmed cell death.

Caspases are indispensable for the execution of apoptosis; activation of executioner caspases appears to occur over a short period of time in an environment highly regulated by competence between promoters and inhibitors of the programmed cell death cascade. As a result, the short half-life of active caspases is thought to be responsible for difficulty in their detection in post mortem tissue. For instance, reports on the detection of active caspase-3 in Alzheimer's disease brain tissue have yielded

conflicting results raising concerns about the role of programmed cell death in Alzheimer's pathology.

Consensus sequences for caspase cleavage have been identified in a wide variety of proteins subserving such diverse functions as cell structure, signalling and DNA integrity. However, several targets have a discrete function that is disrupted in the propagation of the cell death process such as structural proteins that are inactivated by caspases, while other substrates can be activated by caspase cleavage such pro-apoptotic proteins. Because caspases are specific in that they cleave only after aspartic residues in the consensus motif (DXVD), cleavage will reveal *neo*-epitope sequences that can be detected using antibodies raised against these distinct antigenic sites. Using caspase cleavage-site directed antibodies, we have been able to immunohistochemically localize the accumulation of protein-substrates fragmented following caspase cleavage in Alzheimer's disease brains.

Cleavage of APP by caspases has been determined *in vitro* and *in vivo* by developing an antibody that recognizes site-specific caspase activity using the *neo*-epitope carboxy-terminal caspase-consensus cleavage site within the APP cytosolic domain as an immunogen. Extensive characterization of this *neo*-epitope antibody has been performed to ensure that it selectively recognizes the cleaved target protein and not full length APP (Gervais et al., 1999). The selectivity of this antibody has been further confirmed by detection of a discrete band with a molecular weight in Alzheimer's brain that coincided with the corresponding fragment of APP generated by recombinant caspase-3 mediated cleavage of APP in cultured cells undergoing apoptosis. In agreement with our results, a report by Lu et al. (2000) observed accumulation of the carboxy-terminal domain of APP generated by caspase-3 in Alzheimer's disease but not in age-matched control brains.

Cleavage of APP by caspase produces a major fragment of 664 residues that appears to be amyloidogenic (Gervais et al., 1999; LeBlanc et al., 1999) and a minor fragment of 31 residues, which seems to be dissociated from the amyloidogenic process (Soriano et al., 2001), but is by itself neurotoxic (Lu et al., 2000). Cleavage of APP by caspase generates a long N-terminus fragment containing the primary sequence of Aβ, as a consequence it may be amyloidogenic while the C-terminal fragment of 31 amino acid

released by intracellular caspase cleavage of APP is cytotoxic, suggesting that the caspase-3 dependent event on APP may contribute to Alzheimer's pathology. In agreement with this proposal, motor neuron death is associated with an up-regulation of APP followed by amyloidosis and subsequent increased amyloidosis-dependent caspase-3 activation; while inhibition of caspase-3 activity with peptidic inhibitors reduces expression of APP and amyloid Aβ production in these motor neurons (Barnes et al., 1998).

Caspase-cleaved amyloid precursor protein immunoreactivity was found in particulate elements resembling dystrophic neurites sparsely distributed in layers 1 to 6 of the inferior frontal and superior temporal gyri partially associated with dense-core plaques in Alzheimer's disease and diffuse senile plaques in age-matched control brains. In agreement with our findings, recent studies have identified caspase-cleaved amyloid precursor protein immunoreactivity in extracellular deposits surrounding immunopositive neurons, neuronal processes and vacant areas, which may have formerly held neurons. In age-matched control brains, caspase-cleaved APP immunostaining in hippocampal tissue was similar but less intense and with an uneven distribution (Galvan et al., 2002).

Colabeling of a subset of TUNEL-positive pyramidal neurons with the antibody that recognizes caspase-3 cleaved APP ($\alpha\Delta C^{Csp}$-APP) is in agreement with finding of Su et al. (2002). Active caspase-3 immunoreactivity colocalized with TUNEL-positive granulo-vacuolar deposit-bearing hippocampal pyramidal neurons, a characteristic feature of Alzheimer's disease and Down syndrome brains. These findings support a role for the activation of programmed cell death mechanisms in selective intracellular compartments exhibiting granulo-vacuolar deposits (Su et al., 2002).

Evidence of caspase-3 cleaved amyloid precursor protein immunoreactivity in discrete small and medium size particulates partially associated with dense-core senile plaques in Alzheimer disease brains suggests that caspase-3 activation may occur in neurons, particularly in neuronal terminals exposed to the accumulation of fibrillogenic and insoluble amyloid Aβ peptides. Low levels of caspase activation may be sufficient to cleave the amyloid precursor protein or cytoskeletal proteins present in synaptic terminals but may not be sufficient to reach a threshold that propagates the apoptotic signal to the soma. A gradual involvement of promoters and inhibitors of the programmed cell death

may dampen, in the long-term, the complete and full expression of the programmed cell death machinery. In support of this hypothesis, accumulation of anti-apoptotic members of the Bcl-2 family, such as Bcl-xl and Bcl-w, as well as reduced levels of neuronal apoptotic inhibitors in Alzheimer disease and Down syndrome brains is indicative of an imbalance in the ratio of this factors capable of promoting programmed cell death (Kitamura et al., 1998; Pike, 1999; Seidl et al., 1999; Zhu et al., 2002). Furthermore, accumulation of upstream caspases such as caspase-8 and caspase-9, but not of downstream caspases such as caspase-3 and caspase-6 is suggestive of an incomplete expression of molecular components of the programmed cell death or "abortosis" may occur in AD brain (Raina et al., 2001; 2003).

As a proof-of-concept of that programmed cell death occurs in a highly regulated environment of promoters and inhibitors, experimentally induced up-regulation of the neuronal apoptotic inhibitor protein may prevent accelerated degeneration of motor neurons during neurodevelopment of the spinal cord (Liston et al., 1996; Kugler et al., 2000). In addition, induced overexpression of NAIP and the related anti-apoptotic protein XIAP reduces transient ischemic forebrain damage in the rat hippocampus (Xu et al., 1997; 1999).

6.2 Programmed Cell Death Contributes to Early Cortico-cortical Disconnection in Alzheimer's disease

In Alzheimer's disease, loss of synapses may contribute to the initial neuropathological events responsible for mild cognitive impairment and memory loss (Hamos et al., 1989; Scheff and Dekosky, 1990; Dekosky and Scheff, 1990; Masliah et al., 1991; 1996). Accordingly, synaptic loss in association cortices may result in a disconnection syndrome responsible for cognitive impairment in Alzheimer's disease (Hof et al., 1990a; 1990b; Mann, 1996; Bussiere et al 2003). Accumulation of caspase-3 cleaved amyloid precursor protein in neurons and glial cells, as well as caspase-cleaved spectrin in a subset of pyramidal neurons from layers 3 and 5 of the inferior frontal and superior temporal gyri of association cortices indicates that activation of programmed cell death occurs in Alzheimer's disease brain.

Findings from this study indicating that the accumulation of caspase-cleaved amyloid precursor protein proteolytic fragments occurs in neuronal cell bodies but not in thioflavine-S positive paired-helical filaments bearing-neurons, suggests that activation of caspase-3 may occur independently of neurofibrillary tangles. In agreement with this proposal, detection of caspase-3 cleaved spectrin in a subpopulation of non-phosphorylated neurofilaments bearing-neurons that are vulnerable in Alzheimer's disease suggests that programmed cell death occurs as an early event prior to hyperphosphorylation of microtubule associated protein Tau.

The steps of plaque formation have been suggested by immunohistochemical studies in which APP-immunopositive dystrophic neurites appear to occur first in plaque development, followed by the involvement of neurofilaments and then helical paired filaments and finally hyperphosphorylated Tau (Su et al., 1996; 1998). As such, hyperphosphorylation represent a metabolic dead-end that is followed by programmed cell death. By contrast, our data suggest that activation of caspases may occur as a part of the process contributing to neuronal cell loss at each of these stages. Indeed, the amount of neuronal loss exceeds by several orders of magnitude the amount of neurofibrillary tangles (Gomez-Isla et al., 1997).

Infrequent colocalization of caspase-3 cleaved spectrin and senile plaques also implies that activation of caspase-3 may progress in parallel but independently from plaque formation associated more closely with neuronal cell death, than these events. In support of this hypothesis, Rohn et al. (2002) have found no, or an inverse correlation between counts of active caspase-9 immunolabeled neurons and amyloid Aβ deposition or paired-helical filaments-1 bearing neurons. In addition, poor colocalization between active caspase-9 and neurofibrillary tangle bearing-cells as well as the accumulation of caspase cleaved spectrin in dog brains, a species that is recognized not to develop tangles is in support of the hypothesis that amyloidosis or neurofibrillary tangles are dissociated from activation of programmed cell death.

Accumulation of caspase-cleaved spectrin in non-phosphorylated neurofilament immunopositive cells suggests that neurons can be engaged in programmed cell death without neurofibrillary tangle formation. In addition neurons can accumulate proteolytic fragments without an apparent compromise of function. Indeed, cells may live for

decades with neurofibrillary tangles (Morsch et al., 1999). In agreement with this notion, overexpression of mutated forms of APP, presenilin1 as well as accumulation of unpolymerized hyperphosporylated mutated Tau in mice may occur without cell loss (Calhoum et al., 1998; Spittaels et al., 1999; Takeuchi et al., 2000).

6.3 Progressive Pyramidal Degeneration in Alzheimer's disease. A Proposal for Primary Events in Cortical Degeneration

Accumulation of caspase-cleaved spectrin in pyramidal neurons involved in corticocortical communication, as well as in corticofugal projections, known to be glutamatergic, supports the proposal that hypofunction of the N-methyl-D-aspartate (NMDA) receptor subtype is a condition present in the normal aging rodent and primate brain (Gonzales et al., 1991; Magnusson and Cotman, 1993; Saransaari and Oja, 1995) and may be present to a more exaggerated degree in AD brains with respect to age-matched control brains (Ulas and Cotman, 1997; Francis, 2003).

In this study, we have established regional and laminar distribution of programmed cell death events corresponding to the differential involvement of a identifiable neuronal subsets that may play a role in influencing the flow of information processing along cortical systems. Progressive degeneration of nonphosphorylated neurofilaments protein-bearing pyramidal neurons, a subpopulation of neurons specially vulnerable in AD located in layers III and V of association cortices may lead to a cortico-cortical and corticofugal disconnection (Hof et al., 1990a; 1990b; Morrison and Hof, 2002).

Reduced activity of SMI-32 immunopositive pyramidal neurons may elicit, in the short term, an increase in the incoming traffic to the neocortex by disinhibiton of GABAergic interneurons that modulate the basalo-cortical cholinergic and thalamo-cortical glutamatergic projections (Figure 6.1). Our findings are in agreement with reports from Corso et al., (1997) and Farber et al., (2002) which establish that experimentally induced hypofunction of NMDA receptors may elicit a particular neurodegenerative syndrome that coincides with the profile of neurodegeneration as has been established in Alzheimer's disease. However, although hypofunction of the NMDA

receptor during senescence may not be sufficient to trigger widespread neurodegeneration, convergence of unbalanced input to these and downstream cells may be followed by a chronic and amplified uncompensated loop of hyperactivation that leads to cortical disconnection (Olney et al., 1998).

In contrast with the many experimental procedures that have used glutamate-related compounds to trigger an acute excitotoxic process, administration of NMDA antagonists may produce neurodegeneration by an indirect mechanism. According to this scenario, reduced activation of glutamate receptors on GABAergic cells results an uncompensated hyperactivation of cholinergic and glutamatergic pathways that would normally be inhibited by these GABAergic interneurons. As a consequence, disinhibition of these excitatory pathways results in a subtle but prolonged hyperstimulation of corticolimbic neurons. Although blockage of NMDA receptors by administration of antagonists is an acute process, the resultant chronic disinhibition of this network has both profound long-term consequences that may be relevant to the slow progression of Alzheimer's pathology (Wozniak et al., 1998). In support of this proposal, recent studies from Kamenetz et al. (2003) have shown that increased neuronal activity promotes processing of APP and secretion, subsequent synaptic accumulation of Aβ may depress the synaptic transmission before amyloid plaque deposition becomes evident.

6.4 Role of the Calpain Activation in the Adaptive Response of the Cholinergic Septo-Hippocampal Pathway

Axotomy of the fimbria-fornix pathway resulted in a transient increase of ChAT activity in the septum that was concurrent with a reduction in ChAT activity in the dorsal hippocampus. Concordant with these changes in ChAT activity, calpain activation as assessed by accumulation of calpain-cleaved spectrin proteolytic fragments occurred in the septum and dorsal hippocampus.

We did not detect activation of caspase-3 as assessed by accumulation of caspase-cleaved spectrin in the septum or the hippocampus at any time after axotomy. In contrast to the results of this study, neuroinflammation induced by lipopolysaccharide infusion in the basal forebrain produces a reduction in ChAT activity, increase in the

number of activated microglia and in enzymatic activity of caspases -3, -8 and -9. Furthermore, although non-steroidal anti-inflammatory and pan caspase drug therapy reduced the inflammatory response and caspases activation these treatments did not reduce lipopolysaccharide induced death of cholinergic neurons (Wenk et al., 2000).

Our data suggest that calpain activation plays a different role in septo-hippocampal cell bodies and terminals after axotomy. When these axons are cut, the part of the axon that is now disconnected from the cell body disassembles in a characteristic and orderly way. Gradual loss of afferents to the dorsal hippocampus was inferred by lag-period between axotomy, the accumulation of calpain-cleaved spectrin proteolytic fragments and the eventual reduction of ChAT activity in the dorsal hippocampus. ChAT activity of cholinergic cell bodies in the septum increased following axotomy and was accompanied by the accumulation of calpain cleaved -αII-spectrin proteolytic fragments. As a result, calpain activation in these cell bodies may mediate a dynamic and adaptive response, as a consequence of injury of the septohippocampal pathway. In support of this hypothesis, ChAT activity in the septum of axotomized animals was reduced by administration of calpain inhibitors. Since the reduction in somal ChAT activity produced by calpain inhibitors was not associated with a repair of axonal injury of axotomy, it is unlikely that the passive accumulation of ChAT is solely responsible for the increase in ChAT activity in cell bodies produced by axotomy.

Although our data suggest that spectrin degradation can be prevented by intracerebroventricular administration of calpain inhibitors, cholinergic terminals in the hippocampus were not preserved. Insufficient inhibition of calpain proteases, a higher turnover of ChAT reserve in terminals of the dorsal hippocampus than cell bodies in the septum and the devastating nature of axotomy may explain the lack of effect of administration of calpain inhibitors.

More rapid accumulation of calpain-cleaved spectrin proteolytic fragments in the septum with respect to the dorsal hippocampus is suggestive of a differential response occurring in septal cell bodies and terminals after axotomy. Increased ChAT activity and immunoreactivity in the septum, resulting from a transient adaptive response of septal cholinergic cell bodies and/or by passive accumulation of enzyme was correlated with degradation of spectrin. The mechanisms responsible for the elevation of ChAT in the

septum remain to be determined. The cholinergic septo-hippocampal pathway seems to have an intrinsic capacity for platicity. Loss of entorhinal-hippocampal afferents promotes a compensatory response of the medial septal/diagonal band complex (Hyman et al., 1987). Otherwise, resistance to injury seem to be a property of some cholinergic populations of neurons such as the medial septal/diagonal band and anteromedial corticobasalis which have been shown to survive even in the end-stages of Alzheimer's disease (Mufson et al., 1989; Vogels et al., 1990). Noteworthy, is the up-regulation of ChAT activity in the hippocampus and frontal cortex of patients with mild cognitive impairment. Both of these regions are innervated by the medial septal/diagonal band and anteromedial corticobasalis suggesting an adaptive capability or neural reserve, which may offset cognitive decline in the elderly. However, loss of this cholinergic adaptive response in the long-term may explain the significant reduction of ChAT activity in severe Alzheimer's disease and the clinical transition from mild to severe cognitive impairment stage in end-stage (Dekosky and Scheff, 2002).

In summary, I have established a role for calpain activation in the response of septo-hippocampal neurons to fimbria-fornix axotomy. In addition, we have defined surrogate markers for axotomy that are sensitive to potential therapeutic agents, such as calpain inhibitors. Calpain and caspase-3 cysteine proteases are important mediators of cell death and dysfunction in acute and chronic neuronal events. However, differential activation of calpain and caspase-3 may have important implications for targeted therapeutic intervention after acute processes such as axotomy, or in chronic neurodegenerative disorders such as Alzheimer's disease.

6.5 Overview and conclusions

The work developed for this thesis has satisfied primary objectives of establishing the role of caspases in Alzheimer's disease pathology. We found that programmed cell death may contribute to progression of the disease and occurred as an early event in the neurodegenerative process. However, activation of caspases in Alzheimer's brain is not explained exclusively by accumulation and deposition of Aβ and/or neurofibrillary pathology. From our observations, we were able to establish that

pyramidal neurons undergoing programmed cell death may occur independent of amyloidosis or neurofibrillary pathology. Investigating the role of caspase in a rat model of septo-hippocampal disconnection, we determine that axotomy of the fimbria-fornix projection elicited calpain activation but not caspase. Furthermore, administration of calpain inhibitors, partially restore the cholinergic function in the septum but was unable to protect axotomized terminals in the dorsal hippocampus. Thus, we proposed that in acute induced injury, activation of calpain plays a differential role in cholinergic cell bodies and in terminal projections of the dorsal hippocampus.

Figure 6.1 Theoretical proposal of pyramidal dysfunction as an early event in Alzheimer's disease. Dysfunctional SMI-32 immunoreactive pyramidal neurons from layers 3 and 5 of association cortices may create a feed forward exacerbated input traffic to the cortex. In age-matched controls, SMI-32 pyramidal neurons modulate GABAergic interneurons thas upstream cholinergic and glutamatergic afferents maintain a controlled input to the cortex. In mild cognitive impairment, as a result of several insults, oxidative stress, hypoperfusion, amyloidal deposition and neurofibrillary tangles, hypofunctional SMI-32 neurons reduce inhibitory modulation of GABAergic cell increasing basal activity of cholinergic and glutamatergic cells. In late stage of Alzheimer's disease, atrophy of layers 3 and 5 produce cortico-cortical disconnection.

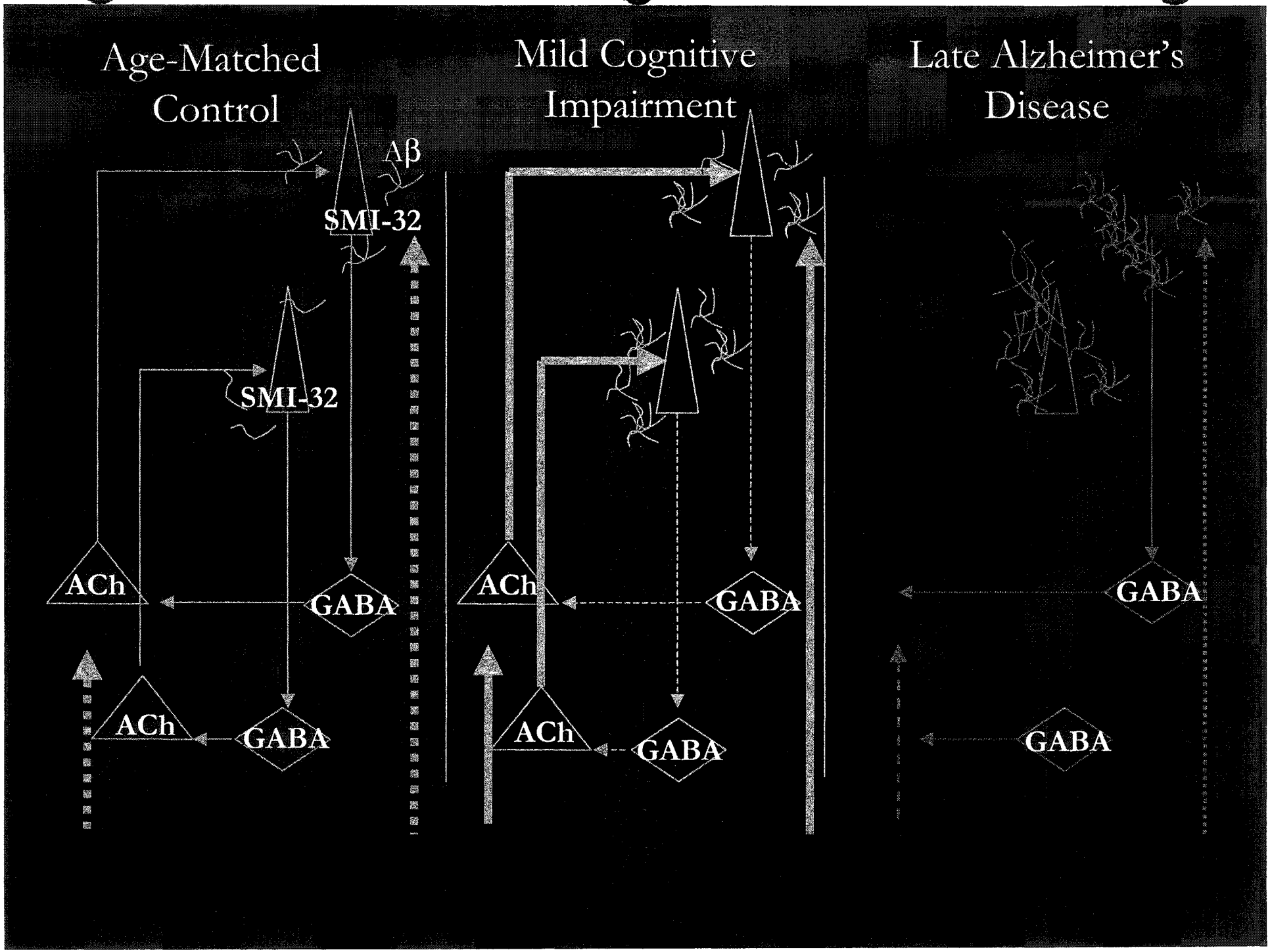
Age-Matched Control
Mild Cognitive Impairment
Late Alzheimer's Disease
Aβ
SMI-32
SMI-32
ACh
GABA
ACh
GABA
ACh
GABA
ACh
GABA
GABA
GABA

7. References

Amaral, D.G. & Kurz, J., (1985). An analysis of the origins of the cholinergic and noncholinergic septal projections to the hippocampal formation of the rat. *J. Comp. Neurol.* 240, 37-59.

Anderson AJ, Cummings BJ, Cotman CW. (1994) Increased immunoreactivity for Jun- and Fos-related proteins in Alzheimer's disease: association with pathology. *Exp Neurol.* 125(2):286-95.

Anderson AJ, Pike CJ, Cotman CW. (1995) Differential induction of immediate early gene proteins in cultured neurons by beta-amyloid (A beta): association of c-Jun with A beta-induced apoptosis. *J Neurochem.* ;65(4):1487-98.

Anguelova, E., Boularand, S., Nowicki, J.P., Benavides, J., Smirnova, T., (2000). Up-regulation of genes involved in cellular stress and apoptosis in a rat model of hippocampal degeneration. *J. Neurosci. Res.* 59, 209-217.

Arendt T, Holzer M, Grossmann A, Zedlick D, Bruckner MK. (1995) Increased expression and subcellular translocation of the mitogen activated protein kinase kinase and mitogen-activated protein kinase in Alzheimer's disease. *Neuroscience.* 68(1):5-18.

Armstrong DM, Ikonomovic MD, Sheffield R, Wenthold RJ. (1994). AMPA-selective glutamate receptor subtype immunoreactivity in the entorhinal cortex of non-demented elderly and patients with Alzheimer's disease. *Brain Res.* 639(2):207-16.

Armstrong, D.M., Terry, R.D., Deteresa, R.M., Bruce, G., Hersh, L.B., Gage, F.H.(1987) Response of septal cholinergic neurons to axotomy. *J Comp Neurol.* 264(3):421-36.

Arriagada, P.V., Growdon, J.H., Hedley-Whyte, E.T., Hyman, B.T., (1992) Neurofibrillary tangles but not senile plaques parallel duration and severity of Alzheimer's disease. *Neurology.* 42(3 Pt 1), 631-639.

Ayala-Grosso C, Ng G, Roy S, Robertson GS. (2002) Caspase-cleaved amyloid precursor protein in Alzheimer's disease. *Brain Pathol.* 12(4):430-41.

Ayala-Grosso, C.A., Urbina-Paez, R., (1999) Septohippocampal adaptive GABAergic responses by AF64A treatment. *J. Neurosci. Res.* 55,178-186.

Bahr BA, Tiriveedhi S, Park GY, Lynch G. (1995) Induction of calpain-mediated spectrin fragments by pathogenic treatments in long-term hippocampal slices. *J Pharmacol Exp Ther.* 273(2):902-8.

Bancher C, Lassmann H, Breitschopf H, Jellinger KA. (1997). Mechanisms of cell death in Alzheimer's disease. *J Neural Transm Suppl* 50:141-52.

Barnes NY, Li L, Yoshikawa K, Schwartz LM, Oppenheim RW, Milligan CE. (1998) Increased production of amyloid precursor protein provides a substrate for caspase-3 in dying motoneurons. *J Neurosci.* 18(15):5869-80.

Bartus RT, Dean RL 3rd, Beer B, Lippa AS. (1982) The cholinergic hypothesis of geriatric memory dysfunction. *Science.* 217(4558):408-14.

Bartus RT. (2000) On neurodegenerative diseases, models, and treatment strategies: lessons learned and lessons forgotten a generation following the cholinergic hypothesis. *Exp Neurol.* 163(2):495-529.

Bartus, Rt., Flicker, C., Dean, R.L., Pontecorvo, M., Figueiredo, J.C., Fisher, Sk., (1985) Selective memory loss following nucleus basalis lesions: long term behavioural recovery despite persistent cholinergic deficiences. *Pharmacol. Biochem. Behav.* 23, 125-35.

Bayer TA, Wirths O, Majtenyi K, Hartmann T, Multhaup G, Beyreuther K, Czech C. (2001) Key factors in Alzheimer's disease: beta-amyloid precursor protein processing, metabolism and intraneuronal transport. *Brain Pathol.* 11(1):1-11.

Behl, C., (2000). Apoptosis and Alzheimer's disease. *J. Neural. Transm.* 107,1325-1344.

Blomer, U., Kafri, T., Randolph-Moore, L., Verma, I.M., Gage, F.H., (1998). Bcl-xL protects adult septal cholinergic neurons from axotomized cell death. *Proc. Nat. Acad. Sci. U S A.* 95, 2603-8.

Braak H, Braak E (1991a) Neuropathological stagging of Alzheimer-related changes. *Acta Neuropathol (Berl)* 82 (4): 239-59

Braak H, Braak E. (1991b) Demonstration of amyloid deposits and neurofibrillary changes in whole brain sections. *Brain Pathol.* 1(3):213-6.

Braak H, Braak E. (1997) Aspects of cortical destruction in Alzheimer disease. In Hyman BT, Duyckaerts C, Christen Y, editors: Connections, Cognition and Alzheimer's Disease. Germany: Springer-Verlag p 1-13.

Brun A, Englund E. (1981) Regional pattern of degeneration in Alzheimer's disease: neuronal loss and histopathological grading. *Histopathology* 5(5):549-64.

Bussiere T, Giannakopoulos P, Bouras C, Perl DP, Morrison JH, Hof PR. (2003) Progressive degeneration of nonphosphorylated neurofilament protein-enriched pyramidal neurons predicts cognitive impairment in Alzheimer's disease: Stereologic analysis of prefrontal cortex area 9. *J Comp Neurol.* 463(3):281-302.

Buzsaki G. (2002) Theta oscillations in the hippocampus. *Neuron.* 33(3):325-40.

Campbell SK, Switzer RC, Martin TL (1987) Alzheimer's plaques and tangles: A controlled and enhanced silver-staining method. *Soc. Neurosci. Abs.* 13: 678

Carro E, Trejo JL, Gomez-Isla T, LeRoith D, Torres-Aleman I. (2002) Serum insulin-like growth factor I regulates brain amyloid-beta levels. *Nat Med.* 8(12):1390-7.

Chan SL, Mattson MP. (1999) Caspase and calpain substrates: roles in synaptic plasticity and cell death. *J Neurosci Res.* 58(1):167-90.

Cohen GM, Sun XM, Fearnhead H, MacFarlane M, Brown DG, Snowden RT, Dinsdale D. (1994) Formation of large molecular weight fragments of DNA is a key committed step of apoptosis in thymocytes. *J Immunol.* 153(2):507-16.

Cohen GM. (1977) Caspases: the executioners of apoptosis. *Biochem J.* 326 (Pt 1):1-16.

Colon EJ. (1973.) The cerebral cortex in presenile dementia. A quantitative analysis. *Acta Neuropathol (Berl).* 23(4):281-90.

Corder EH, Saunders AM, Strittmatter WJ, Schmechel DE, Gaskell PC, Small GW, Roses AD, Haines JL, Pericak-Vance MA. (1993) Gene dose of apolipoprotein E type 4 allele and the risk of Alzheimer's disease in late onset families. *Science.* 261(5123):921-3.

Corso TD, Sesma MA, Tenkova TI, Der TC, Wozniak DF, Farber NB, Olney JW. (1997) Multifocal brain damage induced by phencyclidine is augmented by pilocarpine. *Brain Res.* 752(1-2):1-14.

Cote, S.L., Ribeiro-Da-Silva, A., Cuello, A.C., (1993) Current protocols for light microscopy immunocytochemistry. In Cuello, A.C. (Eds.), Immunohistochemistry II., John Wiley and Sons.

Cotman CW, Su JH. (1996) Mechanisms of neuronal death in Alzheimer's disease. *Brain Pathol.* 6(4):493-506.

Cotman, C.W. & Anderson, A.J. (1995) A potential role for apoptosis in neurodegeneration and Alzheimer's disease. *Mol Neurobiol.* 10(1):19-45.

Cotman, C.W. & Nadler, J.V., (1978). Reactive synaptogenesis in the hippocampus. In: Cotman, C.W. (Eds), Neuronal plasticity. New York: Raven Press. pp. 227-271.

Cowan, C.M., Thai, J., Krajewski, S., Reed, J.C., Nicholson, D.W., Kaufmann, S.H., Roskams, A.J., (2001). Caspases 3 and 9 send a pro-apoptotic signal from synapse to cell body in olfactory receptor neurons. *J. Neurosci.* 21, 7099-7109.

Crutcher, K.A., Madison, R., Davis, J.N., (1981). A study of the rat septohippocampal pathway using anterograde transport of horseradish peroxidase. *Neuroscience.* 6, 1961-1973.

Cullen KM, Halliday GM (1988) Neurofibrillary degeneration and cell loss in the nucleus basalis in comparison to cortical Alzheimer pathology. *Neurobiol Aging.* 19(4):297-306.

Cummings BJ, Pike CJ, Shankle R, Cotman CW. (1996) Beta-amyloid deposition and other measures of neuropathology predict cognitive status in Alzheimer's disease. *Neurobiol Aging.* 17(6):921-33.

Cummings JL, Cole G. (2002) Alzheimer disease. *JAMA* 287(18):2335-8.

Cummings JL, Vinters HV, Cole GM, Khachaturian ZS (1998) Alzheimer's disease. Etiologies, pathophysiology, cognitive reserve and treatment opportunities. *Neurology* 51 (Suppl 1): S2-S17

Czech C, Tremp G, Pradier L. (2000) Presenilins and Alzheimer's disease: biological functions and pathogenic mechanisms. *Prog Neurobiol.* 60(4):363-84.

Davies P, Maloney AJ. (1976) Selective loss of central cholinergic neurons in Alzheimer's disease. *Lancet.* 2(8000):1403.

De la Monte SM, Sohn YK, Ganju N, Wands JR. (1998) CD95-associated apoptosis in neurodegenerative diseases. *Lab Invest.* 1998 Apr;78(4):401-11.

De la Monte SM, Sohn YK, Wands JR. (1997) Correlates of p53- and Fas (CD95)-mediated apoptosis in Alzheimer's disease. *J Neurol Sci.* 152(1):73-83.

De la Torre JC. (1996) Alzheimer disease as a vascular disorder: nosological evidence. *Stroke.* 33(4):1152-62.

De la Torre JC. (2002) Alzheimer's disease: how does it start? *J Alzheimers Dis.* 4(6):497-512.

De Santi S, de Leon MJ, Rusinek H, Convit A, Tarshish CY, Roche A, Tsui WH, Kandil E, Boppana M, Daisley K, Wang GJ, Schlyer D, Fowler J. (2001) Hippocampal formation glucose metabolism and volume losses in MCI and AD. *Neurobiol Aging.* 22(4):529-39.

DeKosky ST, Ikonomovic MD, Styren SD, Beckett L, Wisniewski S, Bennett DA, Cochran EJ, Kordower JH, Mufson EJ. (2002) Upregulation of choline acetyltransferase activity in hippocampus and frontal cortex of elderly subjects with mild cognitive impairment. *Ann Neurol.* 51(2):145-55.

DeKosky ST, Scheff SW. (1990) Synapse loss in frontal cortex biopsies in Alzheimer's disease: correlation with cognitive severity. *Ann Neurol.* 27(5):457-64.

DeKosky, S.T., Scheff, S.W., Styren, S.D., (1996). Structural correlates of cognition in dementia: quantification and assessment of synapse change. *Neurodegeneration.* 5, 417-421.

Delacourte A, Sergeant N, Buee L, Wattez A, Vermersch P, Ghozali F, Fallet-Bianco C, Pasquier F, Lebert F, Petit H, Di Menza C (1999) The biochemical pathway of neurofibrillary degeneration in aging and Alzheimer's disease. *Neurology* 2: 1158-1165

Deweer B, Lehericy S, Pillon B, Baulac M, Chiras J, Marsault C, Agid Y, Dubois B. (1995) Memory disorders in probable Alzheimer's disease: the role of hippocampal atrophy as shown with MRI. *J Neurol Neurosurg Psychiatry.* 58(5):590-7.

Dragoi, G., Carpi, D., Recce, M., Csicsvari, J., Buzsaki, G. (1999) Interactions between hippocampus and medial septum during sharp waves and theta oscillation in the behaving rat. *J Neurosci.* 19(14):6191-9.

Dumanchin-Njock C, Alves da Costa CA, Mercken L, Pradier L, Checler F. (2001) The caspase-derived C-terminal fragment of betaAPP induces caspase-independent toxicity and triggers selective increase of Abeta42 in mammalian cells. *J Neurochem.* 78(5):1153-61.

El Tamer, A., Corey, J., Wulfert, E., Hanin, I., (1992). Reversible cholinergic changes induced by AF64A in rat hippocampus and possible septal compensatory effect. *Neuropharmacology.* 31, 397-402.

Engidawork E, Gulesserian T, Yoo BC, Cairns N, Lubec G. (2001) Alteration of caspases and apoptosis-related proteins in brains of patients with Alzheimer's disease. *Biochem Biophys Res Commun.* 281(1):84-93.

Farber NB, Kim SH, Dikranian K, Jiang XP, Heinkel C. (2002) Receptor mechanisms and circuitry underlying NMDA antagonist neurotoxicity. *Mol Psychiatry.*7(1):32-43.

Fernandez-Shaw C, Marina A, Cazorla P, Valdivieso F, Vazquez J. (1997) Anti-brain spectrin immunoreactivity in Alzheimer's disease: degradation of spectrin in an animal model of cholinergic degeneration. *J Neuroimmunol.* 77(1):91-8.

Ferrer I, Puig B, Krupinsk J, Carmona M, Blanco R. (2001) Fas and Fas ligand expression in Alzheimer's disease. *Acta Neuropathol* 102(2):121-31.

Ferri KF, Kroemer G. (2001) Organelle-specific initiation of cell death pathways. *Nat Cell Biol.* 3(11):E255-63.

Finn JT, Weil M, Archer F, Siman R, Srinivasan A, Raff MC (2000) Evidence that Wallerian degeneration and localized axon degeneration induced by local neurotrophin deprivation do not involve caspases. *J Neurosci.* 20(4):1333-41.

Fischer U, Janicke RU, Schulze-Osthoff K. (2003) Many cuts to ruin: a comprehensive update of caspase substrates. *Cell Death Differ.* 10(1):76-100.

Fonnum, F., (1975). A rapid radiochemical method for the determination of choline acetyltransferase. *J. Neurochem.* 24, 407-9.

Francis PT, Sims NR, Procter AW, Bowen DM. (1963) Cortical pyramidal neurone loss may cause glutamatergic hypoactivity and cognitive impairment in Alzheimer's disease: investigative and therapeutic perspectives. *J Neurochem.* 60(5):1589-604.

Freund TF, Antal M. (1988). GABA-containing neurons in the septum control inhibitory interneurons in the hippocampus. *Nature.* 336(6195):170-3.

Frotscher, M., (1988). Cholinergic neurons in the rat hippocampus do not compensate for the loss of septohippocampal cholinergic fibers. *Neurosci Lett.* 87,18-22

Frotscher, M., Deller, T., Heimrich, B., Forster, E., Haas, C., Naumann, T., (1996). Survival, regeneration and sprouting of central neurons: the rat septohippocampal projection as a model. *Anat. Anz.* 178, 311-315.

Gage, F.H., Bjorklund, A., Stenevi, U., (1983) Reinnervation of the partially deafferented hippocampus by compensatory collateral sprouting from spared cholinergic and noradrenergic afferents. *Brain. Res.* 268, 27-37.

Gage, F.H., Bjorklund, A., Stenevi, U., Dunnett, S.B., Kelly, P.A., (1984). Intrahippocampal septal grafts ameliorate learning impairments in aged rats. *Science.* 225, 533-536.

Gage, F.H., Tuszynski, M.H., Chen, K.S., Armstrong, D., Buzsaki, G., (1989). Survival, growth and function of damaged cholinergic neurons. *EXS.* 57,259-74.

Gage, F.H., Wictorin, K., Fischer, W., Williams, L.R., Varon, S., Bjorklund, A., (1986). A Retrograde cell changes in medial septum and diagonal band following fimbria-fornix transection: quantitative temporal analysis. *Neuroscience.* 19, 241-255.

Gallyas F. (1971). Silver staining of Alzheimer's neurofibrillary changes by means of physical development. *Acta Morphol Acad Sci Hung* 19(1):1-8.

Galvan V, Chen S, Lu D, Logvinova A, Goldsmith P, Koo EH, Bredesen DE. Galvan V, Chen S, Lu D, Logvinova A, Goldsmith P, Koo EH, Bredesen DE. (2002) Caspase cleavage of members of the amyloid precursor family of proteins. *J Neurochem.* 82(2):283-94.

Gasparini L, Gouras GK, Wang R, Gross RS, Beal MF, Greengard P, Xu H. (2001) Stimulation of beta-amyloid precursor protein trafficking by insulin reduces intraneuronal beta-amyloid and requires mitogen-activated protein kinase signaling. *J Neurosci.* 21(8):2561-70.

Gasparini L, Netzer WJ, Greengard P, Xu H. (2002) Does insulin dysfunction play a role in Alzheimer's disease? (2002) *Trends Pharmacol Sci.* 23(6):288-93.

Gasparini L, Xu H. (2003) Potential roles of insulin and IGF-1 in Alzheimer's disease. *Trends Neurosci.* 26(8):404-6.

Gastard MC, Troncoso JC, Koliatsos VE. (2003) Caspase activation in the limbic cortex of subjects with early Alzheimer's disease. *Ann Neurol.* 54(3):393-8.

Gazzaley AH, Benson DL, Huntley GW, Morrison JH. (1997). Differential subcellular regulation of NMDAR1 protein and mRNA in dendrites of dentate gyrus granule cells after perforant path transection. *J Neurosci* 17(6):2006-17.

George, E.B., Glass, JD., Griffin, J.W. (1995) Axotomy-induced axonal degeneration is mediated by calcium influx through ion-specific channels. *J Neurosci.* 15(10):6445-52.

Gervais F, Xu D, Robertson GS, Vaillancourt J, Zhu Y, Vaillancourt JP, Zhu Y, Huang J, LeBlanc A, Smith D, Rigby M, Shearman MS, Clarke EE, Zheng H, Van Der Ploeg LH, Ruffolo SC, Thornberry NA, Xanthoudakis S, Zamboni RJ, Roy S, Nicholson DW. (1999). Involvement of caspase in proteolytic cleavage of Alzheimer's disease amyloid-β precursor protein and amyloidogenic Aβ peptide formation. *Cell* 97: 395-406.

Ginsberg, S.D., Martin, L.J., (2002). Axonal transection in adult rat brain induces transsynaptic apoptosis and persistent atrophy of target neurons. *J. Neurotrauma.* 19, 99-109.

Ginsberg, S.D., Portera-Cailliau, C., Martin, L.J., (1999) Fimbria-fornix transection and excitotoxicity produce similar neurodegeneration in the septum. *Neuroscience* 88, 1059-1071.

Giovannini MG, Scali C, Prosperi C, Bellucci A, Vannucchi MG, Rosi S, Pepeu G, Casamenti F. (2002) Beta-amyloid-induced inflammation and cholinergic hypofunction in the rat brain in vivo: involvement of the p38MAPK pathway. *Neurobiol Dis.* 11(2):257-74.

Glenner GG, Wong CW. (1984) Alzheimer's disease and Down's syndrome: sharing of a unique cerebrovascular amyloid fibril protein. *Biochem Biophys Res Commun.* 122(3):1131-5.

Gomez-Isla T, Growdon WB, McNamara MJ, Nochlin D, Bird TD, Arango JC, Lopera F, Kosik KS, Lantos PL, Cairns NJ, Hyman BT. (1999 The impact of different presenilin 1 and presenilin 2 mutations on amyloid deposition, neurofibrillary changes and neuronal loss in the familial Alzheimer's disease brain: evidence for other phenotype-modifying factors. *Brain.* 122 (Pt 9):1709-19.

Gomez-Isla T, Hollister R, West H, Mui S, Growdon JH, Petersen RC, Parisi JE, Hyman BT (1997) Neuronal loss correlates with but exceeds neurofibrillary tangles in Alzheimer's disease. *Ann Neurol* 41(1): 17-24

Gomez-Isla T, Price JL, McKeel DW Jr, Morris JC, Growdon JH, Hyman BT. (1996) Profound loss of layer II entorhinal cortex neurons occurs in very mild Alzheimer's disease. *J Neurosci.* 16(14):4491-500.

Gotz J, Chen F, van Dorpe J, Nitsch RM. (2001) Formation of neurofibrillary tangles in P301l tau transgenic mice induced by Abeta 42 fibrils. *Science.* 293(5534):1491-5.

Grant SM, Ducatenzeiler A, Szyf M, Cuello AC. (2000) Aβ immunoreactive material is present in several intracellular compartments in transfected neuronally differentiated, P19 cell expressing the human amyloid –precursor protein. *Journal of Alzh Dis.* 2:207-222

Greenamyre JT, Young AB. (1989) Excitatory amino acids and Alzheimer's disease. *Neurobiol Aging.* 10(5):593-602.

Gulyas AI, Toth K, Danos P, Freund TF. (1991) Subpopulations of GABAergic neurons containing parvalbumin, calbindin D28k, and cholecystokinin in the rat hippocampus. *J Comp Neurol.* 312(3):371-8.

Gulyas, A.I., Seress, L., Toth, K., Acsady, L., Antal, M., Freund, T.F. (1991) Septal GABAergic neurons innervate inhibitory interneurons in the hippocampus of the macaque monkey. *Neuroscience.* 41(2-3):381-90.

Guo Q, Fu W, Xie J, Luo H, Sells SF, Geddes JW, Bondada V, Rangnekar VM, Mattson MP (1998) Par-4 is a mediator of neuronal degeneration associated with the pathogenesis of Alzheimer disease. *Nature Medicine.* 4(8): 957-62

Guo Q, Sopher BL, Furukawa K, Pham DG, Robinson N, Martin GM, Mattson MP (1997) Alzheimer's presenilin mutation sensitizes neural cells to apoptosis induced by trophic factor withdrawal and amyloid beta-peptide: involvement of calcium and oxyradicals. *J Neurosci* 17(11): 4212-22

Guttmann, R.P., Sokol, S., Baker, D.L., Simpkins, K.L., Dong, Y., Lynch, D.R., (2002) Proteolysis of the N-methyl-d-aspartate receptor by calpain in situ. *J. Pharmacol. Exp. Ther.* 302,1023-1030.

Hage B, Frotscher M, Naumann T., (1996) Activity of choline acetyltransferase in the rat medial septal nucleus following fimbria-fornix transection or selective immunolesioning with 192 IgG-saporin. *Neurosci Lett.* 205(2), 119-22.

Hagg, T., Manthorpe, M., Vahlsing, H.L., Varon, S., (1988) Delayed treatment with nerve growth factor reverses the apparent loss of cholinergic neurons after acute brain damage. *Exp. Neurol.* 101, 303-312.

Hamos JE, DeGennaro LJ, Drachman DA. (1989) Synaptic loss in Alzheimer's disease and other dementias. *Neurology.* 39(3):355-61.

Hardy J, Duff K, Hardy KG, Perez-Tur J, Hutton M (1998) Genetic dissection of Alzheimer's disease and related dementias: amyloid and its relationship to tau. *Nat Neurosci.* 1(5):355-8.

Hardy J, Selkoe DJ. (2002) The amyloid hypothesis of Alzheimer's disease: progress and problems on the road to therapeutics. *Science.* 297(5580):353-6.

Hardy J. (1997) Amyloid, the presenilins and Alzheimer's disease. *Trends Neurosci.* 20(4):154-9.

Harris A.S. & Morrow J.S. (1988) Proteolytic processing of human brain alpha spectrin (fodrin): identification of a hypersensitive site. *J Neurosci.* 8(7):2640-51.

Harris MH, Thompson CB. (2000) The role of the Bcl-2 family in the regulation of outer mitochondrial membrane permeability. *Cell Death Differ.* 7(12):1182-91.

Hatanpaa K, Brady DR, Stoll J, Rapoport SI, Chandrasekaran K. (1996) Neuronal activity and early neurofibrillary tangles in Alzheimer's disease. *Ann Neurol.* 40(3):411-20.

Hefti, F., (1986) Nerve growth factor promotes survival of septal cholinergic neurons after fimbrial transections. *J. Neurosci.* 6, 2155-2162.

Heimrich, B., Papp, E.C., Freund, T.F., Frotscher, M., (1996). Regeneration of the GABAergic septohippocampal projection in vitro. *Neuroscience.* 72, 409-417.

Heintz, N. & Zoghbi, H.Y., (2000) Insights from mouse models into the molecular basis of neurodegeneration. *Annu. Rev. Physiol.* 62,779-802.

Hell, J.W., Westenbroek, R.E., Breeze, L.J., Wang, K.K., Chavkin, C., Catterall, W.A., (1996) N-methyl-D-aspartate receptor-induced proteolytic conversion of postsynaptic class C L-type calcium channels in hippocampal neurons. *Proc Natl Acad Sci U S A.* 93, 3362-3367.

Henderson, Z., (1996) Responses of basal forebrain cholinergic neurons to damage in the adult brain. *Prog. Neurobiol.* 48, 219-254S.

Hengartner MO. (2000) The biochemistry of apoptosis. *Nature.* 407(6805):770-6.

Hof PR, Cox K, Morrison JH. (1990). Quantitative analysis of a vulnerable subset of pyramidal neurons in Alzheimer's disease: I. Superior frontal and inferior temporal cortex. *J Comp Neurol* 301(1):44-54.

Hof PR, Duan H, Page TL, Einstein M, Wicinski B, He Y, Erwin JM, Morrison JH. (2002) Age-related changes in GluR2 and NMDAR1 glutamate receptor subunit protein immunoreactivity in corticocortically projecting neurons in macaque and patas monkeys. *Brain Res.* 928(1-2):175-86.

Honig, L.S. & Rosenberg, R.N., (2000) Apoptosis and neurologic disease. *Am. J. Med.* 108, 317-330.

Hoyer S, Nitsch R, Oesterreich K. (1991) Predominant abnormality in cerebral glucose utilization in late-onset dementia of the Alzheimer type: a cross-sectional comparison against advanced late-onset and incipient early-onset cases. *J Neural Transm Park Dis Dement Sect.* 3(1):1-14.

Hoyer S, Oesterreich K, Wagner O. (1988) Glucose metabolism as the site of the primary abnormality in early-onset dementia of Alzheimer type? *J Neurol.* 235(3):143-8.

Huang Y, Wang KK. (2001) The calpain family and human disease. *Trends Mol Med.* 7(8):355-62.

Hubbard BM, Anderson JM. 1985. Age-related variations in the neuron content of the cerebral cortex in senile dementia of Alzheimer type. *Neuropathol Appl Neurobiol.* 11(5):369-82.

Hugon, J., Terro, F., Esclaire, F., Yardin, C., (2000) Markers of apoptosis and models of programmed cell death in Alzheimer's disease. *J. Neural. Transm. Suppl.* 59,125-131.

Hyman BT, Kromer LJ, Van Hoesen GW. (1987) Reinnervation of the hippocampal perforant pathway zone in Alzheimer's disease. *Ann Neurol.* 21(3):259-67.

Hyman, B.T., Van Hoesen, G.W., Damasio, A.R., (1990) Memory-related neural systems in Alzheimer's disease: an anatomic study. *Neurology* 40, 1721-1730.

Hyman, B.T., Van Horsen, G.W., Damasio, A.R., Barnes, C.L., (1984) Alzheimer's disease: cell-specific pathology isolates the hippocampal formation. *Science* 225, 1168-1170.

Ikonomovic MD, Nocera R, Mizukami K, Armstrong DM. (2000) Age-related loss of the AMPA receptor subunits GluR2/3 in the human nucleus basalis of Meynert. *Exp Neurol.* 166(2):363-75.

Iversen LL, Mortishire-Smith RJ, Pollack SJ, Shearman MS. (1995) The toxicity in vitro of beta-amyloid protein. *Biochem J.* 311 (Pt 1):1-16.

Ivins KJ, Thornton PL, Rohn TT, Cotman CW (1999) Neuronal apoptosis induced by beta-amyloid is mediated by caspase-8. *Neurobiol Dis* 6(5): 440-9

Janke AL, de Zubicaray G, Rose SE, Griffin M, Chalk JB, Galloway GJ. (2001) 4D deformation modeling of cortical disease progression in Alzheimer's dementia. *Magn Reson Med.* 46(4):661-6.

Johnson GV, Bailey CD. (2003) The p38 MAP kinase signaling pathway in Alzheimer's disease. *Exp Neurol.* 183(2):263-8.

Juottonen K, Laakso MP, Insausti R, Lehtovirta M, Pitkanen A, Partanen K, Soininen H. (1998) Volumes of the entorhinal and perirhinal cortices in Alzheimer's disease. *Neurobiol Aging.* 19(1):15-22.

Kamenetz F, Tomita T, Hsieh H, Seabrook G, Borchelt D, Iwatsubo T, Sisodia S, Malinow R. (2003) APP processing and synaptic function. *Neuron.* 37(6):925-37.

Kang J, Lemaire HG, Unterbeck A, Salbaum JM, Masters CL, Grzeschik KH, Multhaup G, Beyreuther K, Muller-Hill B. (1987) The precursor of Alzheimer's disease amyloid A4 protein resembles a cell-surface receptor. *Nature.*325(6106):733-6.

Katzman R, Terry R, DeTeresa R, Brown T, Davies P, Fuld P, Renbing X, Peck A. (1988) Clinical, pathological, and neurochemical changes in dementia: a subgroup with preserved mental status and numerous neocortical plaques. *Ann Neurol.* 23(2):138-144.

Kermer, P., Naumann, T., Bender, R., Frotscher, M., (1995) Fate of GABAergic septohippocampal neurons after fimbria-fornix transection as revealed by in situ hybridization for glutamate decarboxylase mRNA and parvalbumin immunocytochemistry. *J Comp Neurol.* 362(3),385-399.

Kerr JF, Wyllie AH, Currie AR. (1972) Apoptosis: a basic biological phenomenon with wide-ranging implications in tissue kinetics. Br J Cancer. 26(4):239-57.

Kitamura Y, Ota T, Matsuoka Y, Tooyama I, Kimura H, Shimohama S, Nomura Y, Gebicke-Haerter PJ, Taniguchi T. (1999) Hydrogen peroxide-induced apoptosis mediated by p53 protein in glial cells. *Glia.* 25(2):154-64.

Kitamura Y, Shimohama S, Kamoshima W, Matsuoka Y, Nomura Y, Taniguchi T. (1997) Changes of p53 in the brains of patients with Alzheimer's disease. *Biochem Biophys Res Commun.* 232(2):418-21.

Kitamura Y, Shimohama S, Kamoshima W, Ota T, Matsuoka Y, Nomura Y, Smith MA, Perry G, Whitehouse PJ, Taniguchi T. (1998) Alteration of proteins regulating apoptosis, Bcl-2, Bcl-x, Bax, Bak, Bad, ICH-1 and CPP32, in Alzheimer's disease. *Brain Res.* 780(2):260-9.

Kitamura Y, Taniguchi T, Shimohama S (1999) Apoptotic cell death in neurons and glial cells: implications for Alzheimer's disease. *Jpn J Pharmacol* 79(1): 1-5

Knusell, B., Beck, K.D., Winslow, J.W., Rosenthal, A., Burton, L.E., Widmer, H.R., Nikolics, K., Hefti, F., (1992) Brain-derived neurotrophic factor administration protects basal forebrain cholinergic but not nigral dopaminergic neurons from degenerative changes after axotomy in the adult rat brain. *J. Neurosci.* 12, 4391-4402.

Kohler, C., Chan-Palay, V., Wu, J.Y. (1984) Septal neurons containing glutamic acid decarboxylase immunoreactivity project to the hippocampal region in the rat brain. *Anat Embryol (Berl)* 169(1):41-44.

Kolasa, K. and Harrell, L.E., (2000) Apoptotic protein expression and activation of caspases is changed following cholinergic denervation and hippocampal sympathetic ingrowth in rat hippocampus. *Neuroscience* 101, 541-546.

Koliatsos, V.E. & Price, D.L. (1996) Axotomy as an experimental model of neuronal injury and cell death. *Brain Pathol.* 6(4):447-65.

Kromer, L.F., Bjorklund, A., Stenevi, U., (1983) Intracephalic embryonic neural implants in the adult rat brain. I. Growth and mature organization of brainstem, cerebellar, and hippocampal implants. *J. Comp. Neurol.* 218, 433-459.

Kugler S, Straten G, Kreppel F, Isenmann S, Liston P, Bahr M. (2000) The X-linked inhibitor of apoptosis (XIAP) prevents cell death in axotomized CNS neurons in vivo. Cell Death Differ. 7(9):815-24.

Kwiatkowski, A.P. & King, M.M., (1989) Autophosphorylation of the type II calmodulin-dependent protein kinase is essential for formation of a proteolytic fragment with catalytic activity. Implications for long-term synaptic potentiation. *Biochemistry.* 28, 5380-5385.

Lassmann H, Bancher C, Breitschopf H, Wegiel J, Bobinski M, Jellinger K, Wisniewski HM (1995) Cell death in Alzheimer's disease evaluated by DNA fragmentation in situ. *Acta Neuropathol (Berl)* 89(1): 35-41

LeBlanc A, Liu H, Goodyer C, Bergeron C, Hammond J. (1999) Caspase-6 role in apoptosis of human neurons, amyloidogenesis, and Alzheimer's disease. *J Biol Chem.* 274(33):23426-36.

LeBlanc A. (1995) Increased production of 4 kDa amyloid beta peptide in serum deprived human primary neuron cultures: possible involvement of apoptosis. *J Neurosci.* 15(12):7837-46.

Lee MS, Kwon YT, Li M, Peng J, Friedlander RM, Tsai LH. (2000) Neurotoxicity induces cleavage of p35 to p25 by calpain. *Nature.* 405(6784):360-4.

Lee VM. (2001 Biomedicine. Tauists and beta-aptists united--well almost! *Science.* 293(5534):1446-7

Leranth C, Deller T, Buzsaki G. (1992) Intraseptal connections redefined: lack of a lateral septum to medial septum path. *Brain Res.* 583(1-2):1-11.

Lewis J, Dickson DW, Lin WL, Chisholm L, Corral A, Jones G, Yen SH, Sahara N, Skipper L, Yager D, Eckman C, Hardy J, Hutton M, McGowan E. (2001) Enhanced neurofibrillary degeneration in transgenic mice expressing mutant tau and APP. *Science.* 293(5534):1487-91.

Lewis J, McGowan E, Rockwood J, Melrose H, Nacharaju P, Van Slegtenhorst M, Gwinn-Hardy K, Paul Murphy M, Baker M, Yu X, Duff K, Hardy J, Corral A, Lin WL, Yen SH, Dickson DW, Davies P, Hutton M. (2000) Neurofibrillary tangles, amyotrophy and progressive motor disturbance in mice expressing mutant (P301L) tau protein. *Nat Genet.* 25(4):402-5.

Li, B.S., Sun, M.K., Zhang, L., Takahashi, S., Ma, W., Vinade, L., Kulkarni, A.B., Brady, R.O., Pant, H.C., (2001). Regulation of NMDA receptors by cyclin-dependent kinase-5. *Proc Natl Acad Sci U S A.* 98, 12742-12747.

Linke R, Heimrich B, Frotscher M. (1995) Axonal regeneration of identified septohippocampal projection neurons in vitro. *Neuroscience* 68(1):1-4.

Liston P, Roy N, Tamai K, Lefebvre C, Baird S, Cherton-Horvat G, Farahani R, McLean M, Ikeda JE, MacKenzie A, Korneluk RG (1996) Suppression of apoptosis in mammalian cells by NAIP and a related family of IAP genes. *Nature* 379(6563):349-53.

Lorenzo A, Yuan M, Zhang Z, Paganetti PA, Sturchler-Pierrat C, Staufenbiel M, Mautino J, Vigo FS, Sommer B, Yankner BA. (2000) Amyloid beta interacts with the amyloid precursor protein: a potential toxic mechanism in Alzheimer's disease. *Nat Neurosci.* 3(5):460-4.

Lu DC, Rabizadeh S, Chandra S, Shayya RF, Ellerby LM, Ye X, Salvesen GS, Koo EH, Bredesen DE. (2000) A second cytotoxic proteolytic peptide derived from amyloid beta-protein precursor. *Nature Medicine* 6(4):397-404.

Lu DC, Soriano S, Bredesen DE, Koo EH. (2003) Caspase cleavage of the amyloid precursor protein modulates amyloid beta-protein toxicity. *J Neurochem.* 87(3):733-41

Lu, X., Wyszynski, M., Sheng, M., Baudry, M., (2001) Proteolysis of glutamate receptor-interacting protein by calpain in rat brain: implications for synaptic plasticity. *J. Neurochem.* 77, 1553-1560.

Lucassen PJ, Chung WC, Kamphorst W, Swaab DF (1997) DNA damage distribution in the human brain as shown by in situ end labeling; area-specific differences in aging and Alzheimer disease in the absence of apoptotic morphology. *J Neuropathol Exp Neurol* 56 (8): 887-900

Lynch, G. and Baudry, M., (1984) The biochemistry of memory: a new and specific hypothesis. *Science.* 224, 1057-1063.

Mann DM, Yates PO, Marcyniuk B. (1985). Some morphometric observations on the cerebral cortex and hippocampus in presenile Alzheimer's disease, senile dementia of Alzheimer type and Down's syndrome in middle age. *J Neurol Sci.* 69(3):139-59.

Marks N, Berg MJ (1999) Recent advances on neuronal caspases in development and neurodegeneration. *Neurochem Int* 35(3): 195-220

Martin SJ, Reutelingsperger CP, McGahon AJ, Rader JA, van Schie RC, LaFace DM, Green DR.(1995) Early redistribution of plasma membrane phosphatidylserine is a general feature of apoptosis regardless of the initiating stimulus: inhibition by overexpression of Bcl-2 and Abl. *J Exp Med.* 182(5):1545-56.

Masliah E, Iwai A, Mallory M, Ueda K, Saitoh T. (1996) Altered presynaptic protein NACP is associated with plaque formation and neurodegeneration in Alzheimer's disease. *Am J Pathol.* ;148(1):201-10.

Masliah E, Mallory M, Alford M, Tanaka S, Hansen LA (1998) Caspase dependent fragmentation might be associated with excitotoxicity in Alzheimer disease. *Journal Neuropathol Exp Neurol* 57(11): 1041-1052

Masliah E, Terry RD, Alford M, DeTeresa R, Hansen LA. (1991) Cortical and subcortical patterns of synaptophysinlike immunoreactivity in Alzheimer's disease. *Am J Pathol.* 138(1):235-46.

Masliah, E., Terry, R.D., Alford, M., DeTeresa, R., (1990) Quantitative immunohistochemistry of synaptophysin in human neocortex: an alternative method to estimate density of presynaptic terminals in paraffin sections. *J. Histochem. Cytochem.* 38, 837-844.

Masters CL, Simms G, Weinman NA, Multhaup G, McDonald BL, Beyreuther K. (1984) Amyloid plaque core protein in Alzheimer disease and Down syndrome. *Proc Natl Acad Sci U S A.* 82(12):4245-9.

Mattson MP, Duan W, Pedersen WA, Culmsee C (2001) Neurodegenerative disorders and ischemic brain diseases. *Apoptosis* 6(1-2): 69-81

Mattson MP, Duan W. (1999) "Apoptotic" biochemical cascades in synaptic compartments: roles in adaptive plasticity and neurodegenerative disorders. *J Neurosci Res.* 58(1):152-66.

Mattson MP. (1997) Cellular actions of beta-amyloid precursor protein and its soluble and fibrillogenic derivatives. *Physiol Rev.* 77(4):1081-132.

McEwen BS, Conrad CD, Kuroda Y, Frankfurt M, Magarinos AM, McKittrick C. (1997) Prevention of stress-induced morphological and cognitive consequences. *Eur Neuropsychopharmacol.* 7 Suppl 3:S323-8.

McKinney, M., Coyle, J.T., Hedreen, J.C., (1983) Topographic analysis of the innervation of the rat neocortex and hippocampus by the basal forebrain cholinergic system. *J. Comp. Neuro.* 217, 103-121.

McLean CA, Cherny RA, Fraser FW, Fuller SJ, Smith MJ, Beyreuther K, Bush AI, Masters CL. (1999) Soluble pool of Abeta amyloid as a determinant of severity of neurodegeneration in Alzheimer's disease. *Ann Neurol.* 46(6):860-6.

Meibach, R.C. and Siegel, A., (1977) Efferent connections of the septal area in the rat: an analysis utilizing retrograde and anterograde transport methods. *Brain. Res.* 119, 1-10.

Morishima-Kawashima M, Ihara Y. (2002) Alzheimer's disease: beta-Amyloid protein and tau. *J Neurosci Res.* 70(3):392-401.

Morris JC, Price AL. (2001) Pathologic correlates of nondemented aging, mild cognitive impairment, and early-stage Alzheimer's disease. *J Mol Neurosci.* 17(2):101-18.

Morrison JH, Hof PR. (1997) Life and death of neurons in the aging brain. *Science* 278(5337):412-9.

Morrison RS, Kinoshita Y, Johnson MD, Ghatan S, Ho JT, Garden G. (2002) Neuronal survival and cell death signaling pathways. *Adv Exp Med Biol.* 2002;513:41-86.

Morsch R, Simon W, Coleman PD. (1999) Neurons may live for decades with neurofibrillary tangles. *J Neuropathol Exp Neurol.* 58(2):188-97.

Mosko, S., Lynch, G., Cotman, C.W.(1973) The distribution of septal projections to the hippocampus of the rat. *J. Comp. Neurol.* 152, 163-174.

Mudher A, Lovestone S. (2002) Alzheimer's disease-do tauists and baptists finally shake hands? *Trends Neurosci.* 25(1):22-6.

Mufson EJ, Bothwell M, Kordower JH. (1989) Loss of nerve growth factor receptor-containing neurons in Alzheimer's disease: a quantitative analysis across subregions of the basal forebrain. *Exp Neurol.* 105(3):221-32.

Nakagawa T, Zhu H, Morishima N, Li E, Xu J, Yankner BA, Yuan J. (2000) Caspase-12 mediates endoplasmic-reticulum-specific apoptosis and cytotoxicity by amyloid-beta. *Nature.* 403(6765):98-103.

Naslund J, Haroutunian V, Mohs R, Davis KL, Davies P, Greengard P, Buxbaum JD. (2000) Correlation between elevated levels of amyloid beta-peptide in the brain and cognitive decline. *JAMA.* 283(12):1571-7.

Nath R, Davis M, Probert AW, Kupina NC, Ren X, Schielke GP, Wang KK. (2000) Processing of cdk5 activator p35 to its truncated form (p25) by calpain in acutely injured neuronal cells. *Biochem Biophys Res Commun.* 274(1):16-21

Nath, R., Davis, M., Probert, A.W., Kupina, N.C., Ren, X., Schielke, G.P., Wang, K.K., (2000) Processing of cdk5 activator p35 to its truncated form (p25) by calpain in acutely injured neuronal cells. *Biochem. Biophys. Res. Commun.* 274,16-21.

Nath, R., Huggins, M., Glantz, S.B., Morrow, J.S., McGinnis, K., Nadimpalli, R., Wanga, K.K. (2000) Development and characterization of antibodies specific to caspase-3-produced alpha II--spectrin 120 kDa breakdown product: marker for neuronal apoptosis. *Neurochem. Int.* 37, 351-361.

Naumann, T., Kermer, P., Frotscher, M., (1994) Fine structure of rat septohippocampal neurons. III. Recovery of choline acetyltransferase immunoreactivity after fimbria-fornix transection. *J Comp Neurol.* 350(2),161-170.

Naumann, T., Peterson, G.M., Frotscher, M., (1992) Fine structure of rat septohippocampal neurons: II. A time course analysis following axotomy. *J Comp Neurol.* 325(2),219-242.

Neve RL, McPhie DL, Chen Y (2000) Alzheimer's disease: a dysfunction of the amyloid precursor protein. *Brain Res* 886 (1-2): 54-66

Newcomb, J.K., Kampfl, A., Posmantur, R.M., Zhao, X., Pike, B.R., Liu, S.J., Clifton, G.L., Hayes, R.L. (1997) Immunohistochemical study of calpain-mediated breakdown products to alpha-spectrin following controlled cortical impact injury in the rat. *J Neurotrauma.* 14(6):369-83.

Nicholson DW, Thornberry NA. (1997) Caspases: killer proteases. *Trends Biochem Sci.* 22(8):299-306.

Nicotera P, Leist M, Manzo L. (1999) Neuronal cell death: a demise with different shapes. *Trends Pharmacol Sci.* 20(2):46-51.

Nijhawan D, Honarpour N, Wang X (2000) Apoptosis in neural development and disease. *Annu Rev Neurosci* 23: 73-87

Nishimura T, Akiyama H, Yonehara S, Kondo H, Ikeda K, Kato M, Iseki E, Kosaka K. (1995) Fas antigen expression in brains of patients with Alzheimer-type dementia. *Brain Res.* 695(2):137-45.

Nishimura T, Akiyama H, Yonehara S, Kondo H, Ikeda K, Kato M, Iseki E, Kosaka K (1995) Fas antigen expression in brains of patients with Alzheimer-type dementia. *Brain Res* 95 (2): 137-45

Nixon RA, Saito KI, Grynspan F, Griffin WR, Katayama S, Honda T, Mohan PS, Shea TB, Beermann M. (1994) Calcium-activated neutral proteinase (calpain) system in aging and Alzheimer's disease. *Ann N Y Acad Sci.* 747:77-91.

Nixon RA. (1986) Fodrin degradation by calcium-activated neutral proteinase (CANP) in retinal ganglion cell neurons and optic glia: preferential localization of CANP activities in neurons. *J Neurosci.* 6(5):1264-71.

Nixon RA. (2000) A "protease activation cascade" in the pathogenesis of Alzheimer's disease. *Ann N Y Acad Sci.* 924:117-31.

Nixon RA. (2003) The calpains in aging and aging-related diseases. *Ageing Res Rev.* 2(4):407-18.

Nunomura A, Perry G, Pappolla MA, Wade R, Hirai K, Chiba S, Smith MA. (1999) RNA oxidation is a prominent feature of vulnerable neurons in Alzheimer's disease. *J Neurosci.* 19(6):1959-64.

O'Brien, T.S., Svendsen, C.N., Isaacson, O., Sofroniew, M.V., (1990) Loss of true blue labelling from the medial septum following transection of the fimbria-fornix: evidence for the death of cholinergic and non-cholinergic neurons. *Brain. Res.* 508, 249-256.

Olney JW, Wozniak DF, Farber NB. (1998) Glumate Receptor Dysfunction and Alzheimer's Disease. Restor Neurol Neurosci. 13(1,2):75-83.

Oppenheim RW (1991) Cell death during development of the nervous system. *Annu Rev Neurosci.* 14:453-501.

Otto D, Frotscher M, Unsicker K. (1989) Basic fibroblast growth factor and nerve growth factor administered in gel foam rescue medial septal neurons after fimbria fornix transection. *J Neurosci Res.* 22(1):83-91.

Pearson RC, Sofroniew MV, Powell TP. (1985) Hypertrophy of cholinergic neurones of the rat basal nucleus following section of the corpus callosum. *Brain Res.* 338(2):337-40.

Pei JJ, Braak E, Braak H, Grundke-Iqbal I, Iqbal K, Winblad B, Cowburn RF. (2001) Localization of active forms of C-jun kinase (JNK) and p38 kinase in Alzheimer's disease brains at different stages of neurofibrillary degeneration. *J Alzheimers Dis.* 3(1):41-48.

Pei JJ, Braak H, An WL, Winblad B, Cowburn RF, Iqbal K, Grundke-Iqbal I. (2002) Up-regulation of mitogen-activated protein kinases ERK1/2 and MEK1/2 is associated with the progression of neurofibrillary degeneration in Alzheimer's disease. *Brain Res Mol Brain Res.* 109(1-2):45-55.

Pellegrini L, Passer BJ, Tabaton M, Ganjei JK, D'Adamio L (1999) Alternative, non-secretase processing of Alzheimer's beta-amyloid precursor protein during apoptosis by caspase-6 and -8. *J Biol Chem* 274(30): 21011-6

Pellegrini L, Passer BJ, Tabaton M, Ganjei JK, D'Adamio L. (1999) Alternative, non-secretase processing of Alzheimer's beta-amyloid precursor protein during apoptosis by caspase-6 and -8. *J Biol Chem.* 274(30):21011-6.

Perry E, Walker M, Grace J, Perry R. (1999) Acetylcholine in mind: a neurotransmitter correlate of consciousness? *Trends Neurosci.* 22(6):273-80.

Perry EK, Perry RH, Blessed G, Tomlinson BE. (1977) Necropsy evidence of central cholinergic deficits in senile dementia. *Lancet* 1(8004):189.

Perry G, Nunomura A, Lucassen P, Lassmann H, Smith MA (1998) Apoptosis and Alzheimer's disease. *Science.* 282(5392):1268-9.

Perry G, Nunomura A, Smith MA (1998) A suicide note from Alzheimer disease neurons? *Nat Med* 4(8): 957-62

Peterson, G.M., Lanford, G.W., Powell, E.W., (1990) Fate of septohippocampal neurons following fimbria-fornix transection: a time course analysis. *Brain. Res. Bull.* 25, 129-137.

Pike, B.R., Flint, J., Dutta, S., Johnson, E., Wang, K.K., Hayes, R.L., (2001). Accumulation of non-erythroid alpha II--spectrin and calpain-cleaved alpha II--spectrin breakdown products in cerebrospinal fluid after traumatic brain injury in rats. *J. Neurochem.* 78, 1297-1306.

Pike, B.R., Zhao, X., Newcomb, J.K., Posmantur, R.M., Wang, K.K., Hayes, R.L., (1998). Regional calpain and caspase-3 proteolysis of alpha--spectrin after traumatic brain injury. *Neuroreport.* 9,2437-2442.

Pompl PN, Yemul S, Xiang Z, Ho L, Haroutunian V, Purohit D, Mohs R, Pasinetti GM. (2003) Caspase gene expression in the brain as a function of the clinical progression of Alzheimer disease. *Arch Neurol.*;60(3):369-76.

Porter AG, Janicke RU. (1999) Emerging roles of caspase-3 in apoptosis. *Cell Death Differ.* 6(2):99-104.

Price JL, Morris JC. (1999) Tangles and plaques in nondemented aging and "preclinical" Alzheimer's disease. *Ann Neurol.* 45(3):358-68.

Raff MC, Whitmore AV, Finn JT. (2002) Axonal self-destruction and neurodegeneration. *Science.* 296(5569):868-71.

Raina AK, Hochman A, Zhu X, Rottkamp CA, Nunomura A, Siedlak SL, Boux H, Castellani RJ, Perry G, Smith MA. (2001) Abortive apoptosis in Alzheimer's disease. *Acta Neuropathol (Berl).*101(4):305-10.

Raina AK, Hochman A, Ickes H, Zhu X, Ogawa O, Cash AD, Shimohama S, Perry G, Smith MA (2003) Apoptotic promoters and inhibitors in Alzheimer's disease: Who wins out? *Prog Neuropsychopharmacol Biol Psychiatry.* 27(2):251-4.

Raisman, G., (1966) The connexions of the septum. *Brain* 89(2),317-348.

Regeur L, Jensen GB, Pakkenberg H, Evans SM, Pakkenberg B. (1994) No global neocortical nerve cell loss in brains from patients with senile dementia of Alzheimer's type. *Neurobiol Aging.* 15(3):347-52.

Riley KP, Snowdon DA, Markesbery WR. (2002) Alzheimer's neurofibrillary pathology and the spectrum of cognitive function: findings from the Nun Study. *Ann Neurol.* 51(5):567-77.

Rinne JO, Paljarvi L, Rinne UK. (1987). Neuronal size and density in the nucleus basalis of Meynert in Alzheimer's disease. *J Neurol Sci.* 79(1-2):67-76.

Roberts-Lewis JM, Savage MJ, Marcy VR, Pinsker LR, Siman R. (1994) Immunolocalization of calpain I-mediated spectrin degradation to vulnerable neurons in the ischemic gerbil brain. *J Neurosci.* 14(6):3934-44.

Robertson GS, Crocker SJ, Nicholson DW, Schulz JB (2000) Neuroprotection by the inhibition of apoptosis. *Brain Pathology* 2: 283-292

Rohn TT, Head E, Su JH, Anderson AJ, Bahr BA, Cotman CW, Cribbs DH. (2001) Correlation between caspase activation and neurofibrillary tangle formation in Alzheimer's disease. *Am J Pathol* 158(1):189-98.

Rohn TT, Ivins KJ, Bahr BA, Cotman CW, Cribbs DH. (2000) A monoclonal antibody to amyloid precursor protein induces neuronal apoptosis. *J Neurochem.* 74(6):2331-42.

Rohn TT, Rissman RA, Davis MC, Kim YE, Cotman CW, Head E. (2002) Caspase-9 activation and caspase cleavage of tau in the Alzheimer's disease brain. *Neurobiol Dis.* 11(2):341-54.

Rohn TT, Rissman RA, Head E, Cotman CW. (2003) Caspase Activation in the Alzheimer's Disease Brain: Tortuous and Torturous. *Drug News Perspect.*15(9):549-557.

Rong, Y., Lu, X., Bernard, A., Khrestchatisky, M., Baudry, M., (2001). Tyrosine phosphorylation of ionotropic glutamate receptors by Fyn or Src differentially modulates their susceptibility to calpain and enhances their binding to -spectrin and PSD-95. *J. Neurochem.* 79, 382-390.

Saido TC, Yokota M, Nagao S, Yamaura I, Tani E, Tsuchiya T, Suzuki K, Kawashima S. (1993) Spatial resolution of fodrin proteolysis in postischemic brain. *J Biol Chem.* 268(33):25239-43.

Saido, T.C., Sorimachi, H., Suzuki, K., (1994) Calpain: new perspectives in molecular diversity and physiological-pathological involvement. *FASEB. J.* 8, 814-822.

Saito K, Elce JS, Hamos JE, Nixon RA. (1993) Widespread activation of calcium-activated neutral proteinase (calpain) in the brain in Alzheimer disease: a potential molecular basis for neuronal degeneration. *Proc Natl Acad Sci U S A.* 90(7):2628-32.

Salehi A, Lucassen PJ, Pool CW, Gonatas NK, Ravid R, Swaab DF. (1994) Decreased neuronal activity in the nucleus basalis of Meynert in Alzheimer's disease as suggested by the size of the Golgi apparatus. *Neuroscience.* 59(4):871-80.

Salehi A, Verhaagen J, Dijkhuizen PA, Swaab DF. (1996). Co-localization of high-affinity neurotrophin receptors in nucleus basalis of Meynert neurons and their differential reduction in Alzheimer's disease. *Neuroscience.* 75(2):373-87.

Sarter, M., Bruno, J.P., Dudchenko, P. (1990) Activating the damaged basal forebrain cholinergic system: tonic stimulation versus signal amplification. *Psychopharmacology (Berl).*;101(1):1-17.

Sawa, A., (1999) Neuronal cell death in Down's syndrome. *J. Neural. Transm. Suppl.* 57, 87-97.

Sayre LM, Smith MA, Perry G. Chemistry and biochemistry of oxidative stress in neurodegenerative disease. *Curr Med Chem.* 8(7):721-38.

Scahill RI, Schott JM, Stevens JM, Rossor MN, Fox NC. (2002) Mapping the evolution of regional atrophy in Alzheimer's disease: unbiased analysis of fluid-registered serial MRI. *Proc Natl Acad Sci U S A.* 99(7):4703-7.

Schauwecker, P.E. and McNeil, T.H., (1996) Dendritic remodeling of dentate granule cells following a combined entorhinal cortex/fimbria-fornix lesion. *Exp. Neurol.* 141, 145-153.

Scheuner D, Eckman C, Jensen M, Song X, Citron M, Suzuki N, Bird TD, Hardy J, Hutton M, Kukull W, Larson E, Levy-Lahad E, Viitanen M, Peskind E, Poorkaj P, Schellenberg G, Tanzi R, Wasco W, Lannfelt L, Selkoe D, Younkin S. (1996) Secreted amyloid beta-protein similar to that in the senile plaques of Alzheimer's disease is increased in vivo by the presenilin 1 and 2 and APP mutations linked to familial Alzheimer's disease. *Nat Med.* 2(8):864-70.

Seidl R, Bajo M, Bohm K, LaCasse EC, MacKenzie AE, Cairns N, Lubec G. (1999) Neuronal apoptosis inhibitory protein (NAIP)-like immunoreactivity in brains of adult patients with Down syndrome. *J Neural Transm Suppl.* 57:283-91.

Selkoe DJ. (1994) Alzheimer's disease: a central role for amyloid. *J Neuropathol Exp Neurol.* 53(5):438-47.

Selznick LA, Holtzman DM, Han BH, Gokden M, Srinivasan AN, Johnson EM Jr, Roth KA (1999) In situ immunodetection of neuronal caspase-3 activation in Alzheimer disease. *J Neuropathol Exp Neurol* 58(9): 1020-6

Selznick LA, Zheng TS, Flavell RA, Rakic P, Roth KA (2000) Amyloid beta-induced neuronal death is bax-dependent but caspase-independent. *J Neuropathol Exp Neurol.* 59(4): 271-279

Seubert, P., Ivy, G., Larson, J., Lee, J., Shahi, K., Baudry, M., Lynch, G., (1988) Lesions of entorhinal cortex produce a calpain-mediated degradation of brain -spectrin in dentate gyrus. I. Biochemical studies. *Brain Res.* 459, 226-232.

Shefer VF. (1973) Absolute number of neurons and thickness of the cerebral cortex during aging, senile and vascular dementia, and Pick's and Alzheimer's diseases. *Neurosci Behav Physiol.* 6(4):319-24.

Shimohama S, Tanino H, Fujimoto S (1999) Changes in caspase expression in Alzheimer's disease: comparison with development and aging. *Biochem Bioph Res Comm* 256: 381-384

Shimohama, S. (2000) Apoptosis in Alzheimer's disease--an update. *Apoptosis.* 5, 9-16.

Shute CC, Lewis PR. (1966) Cholinergic and monoaminergic pathways in the hypothalamus. *Br Med Bull.* 22(3):221-6.

Sihag RK, Cataldo AM. (1996) Brain beta-spectrin is a component of senile plaques in Alzheimer's disease. *Brain Res.* 743(1-2):249-57.

Siman R, Baudry M, Lynch G. (1983) Purification from synaptosomal plasma membranes of calpain I, a thiol protease activated by micromolar calcium concentrations. *J Neurochem.* 41(4):950-6.

Simic G, Kostovic I, Winblad B, Bogdanovic N. (1997) Volume and number of neurons of the human hippocampal formation in normal aging and Alzheimer's disease. *J Comp Neurol.* 379(4):482-94.

Singleton, R.H., Zhu, J., Stone, J.R., Povlishock, J.T., (2002). Traumatically induced axotomy adjacent to the soma does not result in acute neuronal death. *J. Neurosci.* 22, 791-802.

Slater AF, Stefan C, Nobel I, van den Dobbelsteen DJ, Orrenius S. (1995) Signalling mechanisms and oxidative stress in apoptosis. *Toxicol Lett.* 82-83:149-53.

Smale G, Nichols NR, Brady DR, Finch CE, Horton WE Jr (1995) Evidence for apoptotic cell death in Alzheimer's disease. *Exp Neurol* 133(2): 225-30

Sofroniew MV, Isacson O. (1988) Distribution of degeneration of cholinergic neurons in the septum following axotomy in different portions of the fimbria-fornix: a correlation between degree of cell loss and proximity of neuronal somata to the lesion. *J Chem Neuroanat.* 1(6):327-37.

Sofroniew, M.V., Cooper, J.D., Svendsen, C.N., Crossman, P., Ip, N.Y., Lindsay, R.M., Zafra, F., Lindholm, D., (1993) Atrophy but not death of adult septal cholinergic neurons after ablation of target capacity to produce mRNAs for NGF, BDNF, and NT3. *J Neurosci.* 13(12),5263-5276.

Sofroniew, M.V., Galletly, N.P., Isacson, O., Svendsen, C.N., (1990). Survival of adult basal forebrain cholinergic neurons after loss of target neurons. *Science* 247(4940),338-342.

Sommer B. (2002) Alzheimer's disease and the amyloid cascade hypothesis: ten years on. *Curr Opin Pharmacol.* 2(1):87-92.

Soriano S, Lu DC, Chandra S, Pietrzik CU, Koo EH. (2001) The amyloidogenic pathway of amyloid precursor protein (APP) is independent of its cleavage by caspases. *J Biol Chem.* 276(31):29045-50.

Sorimachi H, Ishiura S, Suzuki K. (1997) Structure and physiological function of calpains. *Biochem J.* 328 (Pt 3):721-32.

Spillantini MG, Goedert M. (1998) Tau protein pathology in neurodegenerative diseases. *Trends Neurosci.* 21(10):428-33.

Spittaels K, Van den Haute C, Van Dorpe J, Bruynseels K, Vandezande K, Laenen I, Geerts H, Mercken M, Sciot R, Van Lommel A, Loos R, Van Leuven F. (1999). Prominent axonopathy in the brain and spinal cord of transgenic mice overexpressing four-repeat human tau protein. *Am J Pathol.* 155(6):2153-65.

Stadelmann C, Bruck W, Bancher C, Jellinger K, Lassmann H (1998) Alzheimer disease: DNA fragmentation indicates increased neuronal vulnerability, but not apoptosis. *J Neuropathol Exp Neurol* 57(5):456-64

Stadelmann C, Deckwerth TL, Srinivasan A, Bancher C, Bruck W, Jellinger K, Lassmann H (1999) Activation of caspase-3 in single neurons and autophagic granules of

granulovacuolar degeneration in Alzheimer's disease. Evidence for apoptotic cell death. *Am J Pathol* 155(5): 1459-66

Stennicke HR, Salvesen GS. (1998) Properties of the caspases. *Biochim Biophys Acta.* 1387(1-2):17-31.

Stone, J.R., Okonkwo, D.O., Singleton, R.H., Mutlu, L.K., Helm, G.A., Povlishock, J.T., (2002) Caspase-3-mediated cleavage of amyloid precursor protein and formation of amyloid Beta peptide in traumatic axonal injury. *J. Neurotrauma.* 19, 601-614.

Storm Mathisen, J. & Blackstad, T.W., (1964). Cholinesterase in the hippocampus region. Distribution and relation to architectonics and afferent systems. *Acta. Anat. (Basel).* 56, 216-253.

Su JH, Anderson AJ, Cribbs DH, Tu C, Tong L, Kesslack P, Cotman CW. (2003) Fas and Fas ligand are associated with neuritic degeneration in the AD brain and participate in beta-amyloid-induced neuronal death. *Neurobiol Dis.* 12(3):182-93.

Su JH, Anderson AJ, Cummings BJ, Cotman CW. (1994). Immunohistochemical evidence for apoptosis in Alzheimer's disease. *Neuroreport* 5(18): 2529-33.

Su JH, Cummings BJ, Cotman CW. (1996) Plaque biogenesis in brain aging and Alzheimer's disease. I. Progressive changes in phosphorylation states of paired helical filaments and neurofilaments. *Brain Res.* 739(1-2):79-87.

Su JH, Cummings BJ, Cotman CW. (1998) Plaque biogenesis in brain aging and Alzheimer's disease. II. Progressive transformation and developmental sequence of dystrophic neurites. *Acta Neuropathol (Berl).* 96(5):463-71.

Su JH, Deng G, Cotman CW (1997) Neuronal DNA damage precedes tangle formation and is associated with up-regulation of nitrotyrosine in Alzheimer's disease brain. *Brain Res* 774(1-2): 193-9.

Su JH, Kesslak JP, Head E, Cotman CW. (2002) Caspase-cleaved amyloid precursor protein and activated caspase-3 are co-localized in the granules of granulovacuolar degeneration in Alzheimer's disease and Down's syndrome brain. *Acta Neuropathol (Berl).* 104(1):1-6.

Su JH, Zhao M, Anderson AJ, Srinivasan A, Cotman CW (2001) Activated caspase-3 expression in Alzheimer's and aged control brain: correlation with Alzheimer pathology. *Brain Res* 898(2): 350-7

Su JH, Zhao M, Anderson AJ, Srinivasan A, Cotman CW. (2001) Activated caspase-3 expression in Alzheimer's and aged control brain: correlation with Alzheimer pathology. *Brain Res* 898(2): 350-7.

Sun A, Liu M, Nguyen XV, Bing G. (2003) P38 MAP kinase is activated at early stages in Alzheimer's disease brain. *Exp Neurol.* 183(2):394-405.

Swaab DF, Lucassen PJ, Salehi A, Scherder EJ, van Someren EJ, Verwer RW. (1998) Reduced neuronal activity and reactivation in Alzheimer's disease. *Prog Brain Res.* 117:343-77.

Sze C, Bi H, Kleinschmidt-DeMasters BK, Filley CM, Martin LJ. (2001) N-Methyl-D-aspartate receptor subunit proteins and their phosphorylation status are altered selectively in Alzheimer's disease. *J Neurol Sci.* 182(2):151-9.

Tamagno E, Parola M, Guglielmotto M, Santoro G, Bardini P, Marra L, Tabaton M, Danni O. (2003) Multiple signaling events in amyloid beta-induced, oxidative stress-dependent neuronal apoptosis. *Free Radic Biol Med.* 35(1):45-58.

Tanaka H, Grooms SY, Bennett MV, Zukin RS. (2000). The AMPAR subunit GluR2: still front and center-stage. *Brain Res.* 886(1-2):190-207.

Terry AV Jr, Buccafusco JJ. (2003) The cholinergic hypothesis of age and Alzheimer's disease-related cognitive deficits: recent challenges and their implications for novel drug development. *J Pharmacol Exp Ther.* 306(3):821-827

Terry RD (2000)Cell death or synaptic loss in Alzheimer disease. *J Neuropathol Exp Neurol* 59 (12): 1118 – 9

Terry RD (2001) An honorable compromise regarding amyloid in Alzheimer disease. *Ann Neurol* 49(5): 684

Terry RD, Masliah E, Salmon DP, Butters N, DeTeresa R, Hill R, Hansen LA, Katzman R. (1991) Physical basis of cognitive alterations in Alzheimer's disease: synapse loss is the major correlate of cognitive impairment. *Ann Neurol.* 30(4):572-80.

Terry RD, Peck A, DeTeresa R, Schechter R, Horoupian DS. (1981) Some morphometric aspects of the brain in senile dementia of the Alzheimer type. *Ann Neurol.* 10(2):184-92.

Terry, R.D., (2000) Cell death or synaptic loss in Alzheimer disease. *J. Neuropathol. Exp. Neurol.* 59, 1118-1119.

Thompson PM, Hayashi KM, de Zubicaray G, Janke AL, Rose SE, Semple J, Herman D, Hong MS, Dittmer SS, Doddrell DM, Toga AW. (2003) Dynamics of gray matter loss in Alzheimer's disease. *J Neurosci.* 23(3):994-1005.

Thornberry NA, Lazebnik Y. (1998) Caspases: enemies within. *Science.* 281(5381):1312-6.

Troncoso JC, Sukhov RR, Kawas CH, Koliatsos VE (1996) In situ labeling of dying cortical neurons in normal aging and in Alzheimer's disease: Correlation with senile plaques and disease progression. *J Neuropathol Exp Neurol* 55(11): 1134-42.

Tsang SY, Tam SC, Bremner I, Burkitt MJ (1996) Copper-1,10-phenanthroline induces internucleosomal DNA fragmentation in HepG2 cells, resulting from direct oxidation by the hydroxyl radical. *Biochem J* 317(Pt 1): 13-16

Uylings HB, de Brabander JM. (2002) Neuronal changes in normal human aging and Alzheimer's disease. *Brain Cogn.* 49(3):268-76.

Van der Zee EA, Luiten PG. (1999) Muscarinic acetylcholine receptors in the hippocampus, neocortex and amygdala: a review of immunocytochemical localization in relation to learning and memory. *Prog Neurobiol.* 58(5):409-71.

Vander Heiden MG, Plas DR, Rathmell JC, Fox CJ, Harris MH, Thompson CB. (2001) Growth factors can influence cell growth and survival through effects on glucose metabolism. *Mol Cell Biol.* 21(17):5899-912.

Vazquez J, Fernandez-Shaw C, Marina A, Haas C, Cacabelos R, Valdivieso F. (1996). Antibodies to human brain spectrin in Alzheimer's disease. *J Neuroimmunol.* 68(1-2):39-44.

Vogels OJ, Broere CA, ter Laak HJ, ten Donkelaar HJ, Nieuwenhuys R, Schulte BP. (1990) Cell loss and shrinkage in the nucleus basalis Meynert complex in Alzheimer's disease. *Neurobiol Aging* 11(1):3-13.

Waldmeier PC. (2003) Prospects for antiapoptotic drug therapy of neurodegenerative diseases. *Prog Neuropsychopharmacol Biol Psychiatry.* 27(2):303-21.

Wang KK. (2000) Calpain and caspase: can you tell the difference? *Trends Neurosci.* 23(2):59.

Wang, K.K., Posmantur, R., Nath, R., McGinnis, K., Whitton, M., Talanian, R.V., Glantz, S.B., Morrow, J.S., (1998). Simultaneous degradation of alphaII- and betaII--spectrin by caspase 3 (CPP32) in apoptotic cells. *J. Biol. Chem.* 273, 22490-22497.

Watson GS, Craft S. (2003) The role of insulin resistance in the pathogenesis of Alzheimer's disease: implications for treatment. *CNS Drugs.* 17(1):27-45.

Wechsler, A. and Teichberg, V.I., (1998) Brain -spectrin binding to the NMDA receptor is regulated by phosphorylation, calcium and calmodulin. *EMBO. J.* 17, 3931-3939.

Weidemann A, Paliga K, Durrwang U, Reinhard FB, Schuckert O, Evin G, Masters CL. (1999) Proteolytic processing of the Alzheimer's disease amyloid precursor protein within its cytoplasmic domain by caspase-like proteases. *J Biol Chem.* 274(9):5823-9.

Wenk GL, McGann K, Mencarelli A, Hauss-Wegrzyniak B, Del Soldato P, Fiorucci S. (2000) Mechanisms to prevent the toxicity of chronic neuroinflammation on forebrain cholinergic neurons. *Eur J Pharmacol.* 402(1-2):77-85.

West MJ, Coleman PD, Flood DG, Troncoso JC. (1994). Differences in the pattern of hippocampal neuronal loss in normal ageing and Alzheimer's disease. *Lancet.* 344(8925):769-72.

West MJ. (1993) Regionally specific loss of neurons in the aging human hippocampus. *Neurobiol Aging.* 14(4):287-93

Whitehouse PJ, Price DL, Struble RG, Clark AW, Coyle JT, Delon MR. 1982) Alzheimer's disease and senile dementia: loss of neurons in the basal forebrain. *Science.* 215(4537):1237-1239.

Williams, L.R., Varon, S., Peterson, G.M., Wictorin, K., Fischer, W., Bjorklund, A., Gage, F.H., 1986. Continuous infusion of nerve growth factor prevents basal forebrain neuronal death after fimbria fornix transection. *Proc. Natl. Acad. Sci. U S A.* 83, 9231-9235.

Wolozin B, Iwasaki K, Vito P, Ganjei JK, Lacana E, Sunderland T, Zhao B, Kusiak JW, Wasco W, D'Adamio L (1996) Participation of presenilin 2 in apoptosis: enhanced basal activity conferred by an Alzheimer mutation. *Science* 274(5293): 1710-3

Wozniak DF, Dikranian K, Ishimaru MJ, Nardi A, Corso TD, Tenkova T, Olney JW, Fix AS. (1998) Disseminated corticolimbic neuronal degeneration induced in rat brain by MK-801: potential relevance to Alzheimer's disease. Neurobiol Dis. 5(5):305-22.

Xie, X.Y. and Barrett, J.N., (1991). Membrane resealing in cultured rat septal neurons after neurite transection: evidence for enhancement by Ca(2+)-triggered protease activity and cytoskeletal disassembly. *J Neurosci* 11(10), 3257-3267.

Yamatsuji T, Matsui T, Okamoto T, Komatsuzaki K, Takeda S, Fukumoto H, Iwatsubo T, Suzuki N, Asami-Odaka A, Ireland S, Kinane TB, Giambarella U, Nishimoto I (1996) G protein-mediated neuronal DNA fragmentation induced by familial Alzheimer's disease-associated mutants of APP. *Science* 272(5266): 1349-52

Yan, B., Calderwood, D.A., Yaspan, B., Ginsberg, M.H., (2001) Calpain cleavage promotes talin binding to the beta 3 integrin cytoplasmic domain. *J. Biol. Chem.* 276, 28164-28170.

Yang F, Sun X, Beech W, Teter B, Wu S, Sigel J, Vinters HV, Frautschy SA, Cole GM. (1998). Antibody to caspase-cleaved actin detects apoptosis in differentiated neuroblastoma and plaque-associated neurons and microglia in Alzheimer's disease. *Am J Pathol* 152 (2):379-89.

Yankner BA (1996) Mechanisms of neuronal degeneration in Alzheimer's disease. *Neuron.* 16(5):921-32.

Yuan J, Yankner BA (2000) Apoptosis in the nervous system *Nature* 407 (6805): 802-809

Zheng TS, Hunot S, Kuida K, Momoi T, Srinivasan A, Nicholson DW, Lazebnik Y, Flavell RA (2000) Deficiency in caspase-9 or caspase-3 induces compensatory caspase activation. *Nat Med* (11): 1241-1247

Zhu X, Castellani RJ, Takeda A, Nunomura A, Atwood CS, Perry G, Smith MA. (2001) Differential activation of neuronal ERK, JNK/SAPK and p38 in Alzheimer disease: the 'two hit' hypothesis. *Mech Ageing Dev.* 123(1):39-46.

Zimmermann KC, Green DR. (2001) How cells die: apoptosis pathways. *J Allergy Clin Immunol.* 108(4 Suppl):S99-103.